

Interactive effects of ocean acidification and
warming on marine phytoplankton
-from physiology to biogeochemical cycling



Submitted by
Scarlett Sett
Kiel, July 2014

Cover: PLANCTON | Christian Sardet

**Interactive effects of ocean acidification and warming on
marine phytoplankton
-from physiology to biogeochemical cycling**



Dissertation
in fulfillment of the requirements for the degree
Dr.rer.nat.
of the Faculty of Mathematics and Natural Sciences
at Christian-Albrechts University Kiel

submitted by
Scarlett Sett

Kiel, July 2014

First referee: Prof. Dr. Ulf Riebesell
Second referee: Prof. Dr. Andreas Oschlies
Date of oral examination: 17.09.2014
Approved for publication: 17.09.2014
Signed: Prof. Dr. Wolfgang J. Duschl

Table of Contents

Summary	1
Zusammenfassung	3
General Introduction	5
Climate change in the 21 st century	5
Ocean warming and acidification	6
Marine phytoplankton	7
The marine carbon cycle	9
Thesis outline.....	10
References	12
Author contributions	15
Chapter I: Temperature modulates coccolithophorid sensitivity of growth, photosynthesis and calcification to increasing seawater $p\text{CO}_2$	17
Chapter II: Shifts from smaller to larger diatoms during a natural phytoplankton bloom under combined high CO_2 and warming conditions.....	27
Chapter III: Particulate and dissolved organic matter dynamics during an induced Mediterranean plankton bloom under ocean acidification and warming scenarios	57
Synthesis and future perspectives	79
Effects of climate change on phytoplankton physiology.....	79
The use of mesocosms to study whole community responses	81
Effects of climate change on natural phytoplankton communities	83
Implications for coastal ecosystems.....	85
Future perspectives	85
References	87
Acknowledgments	91
Curriculum Vitae	93
Erklärung	95

Table of Contents

Summary

Climate change driven by anthropogenic utilization of fossil fuels and deforestation over the past 250 years is leading to ongoing changes in sea surface temperature (i.e. ocean warming) and seawater carbonate chemistry speciation (i.e. ocean acidification, OA) at an unprecedented pace. Both of these environmental stressors are expected to impact marine ecosystem functioning in the near future with consequences for marine biogeochemical cycling. In the context of this doctoral thesis, phytoplankton physiology and biogeochemical dynamics were investigated under the individual and combined effects of OA and warming through experimental work.

Chapter I of this thesis presents data on the individual and synergistic effects of OA and warming on coccolithophore physiology. In order to test for possible synergistic effects, two coccolithophore species, *Emiliana huxleyi* and *Gephyrocapsa oceanica*, were exposed to a broad range in CO₂ concentrations at three different temperatures. The results from this study showed that both species displayed optimum-curve responses for key metabolic processes (i.e. growth, photosynthesis and calcification) at all temperatures, with species-specific sensitivities. Most importantly, increasing temperature modulated the optimum CO₂ concentration and sensitivity of metabolic processes. Our results enabled us to propose a conceptual model showing that the temperature sensitivity of metabolic processes in these organisms could help explain the discrepancies found in the literature on coccolithophore physiology in response to OA.

Interested by the results from experiments in **Chapter I** with single species, mesocosm experiments were carried out in **Chapters II** and **III** with natural plankton communities. Since most of the literature with natural communities has focused on effects of individual environmental factors, experiments in **Chapters II** and **III** investigated the combined effects of OA and warming during a natural spring bloom (Kiel Bight) and a nutrient-induced summer bloom (Thau lagoon, France). During experiments in **Chapter II** a shift in phytoplankton community composition towards larger diatoms under combined OA and warming conditions (i.e. 'Greenhouse' scenario) was observed. Possible explanations for the observed shift in size are discussed in detail and compared with results in the literature. Furthermore, the shift in species composition significantly increased losses of organic matter at the end of the experiment in the Greenhouse treatment were larger species dominated. **Chapter III** focused on the temporal development of phytoplankton derived particulate and dissolved organic matter (i.e. POM and DOM, respectively). Increased CO₂, individually and in combination with warming, enhanced biomass build-up and modulated the negative effects of warming (i.e. decreased biomass build-up).

In summary, the experimental data from the work presented in this doctoral thesis shows the importance of investigating the synergistic effects of changing environmental factors when trying to understand the response of marine ecosystems to climate change and its importance when

Summary

assessing the future of marine ecosystem functioning. Some suggestions for experimental work are proposed to follow up on the results from experiments presented in this doctoral thesis.

Zusammenfassung

Der Klimawandel, der hauptsächlich durch die anthropogene Nutzung fossiler Energieträger und die Entwaldung in den letzten 250 Jahren verursacht wurde, führt in einem nie dagewesenen Tempo zu anhaltenden Temperaturveränderungen des Wassers der Meeresoberfläche (Ozeanerwärmung) und zu Ozeanversauerung (d.h. OA). Es wird erwartet, dass beide Stressfaktoren in naher Zukunft das Funktionieren mariner Ökosysteme beeinflussen werden, was schwerwiegende Folgen für marine biogeochemische Stoffkreisläufe nach sich ziehen kann. Im Rahmen dieser Doktorarbeit werden die Auswirkungen von Ozeanversauerung und Ozeanerwärmung – als Einzeleffekte und im Zusammenspiel als Synergieeffekte – auf die Physiologie von Phytoplankton und die Dynamik von biogeochemischen Stoffkreisläufen experimentell untersucht.

Kapitel I dieser Arbeit präsentiert Daten von Einzel- und Synergieeffekten von OA und Ozeanerwärmung auf die Physiologie von Coccolithophoriden. Um mögliche Synergieeffekte zu identifizieren, wurden zwei Coccolithophorid-Arten, *E. huxleyi* und *G. Oceanica*, einem breiten Spektrum von CO₂-Konzentration bei gleichzeitig drei verschiedenen Temperaturen ausgesetzt. Die Ergebnisse aus dieser Studie zeigten, dass beide Arten bei allen Temperaturen einer Optimumkurve für bestimmte Schlüsselprozesse ihres Stoffwechsels (d.h. Wachstum, Photosynthese und Kalzifizierung) besitzen, mit jeweils artspezifischen Sensitivitäten. Das wichtigste Ergebnis ist aber, dass die Temperaturerhöhungen das CO₂-Konzentrationsoptimum und -sensitivität der Stoffwechselvorgänge moduliert. Die dargestellte Temperaturempfindlichkeit der Stoffwechselprozess in diesen Organismen könnte zur Klärung beitragen, warum in der Fachliteratur Diskrepanzen zur physiologischen Antwort von Coccolithophoriden auf OA vorliegen.

Da die Ergebnisse der Experimente aus **Kapitel I**, die die Auswirkungen von Stressfaktoren auf einzelne Spezies untersuchten sich als sehr interessant und vielversprechend heraus gestellt haben, wurden in **Kapitel II und III** Mesokosmen-Experimente mit Planktongemeinschaften durchgeführt. Da der Großteil der Fachliteratur, der sich auf natürliche Planktongemeinschaften bezieht, sich auf Einzelauswirkungen von Umweltstressfaktoren (wie Temperatur oder CO₂) beschränkt, wurden die Experimente im **Kapitel II und III** so angelegt, dass sie die kombinierten Effekte während einer natürlichen Frühjahrsblüte (Kieler Bucht) und einer nährstoffinduzierten Sommerblüte (Etang de Thau, Frankreich) untersuchten. Bei den Versuchen in **Kapitel II**, dem Zusammenspiel von OA und Ozeanerwärmung (dem "Treibhaus"-Szenario), veränderte sich die Zusammensetzung der Phytoplanktongemeinschaft hin zu größeren Kieselalgen. Diese Veränderung zu größeren Kieselalgen legen nahe, könnten Export von organischem Material am Ende der Blüte verbessern. **Kapitel III** hat die zeitliche Änderung von den vom Phytoplankton abgeleiteten partikulären und gelösten organischen Substanzen (z.B. POM und DOM, jeweilig) im Fokus. In diesen Experimenten milderten die durch die synergistische Effekte von OA und Ozeanerwärmung größere gebildete Biomasse die negativen Auswirkungen der Erwärmung ab.

Zusammenfassung

Die in der vorliegenden Dissertation beschriebenen Experimente und Daten zeigen zusammenfassend, dass die Untersuchung der Auswirkung von mehreren kombinierten (synergistischen), statt einzelner isolierter Umweltstressfaktoren von Bedeutung ist. Dies wird vor allem dann ersichtlich, wenn man die Reaktion mariner Ökosysteme auf den Klimawandel und dessen Bedeutung bei der zukünftigen Beurteilung der Funktionsweise marine Ökosystem ergründen möchte. Einige Vorschläge für künftige experimentelle Versuche werden in dieser Dissertation angeregt, die an die präsentierten Ergebnisse anknüpfen könnten.

Introduction

Climate change in the 21st century

Climate change driven by human activities since the beginning of the industrial revolution is an undeniable and ongoing process affecting all natural systems on Earth (Parmesan & Yohe, 2003; Parry *et al.*, 2007). Whereas climate change has occurred through Earth's history, it is the extraordinary pace at which it is happening of present concern. The anthropocene is an informal geological term (beginning from the industrial revolution some 250 years ago to present) coined to characterize and describe this period of rapid change in climate conditions driven by human activities such as deforestation, land use change and the burning of fossil fuels. All of these activities lead to the accumulation of gases such as: carbon dioxide (CO₂), methane (CH₄), nitrous oxide (N₂O), chlorofluorocarbons (CFC's) and water vapor in the atmosphere (also known as "greenhouse" gases). The natural presence of these greenhouse gases in the atmosphere helps maintain hospitable conditions for life on Earth by trapping heat from escaping to space through a phenomenon called the "greenhouse effect". However, the accumulation of these gases (mostly CO₂) in the atmosphere from anthropogenic sources has exacerbated the natural effect. Over the past 250 years, CO₂ concentrations in the atmosphere increased from 280 ppmv (parts per million volume) to almost 400 ppmv and global average temperatures increased by 0.8°C over the last century (Parry *et al.*, 2007) (Figure 1).

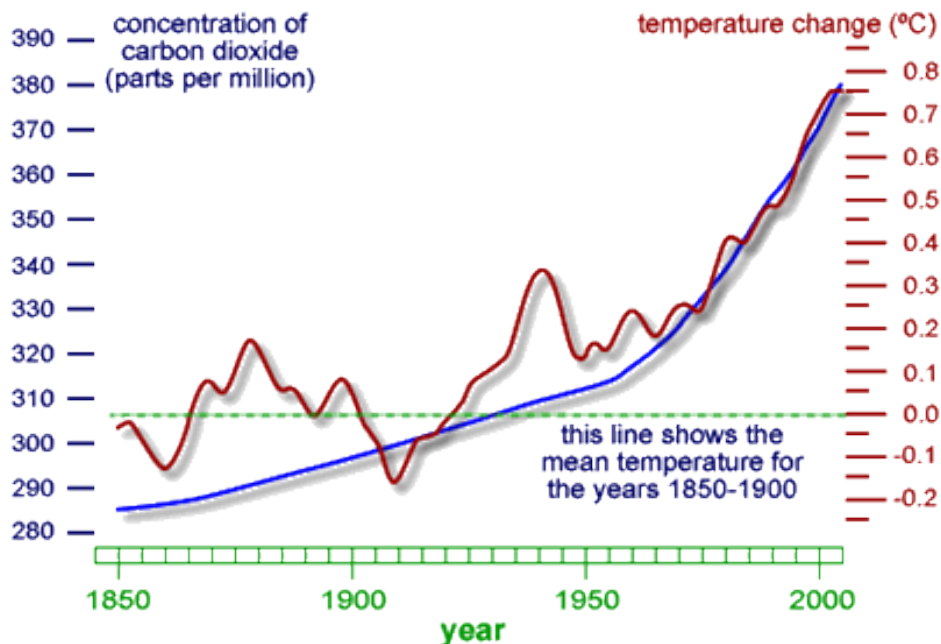


Figure 1. Temperature change (°C) and atmospheric CO₂ concentrations (ppm) over time from the industrial revolution to 2004 (Source: IPCC 2007)

The ocean, covering 71% of the Earth's surface, plays a leading role in mitigating the effect of climate change by storing CO₂ and heat (Sabine *et al.*, 2004; Parry *et al.*, 2007; Levitus *et al.*, 2012).

Introduction

Nevertheless, this 'natural buffer' capacity of the ocean to take up heat and CO₂ comes with consequences for the ocean's chemical and physical properties.

Ocean warming and acidification

Global warming as a consequence of increasing anthropogenic CO₂ concentrations in the atmosphere is observed both on land and in the ocean. However, due to the higher thermal capacity of water, temperature changes in the ocean are slower than those on land. Nevertheless, an increase of 0.6°C in sea surface temperature (SST) over the past 50 years has already been observed with a further projected increase by the end of the century of 1.1-6.2°C (Parry *et al.*, 2007, Figure 2). Even if CO₂ emissions would stabilize, an increase of 0.5°C would still occur by the end of this century (Meehl *et al.*, 2005). Furthermore, while warming was thought to occur most significantly in the upper 700 m of the ocean (Levitus *et al.*, 2005) it was recently showed that 30% of ocean warming was below 700 m leading to a warming trend in the ocean as a whole and not only in the surface (Levitus *et al.*, 2012; Balmaseda *et al.*, 2013).

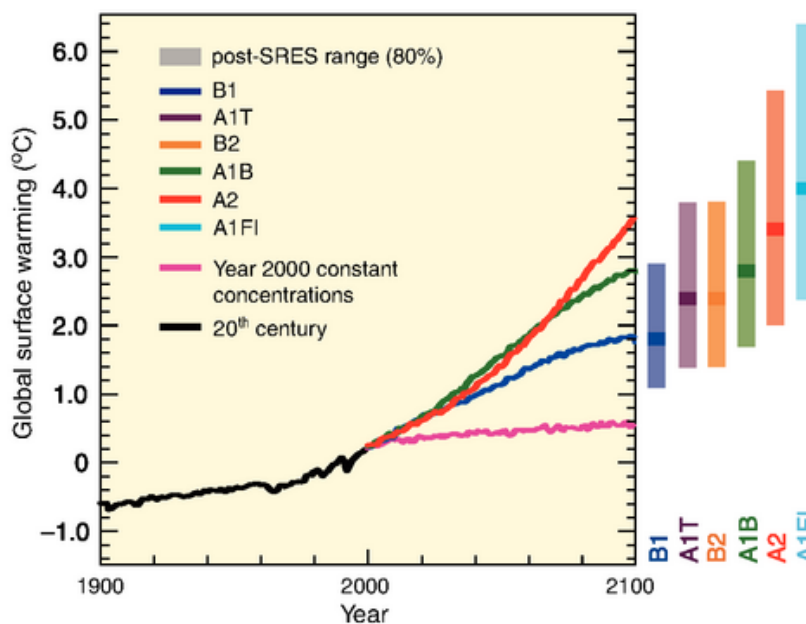


Figure 2. Global surface temperature predictions by the end of the 21st century. Different colors represent different models (Source: IPCC 2007).

Additionally, the ocean has taken up about 1/3 of anthropogenic CO₂ emissions and consequently altered carbonate chemistry speciation in seawater. Ocean acidification (OA) describes the decrease in carbonate ions [CO₃²⁻] and pH and the increase in bicarbonate ions [HCO₃⁻] and dissolved CO₂ (Wolf-Gladrow *et al.*, 1999; Caldeira & Wickett, 2003). With the continuous utilization of fossil fuels, pH is projected to decrease by ~0.4 units towards the end of this century (Orr *et al.*, 2005, Figure 3). These changes in the ocean's chemical and physical properties will potentially modify marine biogeochemical cycling (Rees, 2012) but the challenge remains on to what extent and in which directions (i.e. positive or negative feedbacks) the marine environment will respond.

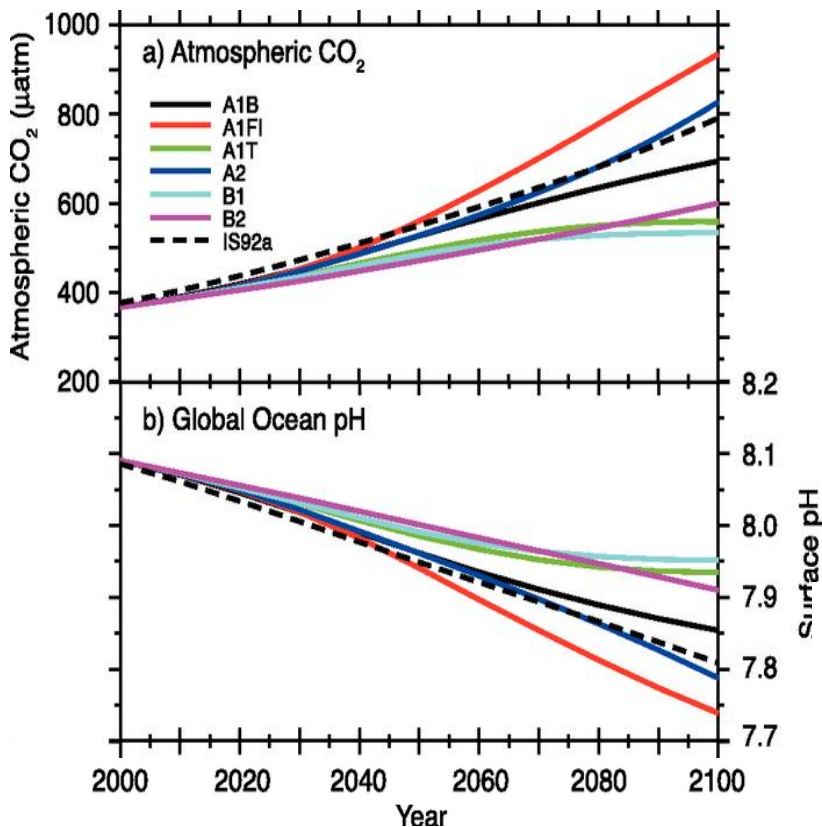


Figure 3. Projected atmospheric CO₂ concentrations (A) and pH (B) under various emission scenarios from 2000-2100 (Source: modified from Orr et al. 2005).

Marine phytoplankton

Despite their invisibility to the naked eye, marine phytoplankton are responsible for ~50% of the global primary production (Falkowski *et al.*, 1998) therefore investigating their response to changing environmental conditions is of great importance to predict the future of marine ecosystems. Although many environmental factors control phytoplankton growth and productivity in the ocean (Beardall & Stojkovic, 2006) the work in this doctoral thesis will focus exclusively on the individual and synergistic effects of OA and warming. Whereas the direct effects of warming in phytoplankton are expected through an acceleration of metabolic activities (Eppley, 1972) the indirect effects are expected through enhanced stratification of the water column and subsequent modulation of nutrients and light availability. Furthermore, increasing CO₂ in seawater is expected to affect marine phytoplankton performance due to their different requirements for inorganic carbon acquisition and specific CO₂ concentrating mechanisms (for a review see Beardall *et al.*, 2009) and thus affect their role as sinks or sources of CO₂. While increases in CO₂ expected by the end of the century have shown to stimulate phytoplankton photosynthesis (Riebesell, 2004) the concomitant decrease in pH negatively affects calcification (Kroeker *et al.*, 2010).

At the base of the marine food web, phytoplankton productivity determines the energy flow to higher trophic levels through an intricate chain of food web dynamics (Pomeroy, 1974). The large phytoplankton diversity and key roles they play in the cycling of carbon (C), nitrogen (N), phosphorus

Introduction

(P) and silica (Si) separate them into 4 main functional clusters: diatoms, coccolithophores, cyanobacteria and dinoflagellates (Falkowski & Raven, 2007). Out of these four functional clusters, this thesis conducted experiments with diatoms and coccolithophores (Figure 4) due to their relevance in the carbon cycle and export production.

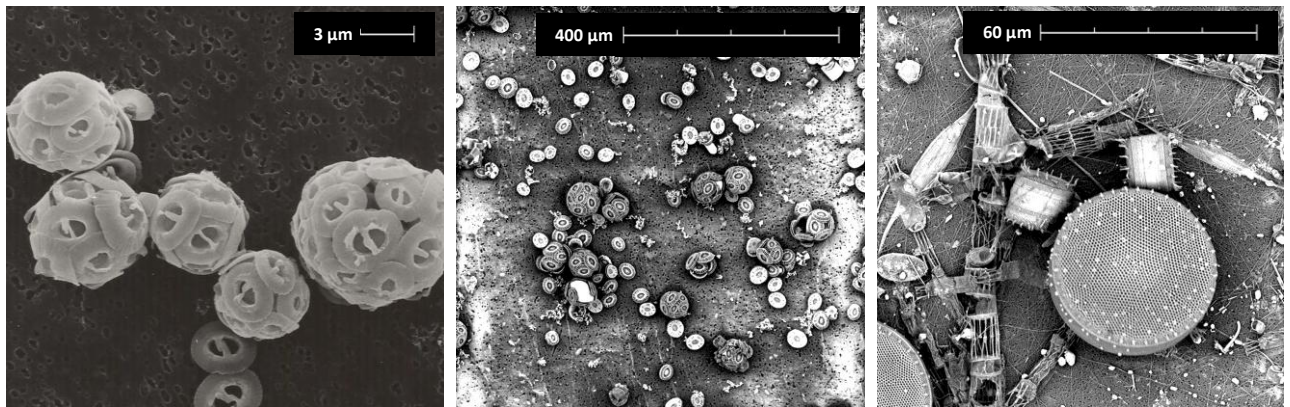


Figure 4. Scanning electron microscope pictures of coccolithophores (A and B) and diatoms (C) taken from experiments in Chapter I and II of this doctoral thesis.

Diatoms are the most abundant of the four groups. They are ubiquitous in distribution and dominate blooms in nutrient rich, high latitude, coastal and upwelling regions due to their many physiological advantages (i.e. high growth and carbon fixation rates, opportunistic consumption of nutrients) while outcompeting other phytoplankton groups (Agawin *et al.*, 2000; Boyd *et al.*, 2010). They are estimated to contribute to ~40% of marine primary production (Sarhou *et al.*, 2005) and utilize silica to build their external shells (“silicified frustules”) and therefore are highly efficient at transporting organic carbon from the surface to the deep ocean (Buesseler, 1998). Coccolithophores are also ubiquitous in distribution but they are only able to produce extensive blooms, which are detectable from space, at high latitudes (Groom & Holligan, 1987; Holligan *et al.*, 1993). While their contribution to marine primary production only accounts for 1-10% (Poulton *et al.*, 2007) their contribution to CaCO_3 in pelagic sediments is ~50% (Broecker & Clark, 2009). Both diatoms and coccolithophores play key roles in the cycling of carbon and therefore investigating their response to changing environmental conditions is of great importance to predict the future of marine biogeochemical element cycling (Sarhou *et al.*, 2005; Boyd *et al.*, 2010). Increased diatom productivity during blooms as a response to climate change, for example, might enhance capacity of the ocean to sequester and store CO_2 and provide a negative feedback to climate change and atmospheric CO_2 (**Chapter II**).

Introduction

The marine carbon cycle

The ocean is the second largest reservoir of carbon on Earth containing about ~40 000 Pg. Out of this large pool, ~39 000 Pg is present as dissolved inorganic carbon (DIC), ~700 Pg as dissolved organic carbon (DOC) and only 3 Pg as particulate organic carbon (POC). The high turnover rates of biogenic material in the ocean compared to those on land (i.e. days-weeks versus years-decades, respectively) explain why the terrestrial biomass is still 200 times higher than in the ocean. The vertical gradient of DIC in the ocean is mediated by physical and a biological carbon pumps (Figure 5, Volk & Hoffert, 1987).

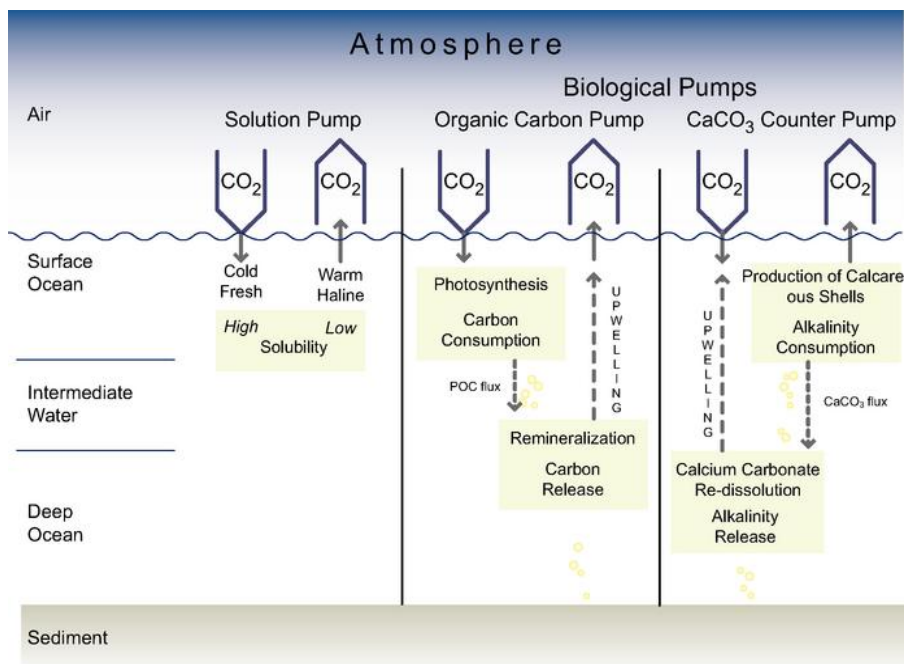


Figure 5. Solubility and carbon pumps in the ocean (Source: Heinze and Maier-Reimer 1991).

The physical (or solubility) pump, as the name implies, mainly describes the vertical fluxes from differences in CO₂ solubility according to temperature. The biological pump, however, is subdivided into the 'organic carbon' and 'carbonate' pump. Simply said, the biological pump is the process of biologically driven CO₂ fixation from the atmosphere into the ocean through the process of phytoplankton photosynthesis with subsequent conversion into particulate organic matter (POM) and thereafter remineralization within the microbial loop or export to the deep ocean (Sarmiento & Gruber, 2006). Whereas the 'organic carbon' pump would sequester and store CO₂ by sinking newly produced POM into the deep ocean, the 'carbonate' (or counter pump) would release CO₂ back into the atmosphere as a result of the production of calcareous material in the euphotic zone. Moreover, the elemental composition of POM is of great importance in determining the efficiency of the carbon pump and ocean's storage capacity for atmospheric CO₂. In 1958, Redfield showed that the elemental composition of phytoplankton was fairly constant across oceanic regions (Redfield, 1958). This was coined as the 'Redfield ratio' and suggested a molar C:N:P proportion of 106:16:1,

Introduction

respectively. However, this concept was challenged in the following years (even presently) because it did not consider the physiological needs of different phytoplankton groups during nutrient acquisition (see review Geider & La Roche, 2002). Deviations away from the canonical 'Redfield' proportions have been shown in a wide selection of scenarios. For example, the excess consumption of inorganic carbon over inorganic nitrogen (above Redfield proportions) during phytoplankton bloom events tends to produce C enriched POM through a process also referred to as carbon overconsumption (Toggweiler, 1993).

Almost all of the newly produced POM is remineralized in the euphotic zone, less than 20% escapes the euphotic zone and only 1-3% reaches the deep ocean (De La Rocha & Passow, 2007). However, 'ballast' minerals such as CaCO_3 and silicate (produced by coccolithophores and diatoms, respectively) are thought to play key roles in the transport of the fraction of POM which would reach the deep ocean (see review by De La Rocha & Passow, 2007).

Thesis outline

The goal of this thesis was to examine the synergistic effects of OA and warming on key phytoplankton species and the potential consequences this could carry for biogeochemical element cycling. Two methodologies were used in order to answer specific scientific questions. First, we conducted single-species culture experiments under controlled conditions in the laboratory to investigate the physiological response of coccolithophores to the individual and interactive effects of OA and warming. The novel results from the culture experiments with single species motivated the work for experiments in **Chapter II** and **III** with natural phytoplankton communities using mesocosms.

Chapter I presents the results from culture experiments with two coccolithophore species, *E. huxleyi* and *G. oceanica*. During these experiments, the response of key metabolic processes (i.e. growth, photosynthesis and calcification) under the individual and combined influence of OA and warming was studied. During the past two decades, coccolithophores have gained considerable attention due to their sensitivity to OA. However, quite a diverse range of responses has been reported and most of the experiments focused only on the individual effects of OA (Ridgwell *et al.*, 2009). Therefore, key uncertainties remained on the interactive effects of CO_2 and other environmental factors on coccolithophore physiology and why the responses varied so widely. The main goal of this study was to investigate whether increasing temperature would systematically modulate sensitivity of key metabolic processes on coccolithophores to OA. We discuss in detail how the temperature sensitivity of metabolic processes can help explain much of the discrepancy found on coccolithophore literature and the importance of combining different environmental stressors to assess the performance of coccolithophores in a future ocean.

Introduction

Whereas the effects of ocean acidification and warming on natural phytoplankton communities has been extensively studied independently there seems to be limited data on the combined effects (Hare *et al.*, 2007; Feng *et al.*, 2010; Kim *et al.*, 2011). Therefore, experiments in **Chapter II** and **III** present the results from two mesocosm experiments investigating the interactive and individual effects of OA and warming on natural phytoplankton communities of two different oceanic regions: Kiel Bight (temperate coastal ecosystem) and Thau Lagoon (Mediterranean Sea). Experiments in **Chapter II** were carried out using the indoor mesocosms in Kiel. These experiments followed the natural development of a spring bloom under combined OA and warming conditions (also only OA). Shifts in community composition suggested that the interaction of OA and warming benefited a larger group size of diatoms with potential consequences for export of organic matter at the end of bloom events. Experiments on **Chapter III** were carried out using floating mesocosms anchored to a platform in the Thau Lagoon, France during a nutrient-induced summer bloom. The experiments followed the temporal development of particulate and dissolved organic matter under the individual and combined effects of OA and warming. Our results suggested that negative effects of warming, such as decreased phytoplankton biomass build-up, were somewhat mitigated by increasing CO₂ (both individually and in combination with warming) and suggested that this could translate into energy transfer to higher trophic levels in this region of the Mediterranean.

A comprehensive summary is presented at the end of this thesis highlighting the findings from the experiments mentioned above and suggesting that the interactive effects of environmental stressors provide more realistic scenarios of a ‘future ocean’ compared to the sum of the individual effects. This should be considered when assessing the future of marine ecosystem in response to climate change in the upcoming decades.

References

- Agawin NSR, Duarte CM, Agusti S (2000) Nutrient and temperature control of the contribution of picoplankton to phytoplankton biomass and production. *Limnology and Oceanography*, **45**, 591–600.
- Balmaseda M, Trenberth KE, Källén E (2013) Distinctive climate signals in reanalysis of global ocean heat content. *Geophysical Research Letters*, **40**, 1754–1759.
- Beardall J, Stojkovic S (2006) Microalgae under Global Environmental Change: Implications for Growth and Productivity, Populations and Trophic Flow. *ScienceAsia*, **1**, 1–10.
- Beardall J, Stojkovic S, Larsen S (2009) Living in a high CO₂ world: impacts of global climate change on marine phytoplankton. *Plant Ecology & Diversity*, **2**, 191–205.
- Boyd PW, Strzepek R, Fu F et al. (2010) Environmental control of open-ocean phytoplankton groups: Now and in the future. *Limnology and Oceanography*, **55**, 1353–1376.

Introduction

- Broecker W, Clark E (2009) Ratio of coccolith CaCO_3 to foraminifera CaCO_3 in late Holocene deep sea sediments. *Paleoceanography*, **24**.
- Buesseler KO (1998) The decoupling of production and particulate export in the surface as a tracer of upper ocean Comparisons between production and. *Global Biogeochemical Cycles*, **12**, 297–310.
- Caldeira K, Wickett M (2003) Anthropogenic carbon and ocean pH. *Nature*, **425**, 2003.
- Eppley RW (1972) Temperature and phytoplankton growth in the sea. *Fishery Bulletin*, **70**, 1063–1085.
- Falkowski PG, Raven J (2007) *Aquatic photosynthesis*. Princeton University Press.
- Falkowski PG, Barber R, Smetacek V (1998) Biogeochemical Controls and Feedbacks on Ocean Primary Production. *Science*, **281**, 200–206.
- Feng Y, Hare CE, Rose JM et al. (2010) Interactive effects of iron, irradiance and CO_2 on Ross Sea phytoplankton. *Deep Sea Research Part I: Oceanographic Research Papers*, **57**, 368–383.
- Geider R, La Roche J (2002) Redfield revisited : variability of C : N : P in marine microalgae and its biochemical basis. *Eu*, **37**, 1–17.
- Groom SB, Holligan PM (1987) Remote sensing of coccolithophore blooms. *Advances in Space Research*, **7**, 73–78.
- Hare C, Leblanc K, DiTullio G et al. (2007) Consequences of increased temperature and CO_2 for phytoplankton community structure in the Bering Sea. *Marine Ecology Progress Series*, **352**, 9–16.
- Heinze C, Maier-Reimer E (1991) Glacial $p\text{CO}_2$ reduction by the world ocean: experiments with the Hamburg Carbon Cycle Model. *Paleoceanography*, **6**, 395–430.
- Holligan PM, Fernandez E, Aiken J et al. (1993) A biogeochemical study of the coccolithophore, *Emiliania huxleyi*, in the North Atlantic. *Global Biogeochemical Cycles*, **7**, 879–900.
- Kim J-M, Lee K, Shin K et al. (2011) Shifts in biogenic carbon flow from particulate to dissolved forms under high carbon dioxide and warm ocean conditions. *Geophysical Research Letters*, **38**.
- Kroeker KJ, Kordas RL, Crim RN et al. (2010) Meta-analysis reveals negative yet variable effects of ocean acidification on marine organisms. *Ecology letters*, **13**, 1419–34.
- De La Rocha CL, Passow U (2007) Factors influencing the sinking of POC and the efficiency of the biological carbon pump. *Deep Sea Research Part II: Topical Studies in Oceanography*, **54**, 639–658.
- Levitus S, Antonov J, Boyer T (2005) Warming of the world ocean, 1955-2003. *Geophysical Research Letters*, **32**.
- Levitus S, Antonov J, Boyer T et al. (2012) World ocean heat content and thermosteric sea level change (0-2000 m) 1955-2010. *Geophysical Research Letters*, **39**.

Introduction

- Meehl G, Washington W, Collins W et al. (2005) How much more global warming and sea level rise? *Science*, **307**.
- Orr JC, Fabry VJ, Aumont O et al. (2005) Anthropogenic ocean acidification over the twenty-first century and its impact on calcifying organisms. *Nature*, **437**, 681–6.
- Parmesan C, Yohe G (2003) A globally coherent fingerprint of climate change impacts across natural systems. *Nature*, **421**, 37–42.
- Parry ML, Canziani OF, Palutikof JP et al. (2007) Climate Change 2007: Impacts, Adaptation and Vulnerability. Contribution of Working Group II to the Fourth Assessment Report of the Intergovernmental Panel on Climate Change. *Journal of Environment Quality*, **37**, 2407.
- Pomeroy LR (1974) The ocean's food web, a changing paradigm. *BioScience*, **24**, 499–504.
- Poulton AJ, Adey TR, Balch WM et al. (2007) Relating coccolithophore calcification rates to phytoplankton community dynamics: Regional differences and implications for carbon export. *Deep Sea Research Part II: Topical Studies in Oceanography*, **54**, 538–557.
- Redfield A (1958) The biological control of chemical factors in the environment. *American Scientist*, 205–221.
- Rees AP (2012) Pressures on the marine environment and the changing climate of ocean biogeochemistry. *Philosophical transactions. Series A, Mathematical, physical, and engineering sciences*, **370**, 5613–35.
- Ridgwell A, Schmidt DN, Turley C et al. (2009) From laboratory manipulations to Earth system models: scaling calcification impacts of ocean acidification. *Biogeosciences*, **6**, 2611–2623.
- Riebesell U (2004) Effects of CO₂ Enrichment on Marine Phytoplankton. *Journal of Oceanography*, **60**, 719–729.
- Sabine CL, Feely R, Gruber N et al. (2004) The oceanic sink for anthropogenic CO₂. *Science*, **305**, 367–371.
- Sarmiento JL, Gruber N (2006) *Ocean biogeochemical dynamics*. Princeton University Press.
- Sarthou G, Timmermans KR, Blain S et al. (2005) Growth physiology and fate of diatoms in the ocean: a review. *Journal of Sea Research*, **53**, 25–42.
- Toggweiler J (1993) Carbon overconsumption. *Nature*, **363**, 210–211.
- Volk T, Hoffert MI (1987) Ocean carbon pumps: analysis of relative strengths and efficiencies in ocean-driven atmospheric CO₂ changes. *Geophysical Monograph Series*, **32**.
- Wolf-Gladrow D, Riebesell U, Burkhardt S (1999) Direct effects of CO₂ concentration on growth and isotopic composition of marine plankton. 461–476.

Introduction

Author Contributions

First author publications and declaration of contribution

Chapter I

Sett, S., Bach, L.T., Schulz, K.G., Koch-Klavsen, S., Lebrato, M., and Riebesell, U. *Temperature Modulates Coccolithophorid Sensitivity of Growth, Photosynthesis and Calcification to Increasing Seawater pCO₂*. **PLoS ONE 9(2)**: e88308. doi:10.1371/journal.pone.0088308

SS, LTB and SKK performed experiments, sampling, analysis and evaluation of the data.

KGS idea for the experiment.

SS wrote the manuscript with suggestions from co-authors.

Chapter II

Sett, S., Schulz, K.G., Bach, L.T., and Riebesell, U. *Shift from smaller to larger diatoms during a natural phytoplankton bloom under combined high CO₂ and warming conditions*. **To be submitted**.

SS performed experiments, sampling, analysis and evaluation of the data.

SS idea for the experiment with suggestions from KGS and LTB.

SS wrote the manuscript with suggestions from co-authors.

Chapter III

Sett, S., Annane, S., Ferreyra, G., Vidussi, F., Mostajir, B., Cantoni, C., Luchetta, A., and Riebesell, U. *Particulate and dissolved organic matter dynamics during a nutrient-induced phytoplankton bloom under ocean acidification and warming scenarios*. **To be submitted**.

SS performed sampling, analysis and evaluation of the data for POM and DOM.

SA, CC, AL, FV provided data sets for nutrients, carbonate chemistry and TEP.

FV, BM idea for the experiment.

SS wrote the manuscript.

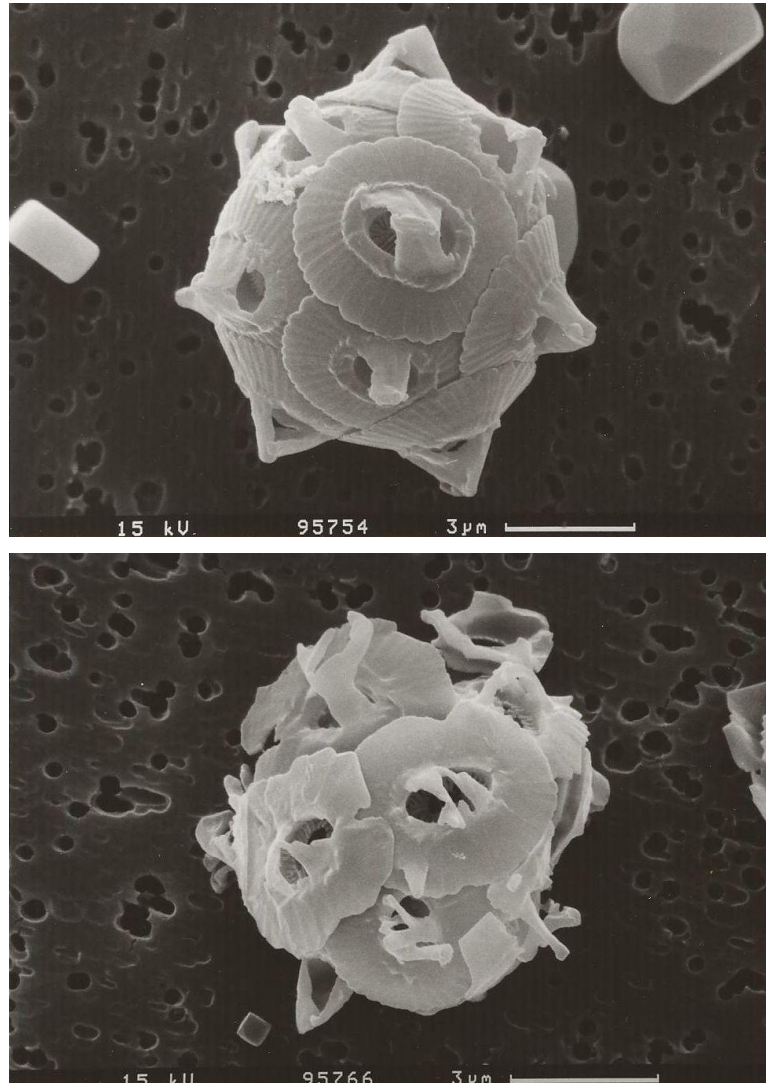
Co-author publications

Barcelos e Ramos, J., Schulz, K.G., Brownlee, C., **Sett, S.**, Azevedo, E.B. (2014) *Effects of increasing seawater carbon dioxide concentrations on chain formation of the diatom Asterionellopsis glacialis*. PLoS ONE 9(3): e90749. doi:10.1371/journal.pone.0090749

Müller, M. N., Lebrato, M., Riebesell, U., Barcelos e Ramos, J., Schulz, K. G., Blanco-Ameijeiras, S., **Sett, S.**, Eisenhauer, A., and Stoll, H. M. (2014) *Influence of temperature and CO₂ on the strontium and magnesium composition of coccolithophore calcite*. Biogeosciences 11, 1065-1075. doi:10.5194/bg-11-1065-2014, 2014.

Bach, L., Riebesell, U., **Sett, S.**, Febiri, S., Rzepka, P. and Schulz, K. G. (2012) *An approach for particle sinking velocity measurements in the 3–400 µm size range and considerations on the effect of temperature on sinking rates*. Marine Biology, 159 (8). pp. 1853-1864. DOI 10.1007/s00227-012-1945-2.

Blanco-Ameijeiras, S., Lebrato, M., Stoll, H. M., Iglesias-Rodriguez, M. D., Mendez-Vicente, A., **Sett, S.**, Müller, M. N., Oschlies, A. and Schulz, K. (2012) *Removal of organic magnesium in coccolithophore carbonates*. Geochimica et Cosmochimica Acta, 89 . pp. 226-239. DOI 10.1016/j.gca.2012.04.043.



Scanning electron microscope pictures of *G. oceanica* under present $p\text{CO}_2$ (top) and projected 2100 $p\text{CO}_2$ levels (bottom)

It is an alarming thought that human interference with the global carbon cycle could put at risk *E. huxleyi* and its relatives in the oceanic coccolithophorid communities. This scenario bears little resemblance to conditions in the Cretaceous and early Tertiary, when CO_2 levels two to six times higher than present (Berner 1990) did not prevent coccolithophorids from flourishing.

E. Paasche

Temperature Modulates Coccolithophorid Sensitivity of Growth, Photosynthesis and Calcification to Increasing Seawater $p\text{CO}_2$

Scarlett Sett^{1*}, Lennart T. Bach¹, Kai G. Schulz^{1,2}, Signe Koch-Klavnsen¹, Mario Lebrato¹, Ulf Riebesell¹

1 Biological Oceanography, GEOMAR Helmholtz Centre for Ocean Research Kiel, Kiel, Germany, **2** Centre for Coastal Biogeochemistry, School of Environmental Science and Management, Southern Cross University, Lismore, Australia

Abstract

Increasing atmospheric CO_2 concentrations are expected to impact pelagic ecosystem functioning in the near future by driving ocean warming and acidification. While numerous studies have investigated impacts of rising temperature and seawater acidification on planktonic organisms separately, little is presently known on their combined effects. To test for possible synergistic effects we exposed two coccolithophore species, *Emiliana huxleyi* and *Gephyrocapsa oceanica*, to a CO_2 gradient ranging from $\sim 0.5\text{--}250 \mu\text{mol kg}^{-1}$ (i.e. $\sim 20\text{--}6000 \mu\text{atm } p\text{CO}_2$) at three different temperatures (i.e. 10, 15, 20°C for *E. huxleyi* and 15, 20, 25°C for *G. oceanica*). Both species showed CO_2 -dependent optimum-curve responses for growth, photosynthesis and calcification rates at all temperatures. Increased temperature generally enhanced growth and production rates and modified sensitivities of metabolic processes to increasing CO_2 . CO_2 optimum concentrations for growth, calcification, and organic carbon fixation rates were only marginally influenced from low to intermediate temperatures. However, there was a clear optimum shift towards higher CO_2 concentrations from intermediate to high temperatures in both species. Our results demonstrate that the CO_2 concentration where optimum growth, calcification and carbon fixation rates occur is modulated by temperature. Thus, the response of a coccolithophore strain to ocean acidification at a given temperature can be negative, neutral or positive depending on that strain's temperature optimum. This emphasizes that the cellular responses of coccolithophores to ocean acidification can only be judged accurately when interpreted in the proper eco-physiological context of a given strain or species. Addressing the synergistic effects of changing carbonate chemistry and temperature is an essential step when assessing the success of coccolithophores in the future ocean.

Citation: Sett S, Bach LT, Schulz KG, Koch-Klavnsen S, Lebrato M, et al. (2014) Temperature Modulates Coccolithophorid Sensitivity of Growth, Photosynthesis and Calcification to Increasing Seawater $p\text{CO}_2$. PLoS ONE 9(2): e88308. doi:10.1371/journal.pone.0088308

Editor: Vengatesen Thiagarajan (Rajan), University of Hong Kong, Hong Kong

Received: August 20, 2013; **Accepted:** January 6, 2014; **Published:** February 5, 2014

Copyright: © 2014 Sett et al. This is an open-access article distributed under the terms of the Creative Commons Attribution License, which permits unrestricted use, distribution, and reproduction in any medium, provided the original author and source are credited.

Funding: The work was funded by the European project Network of leading MESOCOSMS facilities to advance the studies of future AQUATIC ecosystems from the Arctic to the Mediterranean (MESOAQUA, subproject 7) and the German Federal Ministry of Education and Research in the framework of the Biological Impacts of Ocean Acidification (BIOACID, subproject 3.1.1). The funders had no role in study design, data collection and analysis, decision to publish, or preparation of the manuscript.

Competing Interests: The authors have declared that no competing interests exist.

* E-mail: ssett@geomar.de

Introduction

Rapidly increasing fossil fuel emissions and deforestation over the past 250 years have increased atmospheric CO_2 concentrations at an unprecedented pace and caused a rise in global average temperatures as well as changes in ocean carbonate chemistry [1,2]. Presently, the ocean takes up more than 1/4 of the anthropogenic CO_2 emissions, thereby mitigating global warming but changing the ocean's carbonate chemistry equilibrium towards a decrease in carbonate ions [CO_3^{2-}] and pH (i.e. ocean acidification, OA) [2,3] and an increase in bicarbonate ions [HCO_3^-] and [CO_2] (i.e. ocean carbonation). Despite the massive sequestration of anthropogenic CO_2 in the oceans, global warming will still most likely result in an average temperature increase between 1 and 6°C by the end of this century [1]. Ocean warming is expected to influence metabolic rates of marine organisms with unforeseen consequences for marine biogeochemical cycling and ecosystem functioning [4][5].

Coccolithophores are single-celled autotrophic phytoplankton capable to precipitate calcium carbonate (CaCO_3) as small scales (coccoliths) to cover the organic part of the cell. They are considered the most important calcareous primary producers contributing $\sim 1\text{--}10\%$ to today's oceanic primary production [6] and $\sim 50\%$ to CaCO_3 found in pelagic sediments [7]. Hence, they are key players in marine biogeochemical cycles [8,9]. The most important bloom-forming coccolithophore species are *Emiliana huxleyi* [10,11,12] and *Gephyrocapsa oceanica* [13]. Both species have the ability to produce extensive blooms which are detectable from space [14–18]. In modern oceans, *E. huxleyi* is the most abundant species [19], but its contribution to CaCO_3 sedimentation is relatively small owing to its low coccolith weight [20]. *G. oceanica* is generally less abundant than *E. huxleyi* but its contribution to CaCO_3 export into the deep is larger because its coccoliths contain significantly more CaCO_3 [21].

During the last 15 years, coccolithophores have gained considerable attention due to the sensitivity of calcification to changing seawater $p\text{CO}_2$ [22]. To date, experiments investigating

the effects of OA on coccolithophores have shown diverse and sometimes contradictory results (for a review see [23–25]). Nevertheless, the majority of studies show calcification rates to generally decrease in response to OA while growth and carbon fixation rates had less clear trends. Factors potentially responsible for the discrepancies observed have been hypothesized to be related to different culturing conditions, such as temperature and light availability [23,24,26–30] and strain-specific responses [23,31]. Thus, key uncertainties remain on the synergistic effects, and most importantly the understanding of underlying physiological mechanisms, of CO₂ and other environmental factors on coccolithophore physiology. The main goal of our experiments is to understand whether increasing temperature can systematically induce changes in the carbonate chemistry sensitivity of growth, calcification and organic carbon fixation rates of *E. huxleyi* and *G. oceanica*.

Materials and Methods

Experimental set-up

Six experiments are presented in this study with generally similar design. Differences in experimental set-up were restricted to growth temperatures. Monospecific cultures of the coccolithophores *E. huxleyi* (strain PML B92/11 isolated from Bergen, Norway) and *G. oceanica* (strain RCC 1303 isolated from Arcachon Bay, France) were grown in dilute batch cultures [32] in a broad CO₂ gradient (see carbonate chemistry) at three different temperature regimes. The temperature range for each strain was chosen according to its specific biogeographical distribution: 10, 15 and 20°C for *E. huxleyi* [33] and 15, 20 and 25°C for *G. oceanica* [34]. Temperatures will be referred from now on as: “low”, “intermediate” and “high”, respectively. Note that data points for the 15°C experiment with *E. huxleyi* were taken from the constant total alkalinity experiments on Bach et al. 2011 [28]. Cultures were incubated in a thermo constant (+/-0.05°C) climate chamber (RUMED Rubarth Apparate GmbH) at a light:dark cycle of 16:8 and photosynthetic active radiation (PAR) of 150 μmol m⁻² s⁻¹. Cells were pre-acclimated to experimental conditions for at least 7 generations which varied between 5–15 days depending on cell division rate. Initial cell densities varied between 50–600 cells ml⁻¹ depending on treatment. The treatments with the highest cell densities were those at either extremes of the CO₂ range since those had the lowest growth rates. Final cell densities in the main experiments did not exceed 30,000 cells ml⁻¹, minimizing dissolved inorganic carbon drawdown to less than 8% and preventing major changes in the carbonate chemistry speciation [32].

Growth medium

All cultures were grown in artificial seawater (ASW) prepared as described in Kester et al. 1967 [35] but initially without the addition of sodium carbonate (see below carbonate chemistry). ASW was enriched with 64 μmol kg⁻¹ nitrate, 4 μmol kg⁻¹ phosphate, trace metals and vitamins (according to f/4 Guillard and Ryther 1962 [36]), 10 nmol kg⁻¹ selenium, 2 ml kg⁻¹ of 0.2 μm filtered North Sea water.

The nutrient enriched ASW solution (free of dissolved inorganic carbon, DIC, and total alkalinity, TA) was sterile filtered through a 0.2 μm nylon membrane (Whatman® Polycap™ 75 AS) directly into acclimation (0.5 L Nalgene™) or experimental bottles (2 L Nalgene™) leaving only minimal headspace.

Carbonate chemistry

Carbonate chemistry parameters, TA and DIC, were added to the culture medium by calculated additions of hydrochloric acid (certified HCl with a concentration of 3.571 mol L⁻¹, Merck) and Na₂CO₃ (Merck, Suprapur quality and dried for 2 hours at 500°C). This resulted in a DIC gradient of ~1300–2300 μmol kg⁻¹ at constant TA, ~2325±40 μmol kg⁻¹. Samples for TA were taken at the beginning and end of the experiment, respectively. TA samples were filtered through GF/F filters, stored at 4°C and processed within 14 days. Otherwise samples were poisoned with HgCl₂. TA samples were measured in a Metrohm Basic Titrimo 794 titration device according to Dickson et al. 2003 [37].

Unfortunately, DIC samples were lost due to storing problems and had to be estimated from TA and acid additions as described in Bach et al. 2011 [28]. Briefly, initial DIC concentrations (DIC_{initial}) were estimated as:

$$\text{DIC}_{\text{initial}} = \frac{\text{TA} + (\text{Volume}_{\text{acid}} * 3.571)}{2} \quad (1)$$

where TA refers to the measured initial total alkalinity (μmol kg⁻¹) and Volume_{acid} refers to the amount of acid added (μl kg⁻¹) and 3.571 being the molarity of the acid (μmol μl⁻¹). The accuracy of this method is explained in detail in Bach et al. 2011 [28] and shows that the maximum offset of ~30 μmol kg⁻¹ between DIC calculated with equation 1 and DIC calculated from measured TA and pH is small relative to the large DIC ranges (~1300–2600 μmol kg⁻¹). Final DIC concentrations were calculated by subtracting the measured total particulate carbon build-up from DIC_{initial} calculated with equation 1, assuming that the potential error from dissolved organic matter production is small compared to the broad ranges in DIC concentrations [28]. Carbonate chemistry parameters (pH, HCO₃⁻, CO₃²⁻, CO₂) were calculated using the program CO2SYS (Lewis and Wallace 1998 [38]) from measured TA, estimated DIC, temperature, salinity and [PO₄³⁻], and the dissociation constants determined by Roy et al. 1993. pH values are given on the free scale. Note that horizontal error bars on all figures denote for the change of CO₂ concentrations during the course of the experiments and that biological response data is plotted against the average of initial and final [CO₂]. The degree of change in carbonate chemistry conditions from beginning to end of the experiment depended on final cell densities. In some cases, final cell densities were not high and changes in carbonate chemistry were so small that they appear absent in Figure 1.

Particulate organic and inorganic carbon

Sampling started two hours after the onset of the light period and lasted no longer than 2 hours. Samples for particulate carbon were filtered (200 mbar) onto GF/F filters (Whatmann, combusted at 500°C for 6 hours) and stored in glass petri-dishes (pre-combusted at 500°C for 6 hours) at -20°C until analysis. Filters for total particulate carbon (TPC) were dried overnight at 60°C while filters for particulate organic carbon (POC) were first placed in a desiccator above fuming (37%) HCl for 2 hours to remove all inorganic particulate carbon (PIC) and subsequently dried overnight at 60°C. Both TPC and POC samples were analyzed with a EuroEA analyzer according to Sharp 1974 [39] except for experiments with *E. huxleyi* at 15°C and *G. oceanica* at 25°C, for which TPC and POC were measured with an Elemental analyzer coupled to an isotope ratio mass spectrometer (EuroEA, Hekatech GmbH). Both methods use the same analysis but the latter is coupled to an isotope mass spectrometer which gives additional

Chapter I

Temperature Changes Sensitivity to Increasing $p\text{CO}_2$

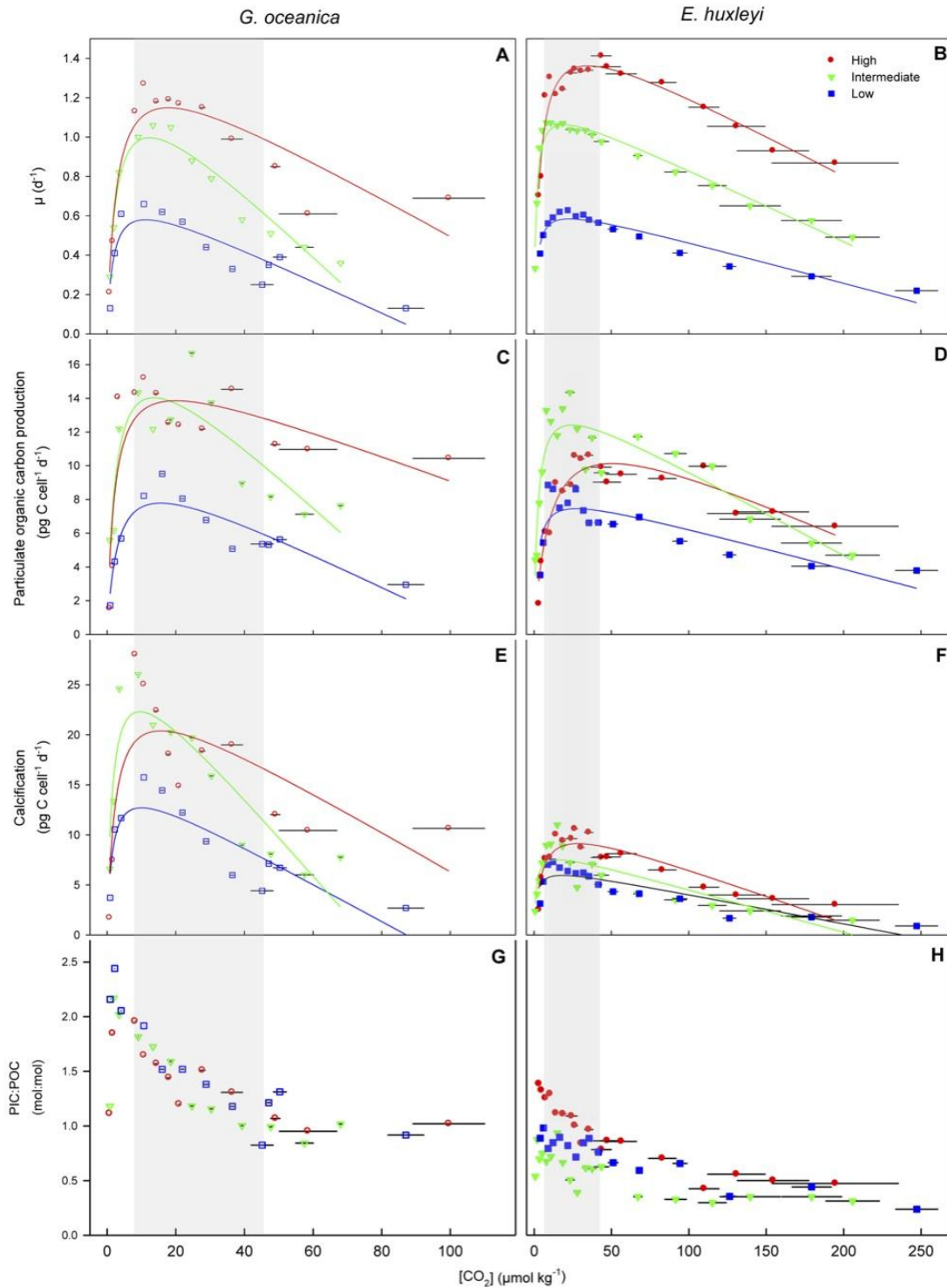


Figure 1. Physiological response of *G. oceanica* and *E. huxleyi* to increasing CO₂ and temperature. Response of growth, POC production, calcification rates and PIC:POC to increasing CO₂ and temperature of *G. oceanica* (left, open symbols) and *E. huxleyi* (right, closed symbols). Horizontal bars indicate change of CO₂ from beginning to end of experiment. In some cases the changes were small and thus appear absent. Shaded areas represent OA relevant ranges (~280–1000 μatm pCO₂). Note that the investigated CO₂ range (x-axis) is only half as broad for experiments with *G. oceanica* compared to the one of *E. huxleyi*. doi:10.1371/journal.pone.0088308.g001

information on isotopic composition, if desired. PIC was calculated by subtracting POC from TPC.

Growth

Cell densities were determined at the beginning and end of the experiment with a Beckman Z2 Coulter® Particle Count and Size Analyzer. Growth rates (μ) were calculated according to:

$$\mu = \frac{\ln(C_{t-final}) - \ln(C_{t_0})}{d} \quad (2)$$

where C_{t-final} represents cell densities at the end of the experiment, C_{t₀} represents initial cell densities and d represents the number of days between t₀ and t_{final}. Calcification and POC production rates were obtained by multiplying growth rates with particulate inorganic or organic carbon cellular quotas, respectively.

Statistics

A nonlinear regression model was used to analyze the data, with a higher number of treatment levels at the expense of replication. This approach is more informative for ecological modelling than the analysis of variance (ANOVA), nevertheless without the loss of statistical power [40]. The Michaelis-Menten kinetics can be used to describe the increase of growth and organic and inorganic carbon production with increasing CO₂ concentrations levelling off at saturating conditions:

$$V = \frac{V_{max} * CO_2}{K_m + CO_2} \quad (3)$$

where V is the growth or production rate at a certain CO₂ concentration, V_{max} is the maximum growth or production rate and K_m is the CO₂ concentration at which the rate is half-saturated. In our experiments growth and production rates decreased after reaching maximum values and thus a linear term was subtracted from equation 3 and the Michaelis-Menten equation modified as follow:

$$V = \frac{X * CO_2}{Y + CO_2} - s * CO_2 \quad (4)$$

where X and Y are random fit parameters and s the 'sensitivity' constant which describes the linear negative effect of increasing CO₂ (decreasing pH) [28]. From the differentiated fit equation (explained in detail in [28]) we calculated optimum CO₂ concentrations for growth, photosynthesis and calcification rates as well as maximum production rates (V_{max}) and half saturation constants (K_m). Coefficients of determination (R²), p-values, F-values and degrees of freedom for each fit are presented in Table 1 and 2. In the following sections optimum and maximum production rates refer to those calculated from the fit equation. Note that in some cases the highest measured values deviated from those determined using the fit equation. The first derivative of eq. 4 was calculated to detect temperature-dependent changes in calcification at specific [CO₂] as follow:

$$f' CO_2 = \frac{X * Y}{(CO_2 + Y)^2} - s \quad (5)$$

a positive value of the first derivative (i.e. a positive slope of a tangent at certain [CO₂]) indicates that there is a positive correlation between increasing CO₂ and the investigated metabolic process while a negative value indicates the opposite. We calculated our values at [CO₂] of 18 μmol kg⁻¹, approximately 375–575 μatm pCO₂, depending on temperature, and thus were able to compare the different temperature-dependent response at the same CO₂ concentration.

Results

The coccolithophores *E. huxleyi* and *G. oceanica* were incubated in a broad CO₂ gradient and three different temperatures. All investigated metabolic processes in both species displayed an optimum-curve response pattern along the CO₂ gradient. However, temperature clearly modified the shape of this response (Figure 1).

Optimum CO₂ concentrations, V_{max} and K_m for growth, photosynthetic carbon fixation and calcification rates were assessed with fit equation (4). Resulting V_{max}, K_m and pCO₂/CO₂ optima as well as statistical results (coefficients of determination (R²), p-values, F values and degrees of freedom) are presented in Table 1 and 2. The underlying carbonate chemistry is presented in the supplement Tables S1–S2 and shows the average values from initial and final calculated CO₂, pCO₂, DIC, pH_{free} and ΩCa. Physiological responses (i.e. growth, POC production, calcification rates and PIC:POC ratios) are also given in supporting information Table S1–S2.

Growth rates (μ)

Increasing temperature stimulated growth rates of *E. huxleyi* and *G. oceanica* (Figure 1A–B). Approximately a doubling in maximum growth rates was observed in both species between the lowest and highest temperature tested (Figure 1A–B, Table 1–2). The CO₂ half-saturation for growth slightly but constantly increased in *G. oceanica* throughout the investigated temperature range (Table 1). In *E. huxleyi*, CO₂ half-saturation slightly decreased from low to intermediate temperatures but increased strongly from intermediate to high temperature (Table 2). Optimum growth for *G. oceanica* was observed at [CO₂] of ~11–13 μmol kg⁻¹ (~300–400 μatm pCO₂) at low and intermediate temperature and ~18 μmol kg⁻¹ (~600 μatm pCO₂) at high temperature (Table 1). Optima for *E. huxleyi* was observed at [CO₂] of ~19–23 μmol kg⁻¹ (~520–620 μatm pCO₂) at low and intermediate temperature and ~35 μmol kg⁻¹ (~1300 μatm pCO₂) at high temperature (Table 2).

POC production

POC production was stimulated from low to intermediate temperatures in both species (Figure 1C–D). The highest temperature did not enhance POC production in *G. oceanica* (Figure 1C) and reduced the rate in *E. huxleyi* (Figure 1D). CO₂ half-saturation showed no clear trend in *G. oceanica* throughout the

Table 1. Parameters from fit equation (4) for *G. oceanica*.

G.oceanica			
Seasonal $T_{\min} = 7^\circ\text{C}$; seasonal $T_{\max} = 27^\circ\text{C}$ [34]	Low	Intermediate	High
CO_2 optima ($\mu\text{mol kg}^{-1}$)	15°C	20°C	25°C
growth rate	11.3	12.4	17.8
POC production	15.6	13.6	20.0
calcification	10.1	9.6	15.6
$p\text{CO}_2$ optima (μatm)			
growth rate	305	403	609
POC production	421	420	835
calcification	269	295	555
V_{\max}			
growth rate (d^{-1})	0.6	1.0	1.1
POC production ($\text{pg C cell}^{-1}\text{d}^{-1}$)	7.8	14.0	13.9
calcification ($\text{pg C cell}^{-1}\text{d}^{-1}$)	12.7	22.3	20.4
K_m ($\mu\text{mol kg}^{-1}$)			
growth rate	1.1	1.4	1.7
POC production	1.8	1.5	1.6
calcification	1.0	1.0	1.5
R^2 (p-value)			
growth rate	0.74 (0.0009)	0.92 (<0.0001)	0.83 (0.0001)
POC production	0.81 (0.0002)	0.70 (0.0018)	0.69 (0.0012)
calcification	0.69 (0.0021)	0.77 (0.0006)	0.58 (0.0081)
F value (degrees of freedom)			
growth rate	16.7 (11)	69.1 (11)	27.7 (11)
POC production	24.7 (11)	13.8 (11)	14.1 (12)
calcification	13.3 (11)	19.1 (11)	8.6 (11)
sensitivity constant			
growth rate	0.008	0.017	0.010
POC production	0.100	0.191	0.076
calcification	0.189	0.398	0.203

doi:10.1371/journal.pone.0088308.t001

entire temperature range (Table 1) while the half-saturation remained unaffected in *E. huxleyi* from low to intermediate temperature but strongly increased at high temperature (Table 2). Optimum CO_2 concentrations for POC production rates in *G. oceanica* were observed at $\sim 13\text{--}16 \mu\text{mol kg}^{-1}$ ($\sim 420 \mu\text{atm } p\text{CO}_2$) at low and intermediate temperature and $\sim 20 \mu\text{mol kg}^{-1}$ ($\sim 835 \mu\text{atm } p\text{CO}_2$) at high temperature (Table 1). The CO_2 optima for *E. huxleyi* were found at $\sim 24\text{--}28 \mu\text{mol kg}^{-1}$ ($\sim 600\text{--}650 \mu\text{atm } p\text{CO}_2$) at low and intermediate temperature and $50 \mu\text{mol kg}^{-1}$ ($\sim 1535 \mu\text{atm } p\text{CO}_2$) at high temperature (Table 2).

Calcification rates

Maximum calcification rates increased in *G. oceanica* from low to intermediate temperature but did not accelerate any further at high temperature levels (Figure 1E, Table 1). In *E. huxleyi*, maximum calcification rates increased steadily over the investigated temperature range (Figure 1F). The CO_2 half-saturation showed in both species very little change from low to intermediate temperatures but increased substantially from intermediate to high temperature (Table 1–2). Optimum calcification rates for *G. oceanica* were observed at $[\text{CO}_2]$ of $\sim 10 \mu\text{mol kg}^{-1}$ ($\sim 260\text{--}300 \mu\text{atm } p\text{CO}_2$) at low and intermediate temperature and at

$\sim 16 \mu\text{mol kg}^{-1}$ ($\sim 550 \mu\text{atm } p\text{CO}_2$) at the highest temperature (Table 1). For *E. huxleyi* optimum calcification rates were observed at $[\text{CO}_2]$ of $\sim 15\text{--}18 \mu\text{mol kg}^{-1}$ ($\sim 400 \mu\text{atm } p\text{CO}_2$) at low and intermediate temperature and at $\sim 30 \mu\text{mol kg}^{-1}$ ($\sim 875 \mu\text{atm } p\text{CO}_2$) at the highest temperature (Table 2).

Increasing temperature did not modulate the effect of increasing CO_2 on the PIC:POC ratio (Figure 1G–H). The PIC:POC ratio was temperature-independent in *G. oceanica* and linearly decreased with increasing CO_2 (Figure 1G). *G. oceanica* had a large fraction of the assimilated particulate carbon as inorganic carbon (calcite) which was then reflected in the higher PIC:POC compared to *E. huxleyi* (Figure 1G–H). Although no clear trends could be observed for *E. huxleyi*, the highest PIC:POC were found at the highest temperature while lowest ratios were observed at intermediate temperature and linearly decreased with a possible stabilization at $[\text{CO}_2]$ levels $> 100 \mu\text{mol kg}^{-1}$ (Figure 1H).

Discussion

Ocean acidification and warming are two ongoing processes potentially affecting marine phytoplankton - in particular calcifying species [5]. Here, we investigated how temperature modulates

Table 2. Parameters from fit equation (4) for *E. huxleyi*.

E.huxleyi			
Seasonal $T_{\min} = 2^\circ\text{C}$; seasonal $T_{\max} = 16^\circ\text{C}$ [33]	Low	Intermediate	High
CO_2 optima ($\mu\text{mol kg}^{-1}$)	10°C	15°C	20°C
growth rate	22.6	19.3	34.9
POC production	27.3	24.5	50.6
calcification	18.1	15.4	28.4
$p\text{CO}_2$ optima (μatm)			
growth rate	519	622	1295
POC production	612	656	1535
calcification	412	414	875
V_{\max}			
growth rate (d^{-1})	0.6	1.1	1.4
POC production ($\text{pg C cell}^{-1}\text{d}^{-1}$)	7.5	12.4	10.1
calcification ($\text{pg C cell}^{-1}\text{d}^{-1}$)	5.9	7.5	9.1
K_m ($\mu\text{mol kg}^{-1}$)			
growth rate	1.4	1.0	2.6
POC production	1.8	1.8	5.9
calcification	1.2	1.0	3.0
R^2 (p-value)			
growth rate	0.90 (<0.0001)	0.95 (<0.0001)	0.90 (<0.0001)
POC production	0.58 (0.0013)	0.81 (<0.0001)	0.87 (<0.0001)
calcification	0.74 (<0.0001)	0.69 (<0.0001)	0.81 (<0.0001)
F value (degrees of freedom)			
growth rate	69.3 (15)	166.9 (18)	81.7 (17)
POC production	11.5 (15)	39.8 (18)	60.3 (17)
calcification	22.2 (15)	20.7 (18)	38.2 (17)
sensitivity constant			
growth rate	0.002	0.004	0.004
POC production	0.024	0.051	0.042
calcification	0.030	0.043	0.055

doi:10.1371/journal.pone.0088308.t002

the sensitivity of key metabolic processes (i.e. growth, photosynthesis and calcification) to increasing CO_2 in the two most abundant coccolithophores *E. huxleyi* and *G. oceanica*. Our experiments confirm that the optimum-curve response of growth, photosynthesis and calcification obtained for *E. huxleyi* over a broad CO_2 gradient [28] also holds under different temperature conditions. Likewise, this response pattern was also displayed by *G. oceanica* at all investigated temperatures.

Despite this similarity in the overall response pattern, the position of optima varied between temperature treatments. In most cases, optimum $[\text{CO}_2]$ where maximum rates were achieved was shifted towards higher CO_2 concentrations with increasing temperature. This underlines the importance of temperature not only in determining absolute growth and production rates but also in systematically modulating sensitivities of these metabolic processes to changing seawater carbonate chemistry speciation.

Additionally, we observed species-specific sensitivities to increasing CO_2 of *E. huxleyi* and *G. oceanica*, as previously pointed out by Riebesell et al. 2000 [22] and Zondervan et al. 2001 [41]. Optimum CO_2 levels for calcification rates were remarkably lower

than those for organic carbon fixation rates in both species (Tables 1–2). However, *G. oceanica* had a narrower CO_2 tolerance range (compare x-axis in Figure 1) and thus the sensitivity constants obtained from the fit equation (4) were about four times higher than in *E. huxleyi* at similar overall rates (compare “sensitivity constant” Tables 1 and 2). Interestingly, sensitivity constants for calcification were about twice as high as those for organic carbon fixation, suggesting that the former process is more susceptible to changes in carbonate chemistry in the high CO_2 range (Table 1). Potentially, *G. oceanica* is more representative of larger coccolithophore species with higher calcification than carbon fixation rates such as *C. leptoporus* and *C. braarudii* [42,43]. For instance, *C. braarudii* stopped calcifying at levels higher than $\sim 80 \mu\text{mol kg}^{-1} \text{CO}_2$ (approx. 2380 $\mu\text{atm } p\text{CO}_2$ [43]) while *C. leptoporus* had an optimum curve response in an even narrower range of $\sim 4\text{--}35 \mu\text{mol kg}^{-1} \text{CO}_2$ (approx. 180–1000 $\mu\text{atm } p\text{CO}_2$ [42]) suggesting that higher CO_2 concentrations (most likely concomitantly lower pH) would be more detrimental to highly calcifying strains compared to those with PIC:POC ratios closer to 1 (i.e. *E. huxleyi*).

Both coccolithophores show highest metabolic activity at temperatures significantly higher than experienced at isolation site

Stimulating effects of increasing temperature have been widely observed in phytoplankton through accelerating metabolic activities [44–46]. In accordance with this, we observed a pronounced acceleration of growth in both species within the investigated temperature range (Figure 1A–B). Maximum growth rates doubled for each 10°C increase, closely matching values reported in the literature for these two species between 6 and 25°C [13,31,47–49]. Interestingly, each species had highest growth rates at temperatures $5\text{--}10^\circ\text{C}$ higher than the maxima observed at their isolation sites when they are the most abundant (Table 1–2 [33,34]). Conte et al. 1998 [47] also observed that an *E. huxleyi* strain had the highest growth rates at temperatures 10°C above those occurring at the strain's natural environment. This could have several implications. Either their biogeographic distribution is relatively broad and both coccolithophore strains tested here occur in large areas which include locations with significantly higher maximum seasonal temperatures or both strains have physiological flexibility which allows them to exploit high temperature anomalies. Both of which, based on the assumption that the strain has optimized its temperature response to its specific environment. The biogeographic distribution and local temperature adaptation of coccolithophores has not been studied in great detail but recent evidence points towards a certain degree of isolation between coccolithophore populations [50,51]. However, there appears to be a strong link between the local environment and the thermal tolerance of marine phytoplankton in the global ocean. Thomas et al. 2012 [52] showed that phytoplankton from polar and temperate regions had optimum growth at temperatures above the annual mean of their region and wider thermal tolerance curves while tropical phytoplankton had their optimum growth below (or at) their annual mean with narrower thermal tolerance curves. They suggested that phytoplankton in the tropics might have a greater risk to future warming scenarios due to their narrow thermal tolerance sensitivities. Nevertheless, for temperate and polar species, being able to exploit high temperature anomalies may be an ecological advantage, in particular for *E. huxleyi* which often blooms during early summer in highly stratified shallow mixed layers [53]. This could have been the case when a large *E. huxleyi* bloom occurred in the Bering Sea in 1997, a year characterized with a particularly shallow mixed layer depth, exceptionally high water temperatures ($\sim 4^\circ\text{C}$ above mean), and high irradiances [54]. Although the occurrence of such blooms was not observed regularly in this oceanic region, there was some indication that *E. huxleyi* progressively entered the region and benefited in this particular year from such climatic anomalies [55].

Rising temperature affects organic carbon fixation and calcification differently

Maximum growth rates increased consistently with increasing temperature in both species suggesting that overall metabolism is generally accelerated within these temperature ranges (Figure 1A–B; Table 1–2). Nevertheless, the temperature sensitivity of both species differed in terms of the maximum organic and inorganic carbon fixation rates. In *G. oceanica*, maximum organic carbon fixation increased strongly from low to intermediate temperature but showed little change thereafter (Figure 1C; Table 1). Maximum calcification rates showed a similar trend from low to intermediate temperatures but even slightly decreased towards the highest investigated temperature (Figure 1E; Table 1). In *E. huxleyi*, maximum organic carbon fixation nearly doubled from low to

intermediate temperature but decreased thereafter, while maximum calcification rates increased linearly over the entire temperature range (Figure 1D, F; Table 2).

The importance of temperature for modulating resource allocation in marine phytoplankton was recently pointed out by Toseland et al. 2013 [56]. Results from their pair-wise gene ontology analysis, as well as their model for optimal resource allocation, indicated that at low temperatures (i.e. temperate and polar regions) cells would preferentially allocate resources into biosynthesis rather than photosynthesis leading to higher allocation of P into rich rRNA and a subsequent decrease of the N:P stoichiometry. Antagonistically, at warmer temperatures resource allocation would preferentially go into photosynthesis and thus higher N:P ratios.

In our experiments, a re-distribution of inorganic carbon among requiring pathways (i.e. photosynthesis and/or calcification) could have occurred. This becomes particularly apparent in *E. huxleyi* at the high temperature treatment (i.e. 20°C) where maximum POC fixation rate clearly has a lower temperature optimum than calcification rate (compare Figure 1D and F; Table 2). Whereas total particulate carbon was similar between the high and intermediate temperature treatments, a high PIC:POC suggested that inorganic carbon was incorporated towards calcification rather than photosynthesis at the high temperature treatment (Figure 1H). Indeed, it was recently postulated that changes in carbonate chemistry affect the redox state inside *E. huxleyi* cells which subsequently causes a reorganization of carbon flux networks within and across cellular compartments (e.g. cytosol, chloroplast and calcification vesicle) [57]. Increasing $p\text{CO}_2$, for example, diverted inorganic carbon away from calcification into pathways involved in the production of organic carbon [30,57].

In this respect it is worth noting that cellular PIC:POC in coccolithophores is a measure for carbon allocation to photosynthesis and calcification and cannot be used to infer potential feedbacks to atmospheric carbon dioxide levels. The latter is ultimately affected by the PIC:POC of export production and while about half of pelagic PIC stems from coccolithophores most of the POC is contributed by other phytoplankton groups such as diatoms. Therefore, it is the changes in the absolute amount of PIC produced by coccolithophores and not in cellular PIC:POC which need to be considered for global biogeochemical element cycling.

Changing temperature shifts the optimum CO_2 concentration for growth, photosynthesis and calcification

CO_2 optima for growth, organic carbon fixation and calcification rates shifted towards higher CO_2 concentrations from intermediate to high temperatures in both coccolithophores examined in this study (Table 1–2). The temperature-induced optimum shift in *E. huxleyi* was even strong enough to reverse the response of calcification rates within the ocean acidification relevant range (i.e. $\sim 7\text{--}45\ \mu\text{mol kg}^{-1}\ \text{CO}_2$, approx. 280–1000 $\mu\text{atm}\ p\text{CO}_2$) from negative at low and intermediate temperatures to positive at high temperature (Figure 2). Hence, a coccolithophore strain can respond to ocean acidification, with both, increasing and decreasing calcification rate, depending on the temperature it was cultured at. This has major implications when trying to compare the responses of different coccolithophore strains cultured at different experimental settings to increasing seawater CO_2 . To account for the modulating effect of temperature on the $\text{CO}_2/p\text{H}$ sensitivity, a direct comparison of species/strain specific responses should occur in the same range of their temperature optimum curves. Investigating the effect of ocean

Temperature Changes Sensitivity to Increasing $p\text{CO}_2$

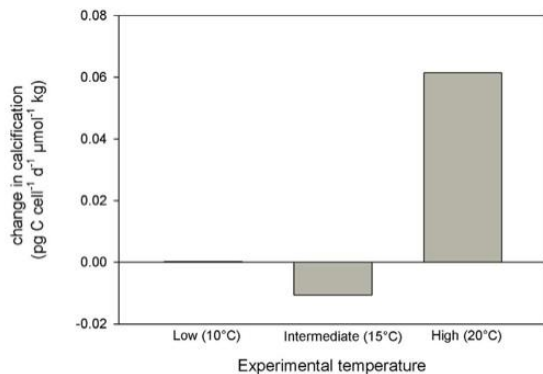


Figure 2. Calcification rate of *E. huxleyi* in response to elevated CO_2 at different temperatures. Depending on the growth temperature the rate of calcification can decrease strongly or moderately or even increase with rising CO_2 levels. The “low”, “intermediate” and “high” refers to experimental temperature of 10, 15 and 20°C, respectively. The slope of a tangent at $[\text{CO}_2]$ of $18 \mu\text{mol kg}^{-1}$ in the 10°C treatment of *E. huxleyi* is almost 0 which means that the optimum curve has reached a plateau in the OA relevant CO_2 range. At 20°C there is a positive slope which means that cells have not yet reached the optimum CO_2 for calcification at $18 \mu\text{mol kg}^{-1}$ in this temperature.
doi:10.1371/journal.pone.0088308.g002

acidification on metabolic processes in coccolithophores therefore requires a sound understanding of the influence of experimental culture conditions (in this study temperature conditions but the same probably also applies to other parameters such as light [30]). If this understanding is missing, then interpretation of the response of coccolithophores to future ocean $p\text{CO}_2$ from laboratory incubations can be misleading because all responses (increase, plateau, decrease) within the OA-relevant $p\text{CO}_2$ range can be attained when growing the investigated cells at certain culture conditions (Figure 3).

The reason for the observed CO_2 optimum shift for growth, organic carbon fixation and calcification at the highest temperature is presently unclear. Possibly the strongly accelerated metabolism at high temperatures, and concomitantly higher demand of inorganic carbon, benefits more from the increased CO_2 substrate availability than it is negatively affected by the increase in proton concentrations (low pH). Or in other words, the balance between a fertilizing effect of additional inorganic carbon and a metabolic repression by high proton concentration observed in previous studies [28,58] is apparently modulated by increasing temperature.

In our study, increasing temperature partly compensates the negative effect of increasing proton concentrations on calcification rates to some extent. However, Feng et al. 2008[59] and De Bodt et al. 2010 [60] found the opposite – i.e. a negative feedback of

References

1. Parry ML, Canziani OF, Palutikof JP, van der Linden PJ, Hanson CE (2007) Climate Change 2007: Impacts, Adaptation and Vulnerability. Contribution of Working Group II to the Fourth Assessment Report of the Intergovernmental Panel on Climate Change. J Environ Qual 37: 2407. doi: 10.2134/jeq2008.0015br.
2. Wolf-Gladrow DA, Riebesell U, Burkhardt S, Bijma J (1999) Direct effects of CO_2 concentration on growth and isotopic composition of marine plankton. Tellus 51B: 461–476.
3. Calderia K, Wickett ME (2003) Anthropogenic carbon and ocean pH. Nature 425: 365.

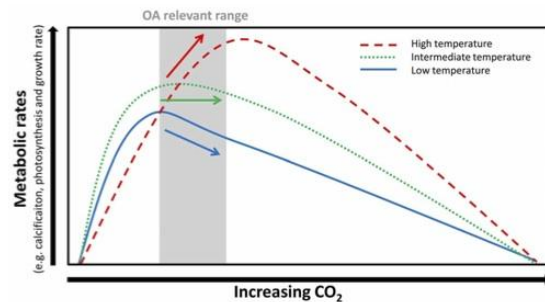


Figure 3. Conceptual graph depicting the modulating effect of temperature on the CO_2/pH sensitivity of key metabolic rates in coccolithophores. The arrows emphasize the trends of key metabolic processes (i.e. calcification, photosynthesis and growth) vs. CO_2 relationship in the range relevant to future ocean acidification.
doi:10.1371/journal.pone.0088308.g003

increasing temperature on calcification rates under high CO_2 conditions at very different temperature regimes (13 and 18°C and 20 and 24°C, respectively). This apparent contradiction can potentially be resolved when considering the diverse temperature sensitivities among strains [47,49]. In case increasing temperature stimulates the investigated strain (as in our study) a partial compensation of the negative influence of high proton concentrations seems to be likely. However, as soon as increasing temperature becomes a stress factor, excess proton concentrations may exacerbate the temperature effect. In the latter case, rising temperature and proton concentration could synergistically reduce metabolic rates in coccolithophores.

Supporting Information

Table S1 Carbonate chemistry and physiological parameters for *G. oceanica*. (PDF)

Table S2 Carbonate chemistry and physiological parameters for *E. huxleyi*. (PDF)

Acknowledgments

We thank Aljosa Zavisic and Kerstin Nachtigall for their support on particulate carbon measurements and Prof. Andreas Oschlies for valuable comments on the manuscript.

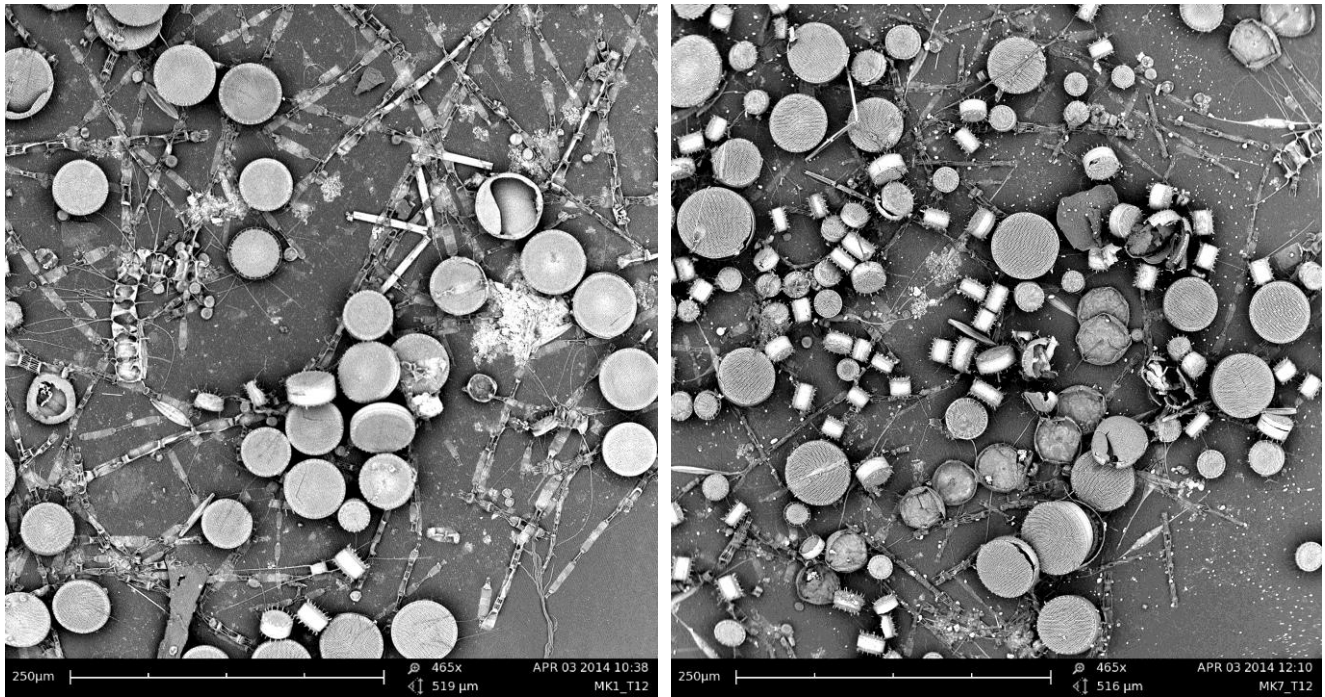
Author Contributions

Conceived and designed the experiments: KGS ML SS. Performed the experiments: SS LTB SKK. Analyzed the data: SS LTB SKK. Wrote the paper: SS KGS LTB SKK ML UR.

4. Taucher J, Oschlies A (2011) Can we predict the direction of marine primary production change under global warming?. Geophys Res Lett 38. doi: 10.1029/2010GL045934.
5. Riebesell U, Tortell P (2011) Effects of ocean acidification on pelagic organisms and ecosystems. Ocean Acidification. Oxford University Press. pp. 99–116.
6. Poulton AJ, Adey TR, Balch WM, Holligan PM (2007) Relating coccolithophore calcification rates to phytoplankton community dynamics: Regional differences and implications for carbon export. Deep Sea Res Part II 54: 538–557.
7. Broecker W, Clark E (2009) Ratio of coccolith CaCO_3 to foraminifera CaCO_3 in late Holocene deep sea sediments. Paleoceanography 24: PA3205. doi: 10.1029/2009PA001731.

8. Balch W, Drapeau D, Bowler B, Booth E (2007) Prediction of pelagic calcification rates using satellite measurements. *Deep Sea Res Part II* 54: 538–557.
9. Bollmann J, Klaas C (2008) Morphological variation of *Gephyrocapsa oceanica* Kamptner 1943 in plankton samples: implications for ecologic and taxonomic interpretations. *Protist* 159: 369–381.
10. Balch WM, Holligan PM, Kilpatrick KA (1992) Calcification, photosynthesis and growth of the bloom-forming coccolithophore, *Emiliania huxleyi*. *Cont Shelf Res* 12: 1353–1374.
11. Winter A, Jordan RW, Roth PH (1994) Biogeography of living coccolithophores in ocean waters. New York: Cambridge University Press.
12. Broerse T, Tyrrell T, Young J, Poulton A, Merico A (2003) The cause of bright waters in the Bering Sea in winter. *Cont Shelf Res* 23: 1579–1596.
13. Rhodes LL, Peake BM, Mackenzie AL, Marwick S (1995) Coccolithophores *Gephyrocapsa oceanica* and *Emiliania huxleyi* (Prymnesiophyceae = Haptophyceae) in New Zealand's coastal waters: characteristics of blooms and growth in laboratory culture. *New Zeal J Mar Fresh* 29: 345–357.
14. Holligan PM, Viollier M, Harboure DS, Camus P, Champagne-Philippe M (1983) Satellite and ship studies of coccolithophore production along a continental shelf edge. *Nature* 304: 339–342.
15. Holligan PM, Fernandez E, Balch WM, Boyd P, Peter H (1993) A biogeochemical study of the coccolithophore, *Emiliania huxleyi*, in the North Atlantic. *Global Biogeochem Cycles* 7: 879–900.
16. Groom SB, Holligan PM (1987) Remote sensing of coccolithophore blooms. *Adv Sp Res* 7: 73–78.
17. Balch M, Holligan PM, Ackleson SG, Voss KJ (1991) Biological and optical properties of mesoscale coccolithophore blooms in the Gulf of Maine. *Limnol Oceanogr* 36: 629–643.
18. Tyrrell T, Taylor AH (1996) A modelling study of *Emiliania huxleyi* in the NE Atlantic. *J Mar Syst* 9: 83–112.
19. Paasche E (2002) A review of the coccolithophorid *Emiliania huxleyi* (Prymnesiophyceae), with particular reference to growth, coccolith formation, and calcification-photosynthesis interactions. *Phycologia* 40: 503–529.
20. Baumann EA, Böckel B, Frenz M (2004) Coccolith contribution to South Atlantic carbonate sedimentation. Coccolithophores: from molecular processes to global impact. Springer. pp. 99–125.
21. Saavedra-Pellitero M, Flores JA, Baumann KH, Sierro FJ (2010) Coccolith distribution patterns in surface sediments of Equatorial and Southeastern Pacific Ocean. *Geobios* 43: 131–149.
22. Riebesell U, Zondervan I, Rost B, Tortell PD, Zeebe RE, et al. (2000) Reduced calcification of marine plankton in response to increased atmospheric CO₂. *Nature* 407: 364–367.
23. Ridgwell A, Schmidt DN, Turley C, Brownlee C, Maldonado MT, et al. (2009) From laboratory manipulations to Earth system models: scaling calcification impacts of ocean acidification. *Biogeosciences* 6: 2611–2623.
24. Hoppe CJM, Langer G, Rost B (2011) *Emiliania huxleyi* shows identical responses to elevated pCO₂ in TA and DIC manipulations. *J Exp Mar Bio Ecol* 406: 54–62.
25. Benner I, Diner RE, Lefebvre SC, Li D, Komada T, et al. (2013) *Emiliania huxleyi* increases calcification but not expression of calcification-related genes in long-term exposure to elevated temperature and pCO₂. *Philos Trans R Soc B* 368. doi: 10.1098/rstb.2013.0049.
26. Zondervan I (2007) The effects of light, macronutrients, trace metals and CO₂ on the production of calcium carbonate and organic carbon in coccolithophores—A review. *Deep Sea Res Part II* 54: 521–537.
27. Shi D, Xu Y, Morel FMM (2009) Effects of the pH/pCO₂ control method on medium chemistry and phytoplankton growth. *Biogeosciences* 6: 1199–1207.
28. Bach LT, Riebesell U, Schulz KG (2011) Distinguishing between the effects of ocean acidification and ocean carbonation in the coccolithophore *Emiliania huxleyi*. *Limnol Oceanogr* 56: 2040–2050.
29. Raven J, Crawford K (2012) Environmental controls on coccolithophore calcification. *Mar Ecol Prog Ser* 470: 137–166.
30. Rokitta SD, Rost B (2012) Effects of CO₂ and their modulation by light in the life-cycle stages of the coccolithophore *Emiliania huxleyi*. *Limnol Oceanogr* 57: 607–618.
31. Langer G, Nehrke G, Probert I, Ly J, Ziveri P (2009) Strain-specific responses of *Emiliania huxleyi* to changing seawater carbonate chemistry. *Biogeosciences* 6: 2637–2646.
32. LaRoche J, Rost B, Engel A (2010) Bioassay, batch culture and chemostat experimentation. Guide for best practices for ocean acidification research and data reporting. Publications Office of the European Union. pp. 81–94.
33. Brattström H, Heisäter T (1992) The Biological station 1892–1992: An historical review. Bergen: Univ. i Bergen.
34. Glé C, Del Amo Y, Sautour B, Laborde P, Chardy P (2008) Variability of nutrients and phytoplankton primary production in a shallow macrotidal coastal ecosystem (Arcachon Bay, France). *Estuar Coast Shelf Sci* 76: 642–656.
35. Kester DR, Duedall IW, Connors DN, Pytkowicz RM (1967) Preparation of artificial seawater. *Limnol Oceanogr* 12: 176–179.
36. Guillard RR, Ryther JH (1962) Studies of marine planktonic diatoms. I. *Cyclotella nana* Husted, and *Detonula confervacea* (Cleve) gran. *Can J Microbiol* 8: 229–239.
37. Dickson AG, Afghan JD, Anderson GC (2003) Reference materials for oceanic CO₂ analysis: A method for the certification of total alkalinity. *Mar Chem* 80: 185–197.
38. Lewis E, Wallace DWR (1998) Program developed for CO₂ system calculations [Internet]. ORNL/CDIAC-105. OakRidge (Tennessee): Carbon Dioxide Information Analysis Center, U.S. Department of Energy. Available: <http://cdiac.ornl.gov/ftp/co2sys>.
39. Sharp JH (1974) Improved analysis for particulate organic carbon and nitrogen from seawater. *Limnol Oceanogr* 19: 984–989.
40. Cottingham KL, Brown BL, Lennon JT (2005) Knowing when to draw the line: designing more informative ecological experiments. *Front Ecol Environ* 3: 145–152. doi: 10.1890/1540-9295(2005)003[0145:KWIDTL]2.0.CO;2.
41. Zondervan I, Zeebe RE, Rost B, Riebesell U (2001) Decreasing marine biogenic calcification: A negative feedback on rising atmospheric pCO₂. *Global Biogeochem Cycles* 15: 507–516.
42. Langer G, Geisen M, Baumann KH, Kläs J, Riebesell U, et al. (2006) Species-specific responses of calcifying algae to changing seawater carbonate chemistry. *Geochemistry, Geophys Geosystems* 7: Q09006. doi: 10.1029/2005GC001227.
43. Krug S, Schulz KG, Riebesell U (2011) Effects of changes in carbonate chemistry speciation on *Coccolithus braarudii*: a discussion of coccolithophorid sensitivities. *Biogeosciences* 8: 771–777.
44. Lund JWG (1949) Studies on *Asterionella*: I. The origin and nature of the cells producing seasonal maxima. *J Ecol* 37: 389–419.
45. Talling JF (1955) The Relative Growth Rates of Three Plankton Diatoms in Relation to Underwater Radiation and Temperature. *Ann Bot XIX*: 329–341.
46. Eppley RW (1972) Temperature and phytoplankton growth in the sea. *Fish Bull* 70: 1063–1085.
47. Conte MH, Thompson A, Lesley D, Harris RP (1998) Genetic and physiological influences on the alkenone/alkenoate versus growth temperature relationship in *Emiliania huxleyi* and *Gephyrocapsa oceanica*. *Geochim Cosmochim Acta* 62: 51–68.
48. Buitenhuis ET, Pangerc T, Franklin DJ, Le Quere C, Malin G (2008) Growth rates of six coccolithophorid strains as a function of temperature. *Limnol Oceanogr* 53: 1181–1185.
49. Langer G, Gussone N, Nehrke G, Riebesell U, Eisenhauer A, et al. (2007) Calcium isotope fractionation during coccolith formation in *Emiliania huxleyi*: Independence of growth and calcification rate. *Geochem Geophys Geosyst* 8: Q05007. doi: 10.1029/2006GC001422.
50. Eynaud F, Giraudeau J, Pichon JJ, Pudsey CJ (1999) Sea-surface distribution of coccolithophores, diatoms, silicoflagellates and dinoflagellates in the South Atlantic Ocean during the late austral summer 1995. *Deep Sea Res Part I* 46: 451–482.
51. Hagino K, Bendif EM, Young JR, Kogame K, Probert I, et al. (2011) New evidence for morphological and genetic variation in the cosmopolitan coccolithophore *Emiliania huxleyi* (Prymnesiophyceae) from the COX1b-ATP4 genes. *J Phycol* 47: 1164–1176. doi: 10.1111/j.1529-8817.2011.01053.x.
52. Thomas MK, Kremer CT, Klausmeier C, Litchman E (2012) A global pattern of thermal adaptation in marine phytoplankton. *Science* 338: 1085–1088.
53. Tyrrell T, Merico A (2004) *Emiliania huxleyi*: bloom observations and the conditions that induce them. Coccolithophores: from molecular processes to global impact. Springer pp. 75–98.
54. Merico A, Tyrrell T, Lessard EJ, Oguz T, Stabeno PJ, et al. (2004) Modelling phytoplankton succession on the Bering Sea shelf: role of climate influences and trophic interactions in generating *Emiliania huxleyi* blooms 1997–2000. *Deep Sea Res Part I* 51: 1803–1826.
55. Merico A, Tyrrell T, Brown CW, Groom SB, Miller PI (2003) Analysis of satellite imagery for *Emiliania huxleyi* blooms in the Bering Sea before 1997. *Geophys Res Lett* 30: 1337. doi: 10.1029/2002GL016648.
56. Toseland A, Daines SJ, Clark JR, Kirkham A, Strauss J, et al. (2013) The impact of temperature on marine phytoplankton resource allocation and metabolism. *Nat Clim Chang* 3: 979–984.
57. Rokitta SD, John U, Rost B (2012) Ocean acidification affects redox-balance and ion-homeostasis in the life-cycle stages of *Emiliania huxleyi*. *PLoS One* 7: e52212.
58. Bach LT, Mackinder LCM, Schulz KG, Wheeler G, Schroeder DC, et al. (2013) Dissecting the impact of CO₂ and pH on the mechanisms of photosynthesis and calcification in the coccolithophore *Emiliania huxleyi*. *New Phytol* 199: 121–134.
59. Feng Y, Warner ME, Zhang Y, Sun J, Fu FX, et al. (2008) Interactive effects of increased pCO₂, temperature and irradiance on the marine coccolithophore *Emiliania huxleyi* (Prymnesiophyceae). *Eur J Phycol* 43: 87–98. doi: 10.1080/09670260701664674.
60. De Bodt C, Van Oostende N, Harlay J, Sabbe K, Chou I (2010) Individual and interacting effects of pCO₂ and temperature on *Emiliania huxleyi* calcification: study of the calcite production, the coccolith morphology and the coccosphere size. *Biogeosciences* 7: 1401–1412.

Chapter II



Scanning electron microscope pictures of a natural diatom bloom under present conditions (left) and future ocean conditions (right)

We cannot cheat on DNA. We cannot get 'round photosynthesis.
We cannot say I am not going to give a damn about
phytoplankton. All these tiny mechanisms provide the
preconditions of our planetary life. To say we do not care is
to say in the most literal sense that "we choose death."

Barbara Ward

Shift from smaller to larger diatoms during a natural phytoplankton bloom under combined high CO₂ and warming conditions

Overhead title: ***Shifts to larger diatoms under future ocean conditions***

Scarlett Sett^{1*}, Kai G. Schulz², Lennart T. Bach¹ and Ulf Riebesell¹

¹ GEOMAR Helmholtz Centre for Ocean Research Kiel, Düsternbrooker Weg 20, 24105 Kiel, Germany (ssett@geomar.de)

² Centre for Coastal Biogeochemistry, School of Environmental Science and Management, Southern Cross University, P.O. Box 157, Lismore, NSW 2480 Australia

Abstract

An indoor mesocosm experiment was carried out to investigate the combined effects of ocean acidification and warming on the species composition and biogeochemical cycling during a natural winter/spring phytoplankton bloom from the Kiel fjord. The experimental setup consisted of a “control” treatment (ambient temperature and $p\text{CO}_2$), a “High CO₂” treatment (ambient temperature and initially +450 $\mu\text{atm } p\text{CO}_2$ above ambient) and a “Greenhouse” treatment (+4°C and initially +450 $\mu\text{atm } p\text{CO}_2$ above ambient). Nutrient replete conditions were naturally available at the beginning of the experiment and once the temperature and $p\text{CO}_2$ target levels were set, light was provided at *in-situ* conditions. A diatom-dominated bloom developed in all treatments with *Skeletonema costatum* being the most dominant species but with an increased abundance of large diatom species in the Greenhouse treatment (i.e. *Thalassiosira* sp and *Nitzschia longissima*). Whereas conditions in the Greenhouse treatment stimulated an early bloom development with faster utilization of inorganic nutrients and timing of maximum biomass, no difference was observed in maximum concentration of particulate organic matter (POM) between the treatments. Losses of POM in the Greenhouse treatment were twice as high as the Control and High CO₂ treatments at the end of the experiment and could be a direct consequence of larger diatom species dominating community composition in the Greenhouse treatment.

Keywords: mesocosm, ocean acidification, warming, diatoms, spring bloom

Chapter II

Introduction

Climate change stemming from anthropogenic CO₂ emissions is an ongoing process changing sea surface temperatures (i.e. ocean warming) and oceanic carbonate chemistry speciation (i.e. ocean acidification) at an unprecedented pace. Projections from the IPCC 2014 (Field *et al.*, 2014) project an increase of 1-6°C and a decrease of ~0.3 units in oceanic pH by the end of this century (Orr *et al.*, 2005). Both of these environmental drivers are expected to affect marine primary producers with potential consequences for marine biogeochemical cycling in the future ocean (Gehlen *et al.*, 2011; Riebesell & Tortell, 2011; Rees, 2012).

Indirect effects of warming are expected through enhanced stratification of the water column and consequent alteration of nutrients and light availability, therefore affecting growth at the base of the food web and modulating energy transfer to higher trophic levels. A direct effect is the enhancement of metabolic activities (Eppley, 1972) which is usually more pronounced in heterotrophs than autotrophs (Pomeroy & Wiebe, 2001). Numerous laboratory and mesocosm based experiments have been carried out to examine the effects of warming on plankton communities. Some of the most common and recurrent patterns observed were increased primary production, PP (Lewandowska *et al.*, 2012), shifts in species composition (Sommer *et al.*, 2007; Lassen *et al.*, 2010), shifts in the partitioning of organic matter into dissolved or particulate pools (Wohlers *et al.*, 2009) and decreased biomass build-up (Keller *et al.*, 1999; Sommer & Lengfellner, 2008; O'Connor *et al.*, 2009; Lassen *et al.*, 2010; Wohlers-Zöllner *et al.*, 2012; Biermann *et al.*, 2014) with one exception (Taucher *et al.*, 2012). Taucher *et al.*, 2012 suggested that the enhanced biomass build-up with warming during their experiments, contradictory to previous results, was most likely due to differences in the phytoplankton community composition.

In addition to warming, increasing CO₂ concentrations in the ocean and concomitant decreasing pH are also expected to affect marine ecosystems in the upcoming decades (Riebesell & Tortell, 2011). While studies looking at the effects of ocean acidification on natural phytoplankton communities have shown that there can be a fertilizing effect of increasing CO₂ on PP (Hein & Sand-Jensen, 1997; Schippers *et al.*, 2004; Tortell *et al.*, 2008; Egge *et al.*, 2009; Engel *et al.*, 2013) there is evidence which points to a negative effect of increasing CO₂ on calcifying phytoplankton (Ridgwell *et al.*, 2009; Hoppe *et al.*, 2011). At the ecological level, shifts in species composition were observed in some studies (Tortell *et al.*, 2002, 2008) with higher CO₂ concentrations profiting diatoms (Tortell *et al.*, 2008; Egge *et al.*, 2009; Feng *et al.*, 2009; Yoshimura *et al.*, 2013). Most importantly, as for the effects of warming, there were differences in the partitioning of organic carbon into the dissolved and particulate pools (Engel *et al.*, 2005; Riebesell *et al.*, 2007; Bellerby *et al.*, 2008; Kim *et al.*, 2011) which in the future could have significant consequences for the export and sequestration of organic

carbon through the biological carbon pump. Nevertheless, ocean acidification and warming are two processes expected to occur simultaneously in the future and whereas their effects on natural phytoplankton communities have been extensively studied independently (as pointed out previously) there seems to be limited data on their combined effects (Hare *et al.*, 2007; Feng *et al.*, 2009; Kim *et al.*, 2011).

By means of indoor mesocosm experiments we were able to follow the temporal development of a natural spring bloom of the Kiel Bight under ocean acidification (i.e. “High CO₂”) and combined ocean acidification and warming conditions (i.e. “Greenhouse”). Coastal ecosystems are highly variable environments, both in terms of temperature and CO₂ (Thomsen *et al.*, 2010; Hofmann *et al.*, 2011; Melzner *et al.*, 2012) and are considered to be environmentally and socio-economically important. In temperate and coastal regions, the spring bloom is the most productive event during the year. Therefore, any changes affecting spring bloom dynamics could impact energy transfer across trophic levels, thereby modifying overall productivity in these ecosystems. The aim of our study was to investigate if these two stressors would affect species composition and biogeochemical cycling during a spring bloom event. The temperature and CO₂ levels applied in our experiments are well within the range expected by the end of this century as projected by the IPCC 2014 (Field *et al.*, 2014).

Materials and methods

Experimental setup

Indoor mesocosm experiments were carried out between January 12 and February 24 2012 at the GEOMAR Helmholtz Centre for Ocean Research Kiel. Six mesocosms with a volume of 1400 L each (1.5 m diameter, 1 m depth) were set up in temperature controlled rooms and filled simultaneously with unfiltered seawater from Kiel Bight containing a representative late winter/early spring phytoplankton community. Dissolved inorganic nutrients at the beginning of the experiment were naturally available and therefore not manipulated in this study. Each mesocosm had a computer-controlled light system equipped with bulbs covering the full natural spectrum of photosynthetically active radiation, PAR: 400-700 nm. The light program allowed for simulation of daily light curves depending on the day of the year and theoretical maximum irradiance intensity around noon (Brock, 1981). Light was provided at conditions representing the mean of a mixed water column of ~10 m depth. Each mesocosm was equipped with a propeller which ensured gentle mixing throughout the experiment allowing small particles to remain in suspension while bigger particles sink through the water column (Sommer *et al.*, 2007). Mesocosms were set up as the following treatments: “Control” treatment (*in situ* temperature of ~5°C and *in situ* pCO₂ of ~550

Chapter II

μatm), “High CO_2 ” treatment (*in situ* temperature and initially $+450 \mu\text{atm } p\text{CO}_2$ above *in situ*) and “Greenhouse” treatment ($+4^\circ\text{C}$ and initially $+450 \mu\text{atm } p\text{CO}_2$ above *in situ*). Target temperature and CO_2 scenarios were chosen according to IPCC 2014 projections for the end of this century (Field *et al.*, 2014).

Temperature and salinity were measured every sampling day with a combined conductivity and temperature probe (WTW Germany). Samples for biogeochemical parameters and phytoplankton analysis were taken daily at 9 a.m. during the bloom period (day 12 to 20) and every other day otherwise. Samples were taken from an intermediate depth (0.5 m below surface) either with a membrane pump directly into measuring vials or a silicone tube into sample canisters. The canisters were gently mixed before any sub sampling took place to ensure representative homogenous samples.

Temperature and CO_2 manipulations

Target temperature for the Greenhouse treatment (i.e. $+4^\circ\text{C}$ above *in situ* conditions) was attained within 12 hrs of filling the mesocosms and remained constant throughout the experiment. For the CO_2 manipulation, 25 L of seawater (same water used for filling the mesocosms) were aerated with pure CO_2 (99.99%) for ~ 24 hrs before the manipulation. The enriched seawater was used to manipulate the total dissolved inorganic carbon (DIC) in the High CO_2 and Greenhouse treatments while leaving total alkalinity (TA) unaffected. The CO_2 manipulation was performed gradually over 2-days to avoid rapid changes and acute stress of the plankton community. During the CO_2 manipulation, the light conditions were kept at 10% of the normal surface irradiance to acclimatize to the new carbonate chemistry. Once target CO_2 levels were attained (experiment day 3) the regular daily light curve regime was started. Transparent floating lids (Polyethylene, 0.3 mm thick) were placed on the water surface for the duration of the experiment to minimize gas exchange with the atmosphere. A gas tracer (N_2O) was used to estimate gas exchange fluxes (Czerny *et al.*, 2013). Assuming that mesocosms in the same treatment behaved similarly in terms of gas exchange fluxes, N_2O was only added to one mesocosm per treatment and applied for the correction of the duplicate in that same treatment.

Carbonate chemistry

DIC samples were sterile filtered ($0.2 \mu\text{m}$) with a membrane pump at a constant 50 ml min^{-1} flow into 50 ml Schott Duran bottles and measured immediately afterwards using an infra red detection method of CO_2 (AIRICA-automated infra red inorganic carbon analyzer) with $\sim 2 \mu\text{mol kg}^{-1}$ precision. CO_2 fluxes obtained from gas exchange calculations with N_2O were then added or

Chapter II

subtracted from measured DIC concentrations to account for CO₂ out gassing or in-gassing, respectively. DIC concentrations presented in this study have been corrected for gas exchange and drawdown is therefore representative for biological consumption, unless otherwise clarified. DIC drawdown (Δ DIC) was calculated by averaging the first two days once p CO₂ targets were set (day 3 and 5) minus each respective experimental day. Maximum DIC consumption (Δ DIC_{max}) was calculated from the difference of initial DIC concentrations (after CO₂ manipulation, days 3 and 5) and minimum DIC concentrations (DIC_{min}). DIC_{min} concentrations were averaged starting around day 20 until the end of the experiment while concentrations remained relatively stable. As one of the mesocosms had a faulty lid, it was not considered for this calculation.

Samples for TA were filtered through GF/F filters and measured within 2 days in a Metrohm Basic Titrino 794 titration device according to Dickson et al. 2003 (Dickson *et al.*, 2003). Measurements for TA and DIC were corrected with certified reference material (Dickson *et al.*, 2003). Calculation for carbonate chemistry speciation was carried out with the program CO2SYS (Lewis & Wallace, 1998) from measured DIC, TA, temperature, salinity and nutrients (i.e. PO₄ and Si), using the dissociation constants by Merbach et al. 1973 as refitted by Dickson & Millero (1987).

Biological and chemical analysis

Dissolved inorganic nutrients: nitrate (NO₃⁻), phosphate (PO₄³⁻) and silicate (H₄SiO₄) as well as dissolved organic carbon (DOC), dissolved organic nitrogen (DON) and dissolved organic phosphorus (DOP) were filtered through pre-combusted (450°C, 6 hrs) GF/F filters with a membrane pump at a rate of 100 ml min⁻¹ directly into their respective vials. Besides DOC samples, which were fixed with 85% phosphoric acid (H₃PO₄) and refrigerated, all samples were frozen at -20°C until analysis. Nutrients were measured on a segmented flow autoanalyzer (SEAL QuAatro) according to Hansen & Koroleff, 1999. DOC samples were analyzed using the HTCO method (high-temperature catalytic oxidation) on a Shimadzu TOC-V analyzer according to Wurl & Min Sin, 2009. Accuracy of the method was calibrated against deep-sea reference material provided by the University of Miami. DON/DOP samples were cooked with Oxisolv (MERCK) and once oxidized; both organic nitrogen and phosphorus were measured as nitrate and phosphate in a two-channel autoanalyzer (SEAL QuAarto) according to Hansen & Koroleff, 1999. DON/DOP concentrations were obtained by subtracting respective inorganic nutrient concentrations.

Samples for particulate organic carbon (POC), particulate organic nitrogen (PON) and particulate organic phosphorus (POP) were filtered at low vacuum (<200 mbar) onto pre-combusted (450°C, 6 hrs) GF/F filters and stored at -20°C until analysis. Filters for POC/PON were fumed with hydrochloric acid (37% HCl) for 2 hours to remove all inorganic carbon and subsequently

Chapter II

dried overnight at 60°C. Samples were analyzed with a EuroEA analyzer according to Sharp (Sharp, 1974). POP filters were cooked with Oxisolv (Merck) and oxidized into orthophosphate. Later POP was measured photometrically as phosphate according to Hansen & Koroleff, 1999. Samples for particulate biogenic silica (BSi) were filtered at low vacuum (<200 mbar) onto cellulose acetate filters. Samples were cooked for 2 hrs and 15 min at ~85°C to extract all biogenic silica into solution and then analyzed as silicate according to Hansen & Koroleff, 1999.

Initial POM values were calculated by averaging concentrations of all treatments on the first two days of the experiment (\pm standard deviation). Build-up of POM was calculated by subtracting the average of the first two days (once target $p\text{CO}_2$ levels were established) to each experimental day. In most cases, maximum POM build-up was observed after nutrient depletion and consisted of more than two experimental days (\pm standard deviation of duplicate).

Phytoplankton composition analysis

Phytoplankton species composition was analyzed by pigment analysis (high pressure liquid chromatography, HPLC), size categorization by flow cytometry and Utermöhl microscopy (6 sampling days). HPLC samples were filtered onto pre-combusted (450°C, 6 hrs) GF/F filters and stored at -80°C until extraction. Photosynthetic pigments were separated via HPLC with 100% acetone (HPLC grade) according to the method of Van Heukelem & Thomas, 2001. Phytoplankton composition was calculated with the program CHEMTAX (Mackey *et al.*, 1996) which estimates taxon-specific contributions to total Chlorophyll *a* (Chl *a*) according to the presence and amounts of marker pigments.

Samples for flow cytometry were taken from an intermediate depth with a membrane pump directly into 10 ml vials, fixed with 25% Glutaraldehyde and immediately frozen at -80°C until analysis. Samples were thawed for 10 minutes and mixed gently before measuring with an Accuri C6 flow cytometer (BD Biosciences). Three major group sizes were determined. Group I represented the smallest group and approximately phytoplankton in the pico size category (<2 μm). Group II and III represented the largest groups and approximately phytoplankton in the nano and micro size category, respectively. The contribution of each group to total Chl fluorescence was calculated from cell abundances and individual red fluorescence (FL3).

Phytoplankton bigger than 2 μm were counted using the inverted microscopy method according to Utermöhl, 1958 on six different occasions during the experiment (for details refer to Collet, 2013). Four sampling days from the beginning of the experiment until maximum Chl *a* and two sampling days during the decline of the bloom. In order to provide a comparison to the counts from the flow cytometer, diatoms were aggregated by size. Group II from the microscopy counts

Chapter II

included diatoms <20 μm in size such as *Skeletonema costatum* and small *Chaetoceros* sp (~5 μm), while Group III included diatoms > 20 μm such as *Thalassionema nitzschioides*, *Thalassiosira* sp, *Nitzschia longissima*, *Navicula transitans*, *Fragilaria* sp, *Guinardia* sp and *Chaetoceros* sp (>20 μm).

Statistical analysis

Initially, replication consisted of triplicates, unfortunately however, due to technical problems (i.e. propeller and light malfunctioning) one mesocosm in each treatment was lost. Nevertheless, Student's t-test were performed on POM losses at the end of the experiment between the Control – High CO_2 and Control – Greenhouse treatments for significant differences ($p < 0.05$). POM losses were calculated as the difference between the daily change in total organic biomass and utilization of the respective inorganic nutrient as follows:

$$\Delta X_{\text{loss}} = \Delta \text{DIX} - (\Delta \text{POX} + \Delta \text{DOX}) \quad (\text{equation 1})$$

where ΔDIX is the dissolved inorganic, ΔPOX is the particulate organic, ΔDOX is the dissolved organic and “X” can be carbon (C), nitrogen (N), phosphorus (P) or silica (Si). Averaged values (of the duplicates) were used for calculation of POM losses on the last two days of the experiment (\pm standard deviation). Except for the nitrogen pool where ΔDON was not considered in the calculation due to measuring errors.

Results

CO₂ manipulation and initial experimental conditions

Target $p\text{CO}_2$ levels in the High CO_2 and Greenhouse treatments (1017 ± 46 and 990 ± 57 μatm $p\text{CO}_2$, respectively) were established within the first 3 days of the experiment and remained relatively constant for ~10 days. Thereafter, $p\text{CO}_2$ levels decreased to minimum values of 38.8 ± 8.7 μatm (Figure 1A). Starting pH values (on the total scale) were 7.93 ± 0.02 in the Control, 7.67 ± 0.02 in the High CO_2 and 7.69 ± 0.02 in the Greenhouse treatment. pH increased up to maximum values of 8.98 ± 0.04 in the Control, 8.94 ± 0.02 in the High CO_2 and 8.87 ± 0.02 in the Greenhouse treatment (Figure 1B). TA slightly increased after nutrient depletion on day 15 from an initial average of 2072.2 ± 3.3 $\mu\text{mol kg}^{-1}$ to final concentrations of 2083.8 ± 2.4 $\mu\text{mol kg}^{-1}$ (Figure 1C). A summary of initial nutrient and $p\text{CO}_2$ conditions as well as temperature and salinity over the experimental period is presented in Table 1.

Chapter II

Characterization of bloom development

Start of autotrophic growth was marked by a rapid decrease in major dissolved inorganic nutrients (Figure 2A-C) and parallel increase of Chl *a* (Figure 3). Faster nutrient uptake in combination with an earlier onset of the bloom and earlier timing of maximum biomass of ~2-5 days was observed under the Greenhouse conditions, whereas overall consumption of dissolved inorganic nutrients was the same between treatments (Figure 2A-C). In all treatments, PO₄ was depleted one day earlier than any of the inorganic nitrogen species. All inorganic nutrients were exhausted by day 15 in the Greenhouse treatment and 3-4 days later in the Control and High CO₂. Chl *a* increased on average from $\sim 0.086 \pm 0.01 \mu\text{g L}^{-1}$ to peak averaged concentrations of $37 \pm 2.5 \mu\text{g L}^{-1}$ in all treatments (Figure 3A). The timing of peak Chl *a* concentrations was similar between the treatments.

Development, build-up and decline of particulate and dissolved organic matter

A concomitant increase in particulate organic matter (POM) was observed along decreasing nutrients and increasing Chl *a*. The temporal development of PON, POP and BSi directly followed the drawdown of the corresponding inorganic nutrients (Figure 2D-F). The onset and timing of peak concentrations was slightly earlier, ~3 days, under the Greenhouse conditions but with no differences in absolute maximum concentrations compared to the Control and High CO₂.

PON increased from an initial average of $1.6 \pm 0.22 \mu\text{mol N L}^{-1}$ to maximum concentrations of $12.1 \pm 0.53 \mu\text{mol N L}^{-1}$ in the Control, $11.8 \pm 1.08 \mu\text{mol N L}^{-1}$ in the High CO₂ and $11.8 \pm 1.17 \mu\text{mol N L}^{-1}$ in the Greenhouse treatment. PON concentrations at the end of the experiment were on average $5.9 \pm 1.7 \mu\text{mol L}^{-1}$ in the Control, $5.8 \pm 0.83 \mu\text{mol L}^{-1}$ in the High CO₂ and $3.5 \pm 0.77 \mu\text{mol L}^{-1}$ in the Greenhouse treatment. The variability of DON concentrations was larger than the stock of inorganic nutrients and therefore was not used for any N pool calculations.

POP increased on average from $0.05 \pm 0.01 \mu\text{mol P L}^{-1}$ to maximum concentrations of $0.59 \pm 0.07 \mu\text{mol P L}^{-1}$ in the Control, $0.58 \pm 0.04 \mu\text{mol P L}^{-1}$ in the High CO₂ and $0.54 \pm 0.04 \mu\text{mol P L}^{-1}$ in the Greenhouse treatment. Concentrations of POP at the end of the experiment were almost twice as high in the Control ($0.37 \pm 0.07 \mu\text{mol P L}^{-1}$) and High CO₂ ($0.32 \pm 0.07 \mu\text{mol P L}^{-1}$) compared to the Greenhouse treatment ($0.15 \pm 0.05 \mu\text{mol P L}^{-1}$). After PO₄ exhaustion, DOP slightly increased to maximum concentrations of $0.16 \pm 0.07 \mu\text{mol P L}^{-1}$ in all treatments and remained stable throughout the experiment with no distinct trends between treatments (data not shown).

BSi, indicative for diatoms, followed the development of Chl *a* from the beginning of the experiment up to the peak of the bloom. BSi increased on average from $1.0 \pm 0.13 \mu\text{mol L}^{-1}$ to maximum concentrations of $28.5 \pm 1.22 \mu\text{mol L}^{-1}$ in the Control, $27.9 \pm 1.02 \mu\text{mol L}^{-1}$ in the High CO₂ and $30.0 \pm 0.62 \mu\text{mol L}^{-1}$ in the Greenhouse treatment. BSi concentrations remained relatively high

Chapter II

after the peak of the bloom while the pigment concentrations associated to diatoms decreased similarly to Chl *a* (Figure 3 and 6A). BSi not only represented living diatoms but also silicate frustules which remained suspended in the water column for some time before sinking out. BSi concentrations at the end of the experiment were more than twice as high in the Control and High CO₂ (14.77 ± 3.6 and $11.86 \pm 3.9 \mu\text{mol L}^{-1}$, respectively) compared to the Greenhouse treatment ($4.98 \pm 1.98 \mu\text{mol L}^{-1}$). Losses of POM were significantly higher in the Greenhouse treatment at the end of the experiment in comparison to the control (Figure 4).

Carbon cycling- Photosynthetic uptake of DIC was accompanied by an increase in POC and DOC concentrations (Figure 5A-C). Slightly faster DIC uptake and timing of peak POC concentrations was observed in the Greenhouse treatment. Photosynthetic carbon fixation during the experiment decreased DIC concentrations from $2047.6 \pm 11.2 \mu\text{mol L}^{-1}$ to $1595.8 \pm 30.9 \mu\text{mol L}^{-1}$ in the Control treatment and from $2104.3 \pm 10.2 \mu\text{mol L}^{-1}$ to $1630 \pm 6.9 \mu\text{mol L}^{-1}$ in the High CO₂ and Greenhouse treatments (Figure 5A). A slightly higher DIC drawdown of $485.7 \pm 5.8 \mu\text{mol L}^{-1}$ was calculated in the High CO₂ compared to $461.3 \pm 7.3 \mu\text{mol L}^{-1}$ in the Control and Greenhouse treatments.

During the first part of the experiment (day 1-20) calculated CO₂ out-gassing did not exceed $12 \mu\text{mol kg}^{-1} \text{d}^{-1}$ and during the second half of the experiment (day 20-44) calculated CO₂ in-gassing did not exceed $20 \mu\text{mol kg}^{-1} \text{d}^{-1}$. Naturally, higher in/out gassing occurred in the High CO₂ and Greenhouse treatments where CO₂ gradients were larger. Additionally, the lid in one of the Control mesocosms was not properly covering the water surface and a small air space was created near the propeller increasing gas exchange in this area. DIC concentrations in this treatment steadily increased after day 20 of the experiment, most likely from in-gassing since no change in POC or DOC concentrations was observed (Figure 5).

POC increased from an initial average of $13.2 \pm 1.1 \mu\text{mol C L}^{-1}$ to maximum concentrations of $289.7 \pm 13.6 \mu\text{mol C L}^{-1}$ in the Control, $305.2 \pm 15.8 \mu\text{mol C L}^{-1}$ in the High CO₂ and $301.6 \pm 26.1 \mu\text{mol C L}^{-1}$ in the Greenhouse treatment (Figure 5B). Maximum build-up of POC occurred ~5 days after inorganic nutrient depletion and remained constant for 10-15 days, then decreased rapidly on the last days of the experiment. DOC steadily increased from an average of $220.6 \pm 7.3 \mu\text{mol C L}^{-1}$ to maximum averaged concentrations of $277.4 \pm 13.5 \mu\text{mol C L}^{-1}$ in the Control and Greenhouse treatments and slightly higher in the High CO₂ with $302.3 \pm 7 \mu\text{mol C L}^{-1}$ at the end of the experiment (Figure 5C).

Chapter II

Elemental stoichiometry of particulate organic matter

Inorganic nutrients were assimilated into the respective POM pools according to Redfield proportions up to day 15 of the experiment. Thereafter, due to nutrient limitation relatively constant POC:PON and decreasing POC:POP and PON:POP were observed (Figure 6). Both POC:POP and PON:POP started at values almost twice as high as 106:1 and 16:1 Redfield proportions, respectively, suggesting low living phytoplankton biomass in the POM pool at the beginning of the experiment (Figure 6B-C). After nutrient depletion, carbon fixation continued leading to maximum POC:PON of up to 30-40 and POC:POP of up to 600-800 while PON:POP remained relatively constant. Except for the faster bloom onset in the Greenhouse treatment, no trends were observed between the treatments (Figure 6A-C).

Phytoplankton composition derived from HPLC analysis

Chl *a* was almost exclusively produced by diatoms with minor contributions from cryptophytes, prasinophytes, dinophytes and chlorophytes (Figure 7A-E). Diatoms followed the temporal development of Chl *a* and contributed with a maximum of $\sim 35 \mu\text{g L}^{-1}$ of a total average of $37 \pm 3 \mu\text{g L}^{-1}$ (Figure 7A). Cryptophytes were the second group after diatoms contributing with a maximum of $\sim 1.2 \mu\text{g L}^{-1}$ to Chl *a* while minor contributions from the other phytoplankton groups did not exceed $\sim 0.5 \mu\text{g L}^{-1}$ (Figure 7B-E). The contributions by prasinophytes and cryptophytes to Chl *a* during the peak of the bloom showed opposite responses in the Greenhouse treatment. Contributions of prasinophytes were higher in the Greenhouse treatment compared to the Control and High CO₂ treatments while the opposite was observed for cryptophytes showing twice as high concentrations in the Control and High CO₂ than in the Greenhouse treatment (Figure 7D and E). Chl *a* contributions of chlorophytes and dinophytes showed a similar response, increasing after the peak of the bloom with higher concentrations in the Greenhouse treatment (Figure 7B and C), though at relatively low absolute concentrations.

Phytoplankton composition from flow cytometry and microscopy

Phytoplankton abundances as measured by flow cytometry increased to peak concentrations similarly to the development of Chl *a* (Figure 8A-C). Abundances in Group I (the smallest size) decreased after reaching peak concentrations between days 15-18 while abundances in Group II (intermediate size approximately between $\sim 2-20 \mu\text{m}$) and Group III (largest size fraction approx. $>20 \mu\text{m}$) remained relatively stable for $\sim 10-15$ days. The contribution of Group I to total Chl fluorescence (i.e. cell abundances multiplied by red fluorescence) at the beginning of the experiment was up to 30% but during peak concentrations and thereafter accounted for $<2\%$ (Figure 8D). Group

Chapter II

II showed peak abundances one day after nutrient depletion. Abundances of Group II were ~25% lower in the Greenhouse treatment compared to those in the Control and High CO₂ treatments (Figure 8B). The contribution of Group II to Chl fluorescence during the bloom peak was >60% in the Control and High CO₂ and ~45-50% in the Greenhouse treatment (Figure 8E). Conversely, Group III showed higher abundances in the Greenhouse treatment during peak Chl *a* (and thereafter) compared to the Control and High CO₂ treatments (Figure 8C). The contribution to Chl fluorescence during peak concentrations from Group III was ~50% in the Greenhouse treatment and <40% in the Control and High CO₂ (Figure 8F). Since more than 95% of the Chl could be attributed to diatoms from the peak of the bloom towards the end of the experiment, Group II and Group III as identified by flow cytometry are most likely composed by diatoms only.

Although absolute values were not the same between microscopic and flow cytometry counts, the tendency of larger diatom species dominating the Greenhouse treatment was observed in both (Figure 8B-C, 9). Abundances of *S. costatum* and the small *Chaetoceros sp* (most likely in Group II) remained similar between the treatments while the shift towards larger diatoms in the Greenhouse treatment was mainly driven by *Thalassiosira sp* and *Nitzschia longissima* (Figure 9).

Discussion

Climate change, in the context of ocean acidification and warming, has the potential to significantly affect marine biogeochemical cycling by modifying the balance between primary production and heterotrophic processes (Riebesell & Tortell, 2011). Our study examined the combined effects of these two stressors on the species composition and biogeochemical dynamics during a natural spring phytoplankton bloom from a temperate coastal ecosystem. The majority of experiments in this region have focused on the individual effects of warming (for reviews see Sommer *et al.*, 2012; Wohlers-Zöllner *et al.*, 2012) or CO₂ alone (Schulz & Riebesell, 2013; Engel *et al.*, 2014). However as climate change simultaneously affects both environmental drivers, combining them in experiments creates a more realistic “future ocean” scenario.

Temporal development of the bloom and POM dynamics

In temperate ecosystems, light availability is the primary environmental factor limiting autotrophic phytoplankton growth in early spring (Sommer, 1996). Hence, the phytoplankton bloom was initiated as soon as light was provided at *in-situ* conditions. The temporal development of POM during the nutrient replete phase of the experiment (days 1 to 15) was what would be expected from a natural diatom-dominated spring bloom exhibiting rapid drawdown of inorganic nutrients and accompanied by exponential autotrophic growth (as represented by Chl *a*) and biomass build-up

Chapter II

of POC, PON, POP and BSi. Once inorganic nutrients were completely depleted between days 15-18 (depending on treatment) peak concentrations in the respective particulate pool were observed (Figure 2). During the first part of the experiment (i.e. exponential growth phase) faster nutrient uptake accelerated the POM peak by ~2-5 days in the Greenhouse treatment compared to the Control and the High CO₂ treatments. Such a response (i.e. acceleration of bloom onset and timing of maximum concentrations) has been a common occurrence in similar mesocosm experiments investigating warming (1-1.4 days °C⁻¹, Sommer *et al.*, 2012b) but is most likely irrelevant from an ecological point of view compared to the large inter-annual variability observed in long-term monitoring records in this region (Edwards & Richardson, 2004; Wiltshire *et al.*, 2008).

Peak concentrations of PON, POP and BSi were observed one day after the respective inorganic nutrient was depleted with no differences in maximum POM concentrations between the treatments (Figure 2 D-F). DIC uptake and POC build-up continued for another 5 days after nutrient depletion and thereafter POC concentrations remained constant for ~15 days while DIC concentrations remained at lowest concentrations (Figure 5B-C). In previous experiments, POM concentrations followed the temporal development of Chl *a*, immediately decreasing after peak concentrations and showing a negative correlation with increasing temperature (Wohlers *et al.*, 2009; Biermann *et al.*, 2014). The difference between previous studies and the present was the addition of grazers at the beginning of the experiment. In the former cases, warming enhanced grazing activity of consumers (i.e. copepods and ciliates) and therefore top-down control processes modified biomass build-up (Sommer & Lengfellner, 2008; Lewandowska & Sommer, 2010). The low grazing pressure in our set-up favoured bottom-up processes allowing maximum biomass build-up to be attained in all treatments and maintained at high concentrations after the peak of the bloom. Similar results of relatively stable POM concentrations after the bloom peak were observed during nutrient induced diatom blooms with low grazing pressures (Engel *et al.*, 2002; Wohlers-Zöllner *et al.*, 2011). After a phytoplankton bloom, large marine diatom aggregates have been reported to remain in the surface layer for days before aging, disintegrating and then sinking (Smayda & Boleyn, 1966; Sarthou *et al.*, 2005) most likely explaining the phase of relatively stable POM concentrations we observed in our experiments. Alternatively, during diatom-dominated blooms, the abiotic generation of transparent exopolymer particles (TEP) through the release of extracellular substances might have also been collected and measured within the POM pool and matched the expected TEP C:N of ~26 (Passow, 2002) during the post bloom phase in our experiments. TEP has been directly associated to enhanced sinking rates of diatom aggregates at the end of bloom events (Sarthou *et al.*, 2005) and could explain the rapid loss of POM on the last days in our experiment.

Chapter II

Phytoplankton community composition and shifts in size

The chain-forming diatom *S. costatum* is a typical dominating species during spring blooms in the Kiel Bight (Wasmund *et al.*, 2008) and was the most abundant species during our experiments. However, higher abundances of larger diatom species (such as *Thalassiosira* sp and *Nitzschia longissima*) were observed in the Greenhouse treatment. This result comes as a surprise since there is strong evidence suggesting that warming alone reduces cell size and benefits smaller phytoplankton (Sommer & Lengfellner, 2008; Daufresne *et al.*, 2009; Lewandowska & Sommer, 2010; Morán *et al.*, 2010). The increase of small-sized phytoplankton in warming experiments was mostly associated to higher feeding rates of zooplankton on larger species allowing smaller ones to proliferate (Keller *et al.*, 1999; O'Connor *et al.*, 2009; Lewandowska *et al.*, 2012) while our experiments were more representative of an ecosystem with low grazing pressure. Furthermore, during CO₂ enrichment experiments in natural phytoplankton communities both positive and negative effects of increasing CO₂ were observed on a number of functional groups and species. For instance, small picoeucaryotes profited from higher CO₂ levels (Brussaard *et al.*, 2013; Schulz *et al.*, 2013; Yoshimura *et al.*, 2013). The specific mode of carbon concentrating mechanism (CCM) employed for inorganic carbon acquisition was speculated to be among the reasons for this response, relying more on passive diffusion in very small cells. In this context it is interesting to note that not only relatively small phytoplankton cells have been found to be able to directly profit from higher CO₂ concentrations but also the relatively big ones. Incubation experiments with natural Southern Ocean phytoplankton communities showed that large chain-forming *Chaetoceros* sp profited at high CO₂ conditions at the expense of smaller diatoms such as *Pseudo-nitzschia subcurvata* and *Cylindrotheca closterium* (Tortell *et al.*, 2008; Feng *et al.*, 2010). This could be related to an elevation of carbon limitation in the larger diffusive boundary layer of larger cells compared to smaller ones.

Incubation experiments with natural Bering and North Sea phytoplankton communities observed either no or a negative effect of increased CO₂, increased temperature or both on diatom cell numbers in comparison to a control (Hare *et al.*, 2007) or a positive effect of increased CO₂ alone but not in combination with increased temperature (Feng *et al.*, 2009). In the latter experiment, however one has to keep in mind that nutrient levels applied with silicate to nitrate ratios of about 0.15 are rather disadvantageous for diatom growth, also indicated by lower diatom biomass towards the end of the experiment in most incubations compared to the beginning. One also has to keep in mind that a change in diatom size, as observed in our experiment, is not easily picked up by looking at absolute diatom cell abundances but rather looking at abundances of individual species. In contrast to Hare *et al.* and Feng *et al.* our initial community was dominated by diatoms in terms of

Chapter II

biomass and probably allowed for an easier detection of the otherwise rather subtle changes in diatom community composition in response to increased CO₂ and temperature. Another issue could be the initial phytoplankton community composition. Eggers *et al.*, 2014 showed that initial community composition had a stronger effect on phytoplankton biomass than increased CO₂ and that if the community was initially dominated by diatoms, increased CO₂ tended to select for the larger diatom species.

Furthermore, while mesocosm experiments studying the effects of warming during the spring bloom consistently reported decreased phytoplankton biomass with warming (Sommer & Lengfellner, 2008; Lewandowska & Sommer, 2010) Taucher *et al.*, 2012 reported the opposite. Although the latter experiments were conducted with a summer phytoplankton assemblage at much higher temperatures compared to the spring community at lower temperatures of the former experiments, Taucher *et al.*, 2012 suggested that community composition could have been a possible explanation to the opposing response of biogeochemical dynamics to warming. While the experiments in spring were dominated by the typical “spring bloom” species: *Skeletonema costatum*, the summer experiments were dominated by the diatom: *Dactyliosolen fragilissimus* and shows the strong influence of community composition on the biogeochemical response on a coastal system.

Interestingly the shift in species composition in our experiments was within the same functional group (i.e. diatoms) and mainly driven by two large species: *Thalassiosira* sp and *Nitzschia longissima* in the Greenhouse treatment (Figure 9). We suggest that the shift towards larger diatom species was driven by the combined effect of OA and warming. Although the temperature effect cannot be completely ruled out, there is evidence showing a negative correlation between abundances of large diatoms and warming (Sommer & Lengfellner, 2008; Lewandowska & Sommer, 2010). Additionally, Feng *et al.*, 2009 showed that while diatom abundance increased under high CO₂ conditions the shift to larger species was only observed in the combined treatment (“Greenhouse” conditions) similarly to our experiments were no effect in size shift was observed in the High CO₂ treatment.

Furthermore, the shift in size could have implications for the sinking of particulate organic matter. In fact, the loss of organic matter at the end of the experiments was significantly higher in the Greenhouse treatment suggesting that the shift in size towards larger diatoms did play a role in determining loss processes at the end of the bloom.

Acknowledgements

We gratefully thank Kerstin Nachtigall, Andrea Ludwig, Jana Meyer and Sebastian Fessler for the assistance during carbonate chemistry and nutrient analysis. Student helpers Georg Brandenburger, Yves Trense and Yong Zhang during experimental sampling and Yvonne Collet for the analysis of

Chapter II

phytoplankton composition. This work was funded by the European project MESOAQUA agreement no. 2282224.

Reference list

Bellerby RGJ, Schulz KG, Riebesell U et al. (2008) Marine ecosystem community carbon and nutrient uptake stoichiometry under varying ocean acidification during the PeECE III experiment. *Biogeosciences*, **5**, 1517–1527.

Biermann A, Engel A, Riebesell U (2014) Changes in organic matter cycling in a plankton community exposed to warming under different light intensities. *Journal of Plankton Research*, **36**, 658–671.

Brock TD (1981) Calculating solar radiation for ecological studies. *Ecological Modelling*, **14**, 1–19.

Brussaard CPD, Noordeloos AAM, Witte H et al. (2013) Arctic microbial community dynamics influenced by elevated CO₂ levels. *Biogeosciences*, **10**, 719–731.

Collet Y (2013) *The combined effects of temperature and carbon dioxide on coastal phytoplankton communities in the Kiel Fjord - an indoor mesocosm experiment*. Bachelor thesis. Universität Trier.

Czerny J, Schulz KG, Ludwig A et al. (2013) Technical Note: A simple method for air–sea gas exchange measurements in mesocosms and its application in carbon budgeting. *Biogeosciences*, **10**, 1379–1390.

Daufresne M, Lengfellner K, Sommer U (2009) Global warming benefits the small in aquatic ecosystems. *Proceedings of the National Academy of Sciences of the United States of America*.

Dickson A, Afghan J, Anderson G (2003) Reference materials for oceanic CO₂ analysis: A method for the certification of total alkalinity. *Marine Chemistry*, **80**, 185–197.

Edwards M, Richardson AJ (2004) Impact of climate change on marine pelagic phenology and trophic mismatch. *Nature*, **430**, 881–4.

Egge JK, Thingstad TF, Larsen A et al. (2009) Primary production during nutrient-induced blooms at elevated CO₂ concentrations. *Biogeosciences*, **6**, 877–885.

Eggers SL, Lewandowska AM, Barcelos e Ramos J et al. (2014) Community composition has a greater impact on the functioning of marine phytoplankton communities than ocean acidification. *Global Change Biology*, **20**, 713–723.

Engel A, Goldthwait S, Passow U et al. (2002) Temporal decoupling of carbon and nitrogen dynamics in a mesocosm diatom bloom. *Limnology and Oceanography*, **47**, 753–761.

Engel A, Zondervan I, Beaufort L et al. (2005) Testing the direct effect of CO₂ concentration on a bloom of the coccolithophorid *Emiliana huxleyi* in mesocosm experiments Marie-Dominique Pizay. *Limnology and Oceanography*, **50**, 493–507.

Chapter II

- Engel A, Borchard C, Piontek J et al. (2013) CO₂ increases ¹⁴C primary production in an Arctic plankton community. *Biogeosciences*, **10**, 1291–1308.
- Engel A, Piontek J, Grossart H-P et al. (2014) Impact of CO₂ enrichment on organic matter dynamics during nutrient induced coastal phytoplankton blooms. *Journal of Plankton Research*, **0**, 1–17.
- Eppley RW (1972) Temperature and phytoplankton growth in the sea. *Fishery Bulletin*, **70**, 1063–1085.
- Feng Y, Hare C, Leblanc K et al. (2009) Effects of increased pCO₂ and temperature on the North Atlantic spring bloom. I. The phytoplankton community and biogeochemical response. *Marine Ecology Progress Series*, **388**, 13–25.
- Feng Y, Hare CE, Rose JM et al. (2010) Interactive effects of iron, irradiance and CO₂ on Ross Sea phytoplankton. *Deep Sea Research Part I: Oceanographic Research Papers*, **57**, 368–383.
- Field C, Barros V, Dokken D et al. (2014) IPCC, 2014: Summary for Policymakers. In: *Climate Change 2014: Impacts, Adaptation and Vulnerability. Contribution of Working Group II to the Fifth Assessment Report of the Intergovernmental Panel on Climate Change*, pp. 1–32. Cambridge University Press, United Kingdom and New York.
- Gehlen M, Gruber N, Gangsto R (2011) Biogeochemical consequences of ocean acidification and feedbacks to the earth system. In: *Ocean Acidification* (eds Gattuso J, Hansson L), pp. 99–121. Oxford University Press.
- Hansen H, Koroleff F (1999) Determination of nutrients. In: *Methods of seawater analysis*, 3rd edn (eds Grasshoff K, Kremling K, Ehrhardt M), pp. 159–228. Wiley VCH, Weinheim.
- Hare C, Leblanc K, DiTullio G et al. (2007) Consequences of increased temperature and CO₂ for phytoplankton community structure in the Bering Sea. *Marine Ecology Progress Series*, **352**, 9–16.
- Hein M, Sand-Jensen K (1997) CO₂ increases oceanic primary production. *Nature*, **384**, 526–527.
- Van Heukelem L, Thomas CS (2001) Computer-assisted high-performance liquid chromatography method development with applications to the isolation and analysis of phytoplankton pigments. *Journal of chromatography. A*, **910**, 31–49.
- Hofmann GE, Smith JE, Johnson KS et al. (2011) High-frequency dynamics of ocean pH: a multi-ecosystem comparison. *PLoS one*, **6**, e28983.
- Hoppe CJM, Langer G, Rost B (2011) *Emiliania huxleyi* shows identical responses to elevated pCO₂ in TA and DIC manipulations. *Journal of Experimental Marine Biology and Ecology*, **406**, 54–62.
- Keller A, Oviatt CA, Walker HA et al. (1999) Predicted impacts of elevated temperature on the magnitude of the winter-spring phytoplankton bloom in temperate coastal waters: A mesocosm study. *Limnology and Oceanography*, **44**, 344–356.

Chapter II

- Kim J-M, Lee K, Shin K et al. (2011) Shifts in biogenic carbon flow from particulate to dissolved forms under high carbon dioxide and warm ocean conditions. *Geophysical Research Letters*, **38**.
- Lassen MK, Nielsen KD, Richardson K et al. (2010) The effects of temperature increases on a temperate phytoplankton community — A mesocosm climate change scenario. *Journal of Experimental Marine Biology and Ecology*, **383**, 79–88.
- Legendre L, Rivkin R (2002) Fluxes of carbon in the upper ocean: regulation by food-web control nodes. *Marine Ecology Progress Series*, **242**, 95–109.
- Lewandowska A, Sommer U (2010) Climate change and the spring bloom: a mesocosm study on the influence of light and temperature on phytoplankton and mesozooplankton. *Marine Ecology Progress Series*, **405**, 101–111.
- Lewandowska AM, Breithaupt P, Hillebrand H et al. (2012) Responses of primary productivity to increased temperature and phytoplankton diversity. *Journal of Sea Research*, **72**, 87–93.
- Lewis E, Wallace D (1998) Program developed for CO₂ system calculations [Internet] ORNL/CDIAC-105. OakRidge (Tennessee): Carbon Dioxide Information Analysis Center.
- Mackey M, Mackey D, Higgings H et al. (1996) CHEMTAX - a program for estimating class abundances from chemical markers: application to HPLC measurements of phytoplankton. *Marine Ecology Progress Series*, **144**, 265–283.
- Melzner F, Thomsen J, Koeve W et al. (2012) Future ocean acidification will be amplified by hypoxia in coastal habitats. *Marine Biology*, **160**, 1875–1888.
- Morán XAG, López-Urrutia Á, Calvo-Díaz A et al. (2010) Increasing importance of small phytoplankton in a warmer ocean. *Global Change Biology*, **16**, 1137–1144.
- O'Connor MI, Piehler MF, Leech DM et al. (2009) Warming and resource availability shift food web structure and metabolism. *PLoS biology*, **7**, e1000178.
- Orr JC, Fabry VJ, Aumont O et al. (2005) Anthropogenic ocean acidification over the twenty-first century and its impact on calcifying organisms. *Nature*, **437**, 681–6.
- Passow U (2002) Transparent exopolymer particles (TEP) in aquatic environments. *Progress in Oceanography*, **55**, 287–333.
- Pomeroy L, Wiebe W (2001) Temperature and substrates as interactive limiting factors for marine heterotrophic bacteria. *Aquatic Microbial Ecology*, **23**, 187–204.
- Rees AP (2012) Pressures on the marine environment and the changing climate of ocean biogeochemistry. *Philosophical transactions. Series A, Mathematical, physical, and engineering sciences*, **370**, 5613–35.
- Ridgwell A, Schmidt DN, Turley C et al. (2009) From laboratory manipulations to Earth system models: scaling calcification impacts of ocean acidification. *Biogeosciences*, **6**, 2611–2623.

Chapter II

- Riebesell U, Tortell P (2011) Effects of ocean acidification on pelagic organisms and ecosystems. In: *Ocean Acidification*, pp. 99–116. Oxford University Press.
- Riebesell U, Schulz KG, Bellerby RGJ et al. (2007) Enhanced biological carbon consumption in a high CO₂ ocean. *Nature*, **450**, 545–8.
- Sarthou G, Timmermans KR, Blain S et al. (2005) Growth physiology and fate of diatoms in the ocean: a review. *Journal of Sea Research*, **53**, 25–42.
- Schippers P, Lurling M, Scheffer M (2004) Increase of atmospheric CO₂ promotes phytoplankton productivity. *Ecology Letters*, **7**, 446–451.
- Schulz KG, Riebesell U (2013) Diurnal changes in seawater carbonate chemistry speciation at increasing atmospheric carbon dioxide. *Marine biology*, **160**, 1889–1899.
- Schulz KG, Bellerby RGJ, Brussaard CPD et al. (2013) Temporal biomass dynamics of an Arctic plankton bloom in response to increasing levels of atmospheric carbon dioxide. *Biogeosciences*, **10**, 161–180.
- Sharp JH (1974) Improved analysis for particulate organic carbon and nitrogen from seawater. *Limnology and Oceanography*, **19**, 984–989.
- Smayda T, Boleyn B (1966) Experimental observations on the flotation of marine diatoms. II. *Skeletonema costatum* and *Rhizosolenia setigera*. *Limnology and Oceanography*, **11**, 18–34.
- Sommer U (1996) Plankton Ecology: The past two decades of progress. *Naturwissenschaften Aufsätze*, **83**, 293–301.
- Sommer U, Lengfellner K (2008) Climate change and the timing, magnitude, and composition of the phytoplankton spring bloom. *Global Change Biology*, **14**, 1199–1208.
- Sommer U, Aberle N, Engel A et al. (2007) An indoor mesocosm system to study the effect of climate change on the late winter and spring succession of Baltic Sea phyto- and zooplankton. *Oecologia*, **150**, 655–67.
- Sommer U, Adrian R, Bauer B et al. (2012a) The response of temperate aquatic ecosystems to global warming: novel insights from a multidisciplinary project. *Marine Biology*, **159**, 2367–2377.
- Sommer U, Aberle N, Lengfellner K et al. (2012b) The Baltic Sea spring phytoplankton bloom in a changing climate: an experimental approach. *Marine Biology*, **159**, 2479–2490.
- Taucher J, Schulz KG, Dittmar T et al. (2012) Enhanced carbon overconsumption in response to increasing temperatures during a mesocosm experiment. *Biogeosciences*, **9**, 3531–3545.
- Thomsen J, Gutowska MA, Saphörster J et al. (2010) Calcifying invertebrates succeed in a naturally CO₂-rich coastal habitat but are threatened by high levels of future acidification. *Biogeosciences*, **7**, 3879–3891.

Chapter II

- Tortell P, DiTullio G, Sigman D et al. (2002) CO₂ effects on taxonomic composition and nutrient utilization in an Equatorial Pacific phytoplankton assemblage. *Marine Ecology Progress Series*, **236**, 37–43.
- Tortell PD, Payne CD, Li Y et al. (2008) CO₂ sensitivity of Southern Ocean phytoplankton. *Geophysical Research Letters*, **35**, L04605.
- Utermöhl H (1958) Zur Vervollkommnung der quantitativen Phytoplankton-Methodik. *Mitteilungen der Internationalen Vereinigung für Theoretische und Angewandte Limnologie*, **9**, 263–272.
- Wasmund N, Göbel J, Bodungen BV (2008) 100-years-changes in the phytoplankton community of Kiel Bight (Baltic Sea). *Journal of Marine Systems*, **73**, 300–322.
- Wiltshire KH, Malzahn AM, Wirtz K et al. (2008) Resilience of North Sea phytoplankton spring bloom dynamics: An analysis of long-term data at Helgoland Roads. *Limnology and Oceanography*, **53**, 1294–1302.
- Wohlers J, Engel A, Zöllner E et al. (2009) Changes in biogenic carbon flow in response to sea surface warming. *Proceedings of the National Academy of Sciences of the United States of America*, **106**, 7067–72.
- Wohlers-Zöllner J, Breithaupt P, Walther K et al. (2011) Temperature and nutrient stoichiometry interactively modulate organic matter cycling in a pelagic algal-bacterial community. *Limnology and Oceanography*, **56**, 599–610.
- Wohlers-Zöllner J, Biermann A, Engel A et al. (2012) Effects of rising temperature on pelagic biogeochemistry in mesocosm systems: a comparative analysis of the AQUASHIFT Kiel experiments. *Marine Biology*, **159**, 2503–2518.
- Wurl O, Min Sin T (2009) Analysis of Dissolved and Particulate Organic Carbon with the HTCO Technique. In: *Practical guidelines for the analysis of seawater* (ed Wurl O), pp. 33–48. CRC Press Taylor and Francis group.
- Yoshimura T, Suzuki K, Kiyosawa H et al. (2013) Impacts of elevated CO₂ on particulate and dissolved organic matter production: microcosm experiments using iron-deficient plankton communities in open subarctic waters. *Journal of Oceanography*, **69**, 601–618.

	Control	High CO ₂	Greenhouse
Mean water temperature (°C)	4.8 ± 0.3	5.4 ± 0.3	8.5 ± 0.4
Initial pCO₂ (µatm)	536 ± 25	1017 ± 46	990 ± 57
Initial nutrient concentrations (µmol L⁻¹)			
NO ₃ ⁻		11 ± 0.2	
PO ₄ ⁻³		0.78 ± 0.05	
Si(OH) ₂		30 ± 1.5	
NH ₄ ⁺		2.4 ± 0.2	
Salinity		20	

Table 1. Summary of initial experimental conditions. Mean water temperature for each treatment throughout the experiment, initial partial pressure of CO₂ after CO₂ manipulation (pCO₂), initial dissolved inorganic nutrient concentrations and salinity.

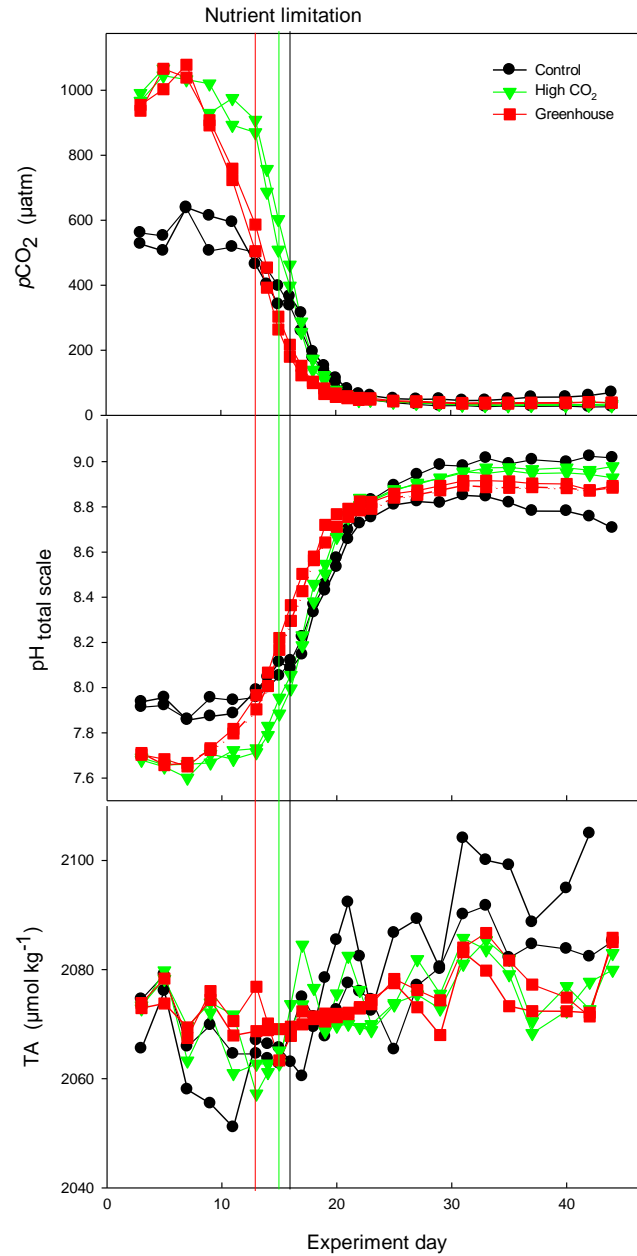


Figure 1. Evolution of A) CO_2 partial pressure ($p\text{CO}_2$), B) pH_{total} and C) total alkalinity during the experiment. Where $p\text{CO}_2$ and pH were calculated from measured TA and measured DIC (see methods for details). Vertical lines indicate time of nitrate depletion; red line corresponds to Greenhouse treatment, green line to High CO_2 and black to Control treatment.

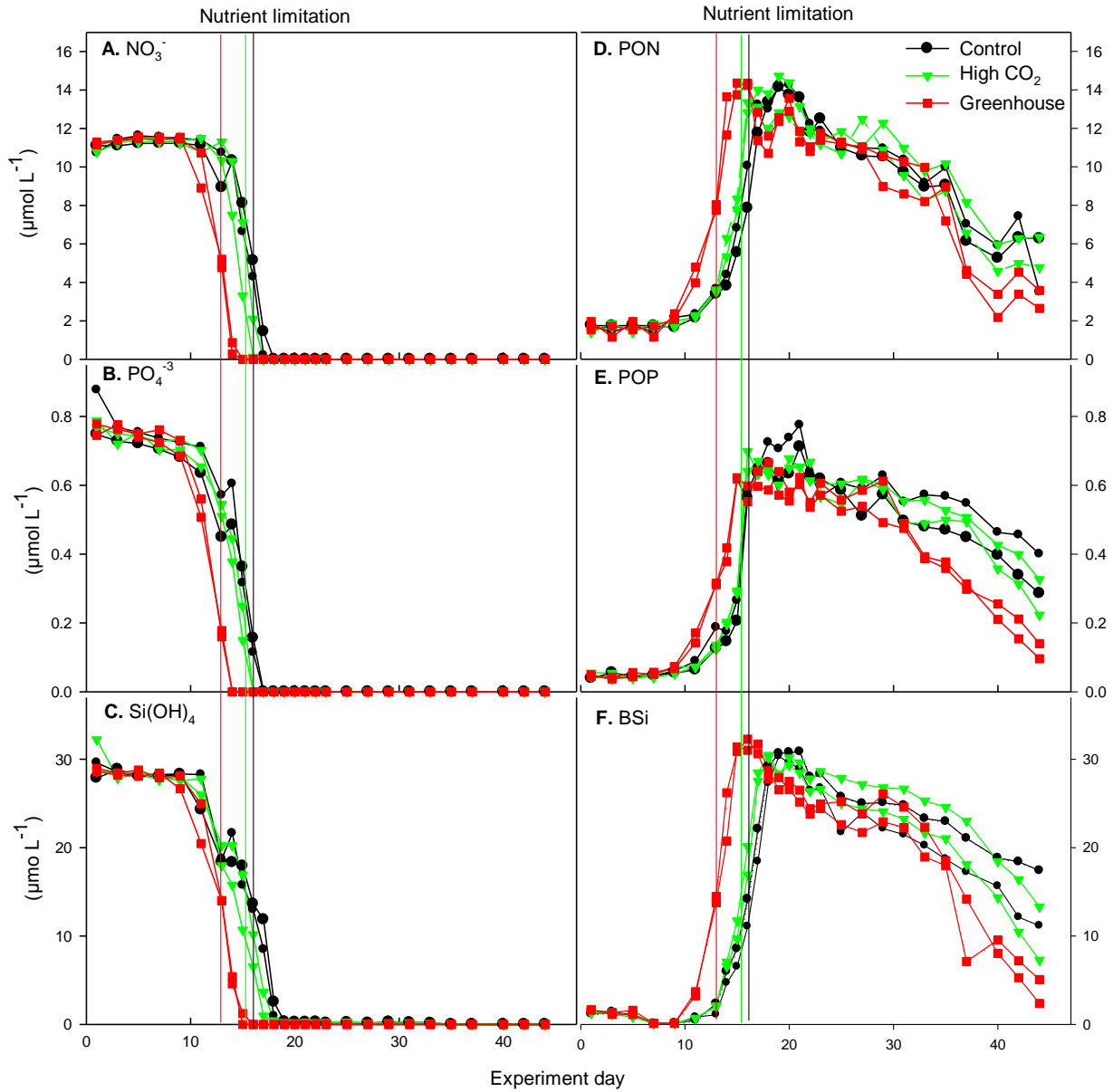


Figure 2. Drawdown of major dissolved inorganic nutrients and development of particulate organic matter during the experiment. (A) nitrate, (B) phosphate, (C) silicate, (D) particulate organic nitrogen, (E) particulate organic phosphorous and (F) biogenic silica. Vertical lines indicate time of nitrate depletion; red line corresponds to Greenhouse treatment, green line to High CO_2 and black to Control treatment.

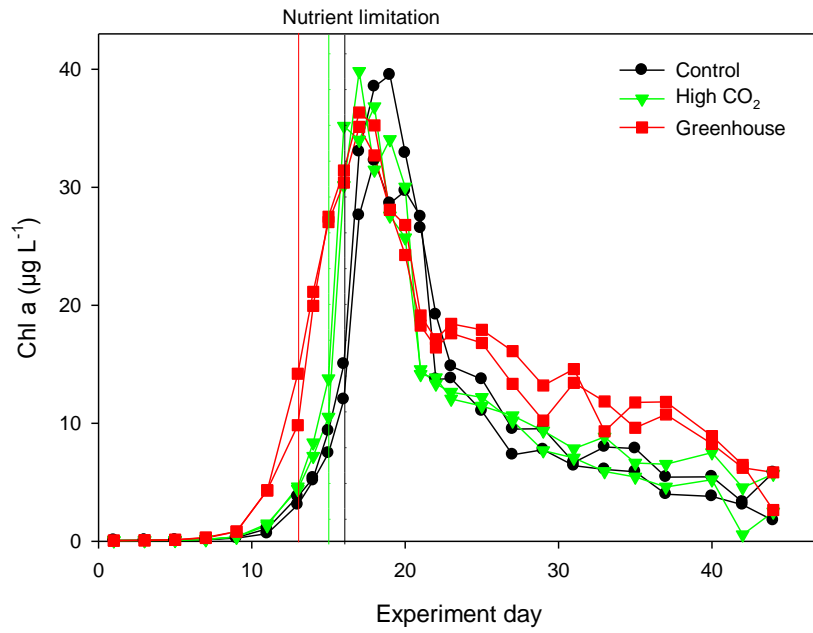


Figure 3. Temporal development of total Chlorophyll *a* during the experiment. Vertical lines indicate time of nitrate depletion; red line corresponds to Greenhouse treatment, green line to High CO₂ and black to Control treatment.

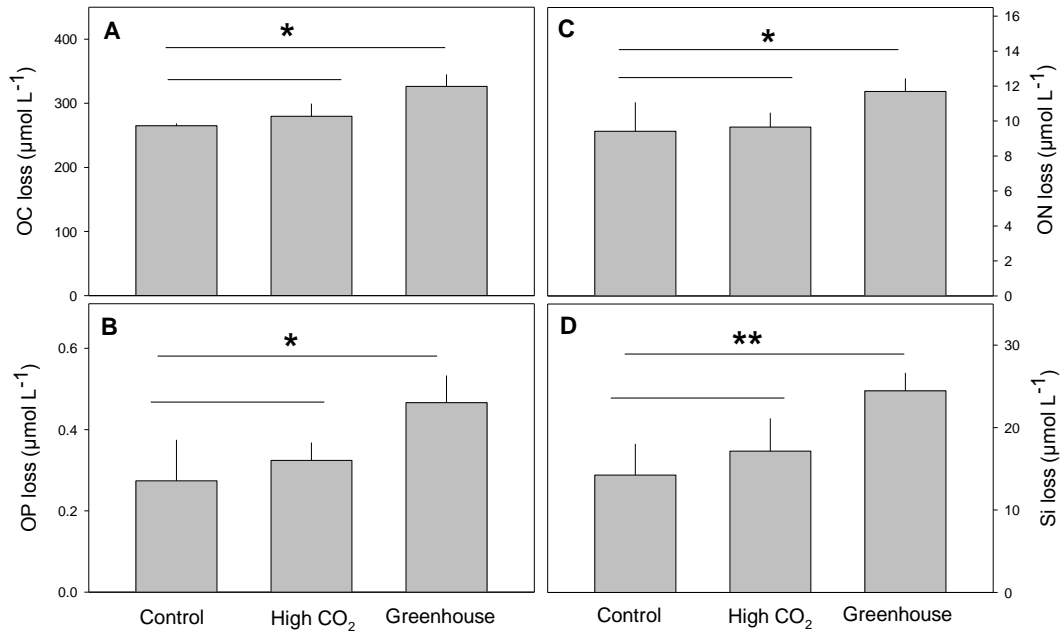


Figure 4. Losses of organic matter at the end of the experiment for A) organic carbon, B) organic phosphorous, C) organic nitrogen and D) silicate. Student's t-test were performed between the Control and High CO₂ treatment and Control and Greenhouse treatment. Stars show significant differences obtained from Student's t-tests (* = $p < 0.05$, ** = $p < 0.01$).

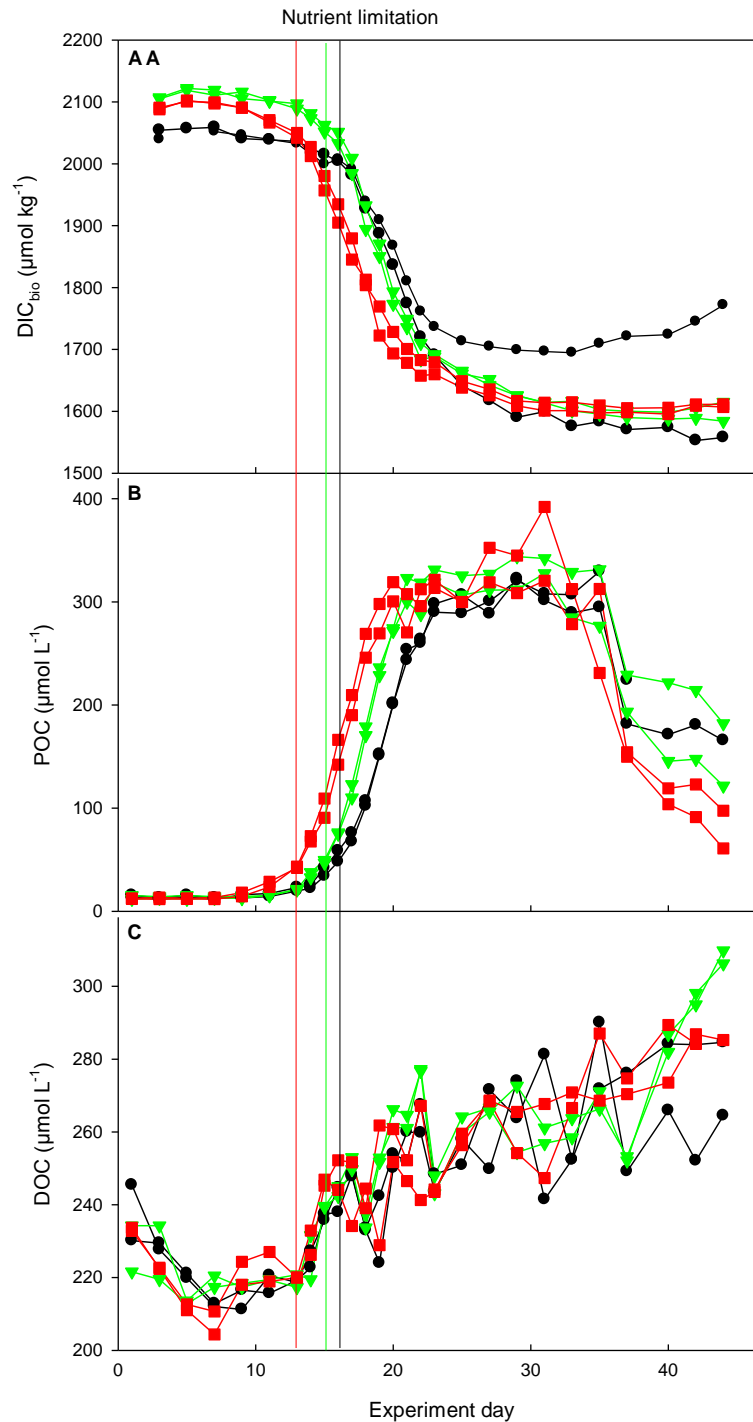


Figure 5. Carbon dynamics during the experiment for A) dissolved inorganic carbon (corrected for gas exchange) B) particulate organic carbon and C) dissolved organic carbon. Color coding according to Figure 1. Vertical lines indicate time of nitrate depletion; red line corresponds to Greenhouse treatment, green line to High CO_2 and black to Control treatment. Please note that concentrations of one of the Controls deviates from its duplicate after the bloom peak due to a faulty lid (see section *Carbon cycling* in the Results for details).

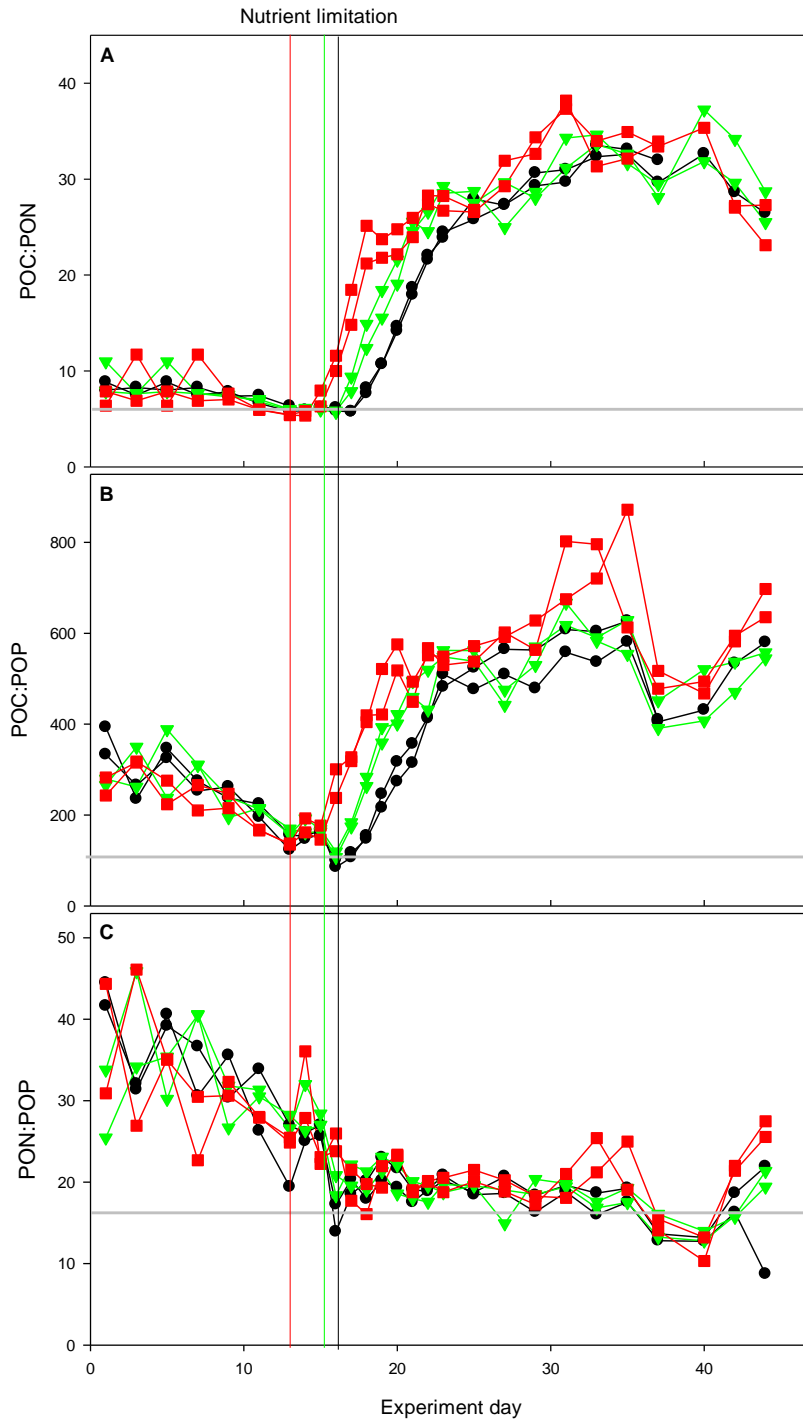


Figure 6. Elemental stoichiometry of particulate organic matter (POM) during the experiment. Color coding according to Figure 1. Vertical lines indicate time of nitrate depletion; red line corresponds to Greenhouse treatment, green line to High CO₂ and black to Control treatment. Grey horizontal lines represent Redfield proportions of A) 6.6 B) 106:1 and C) 16:1.

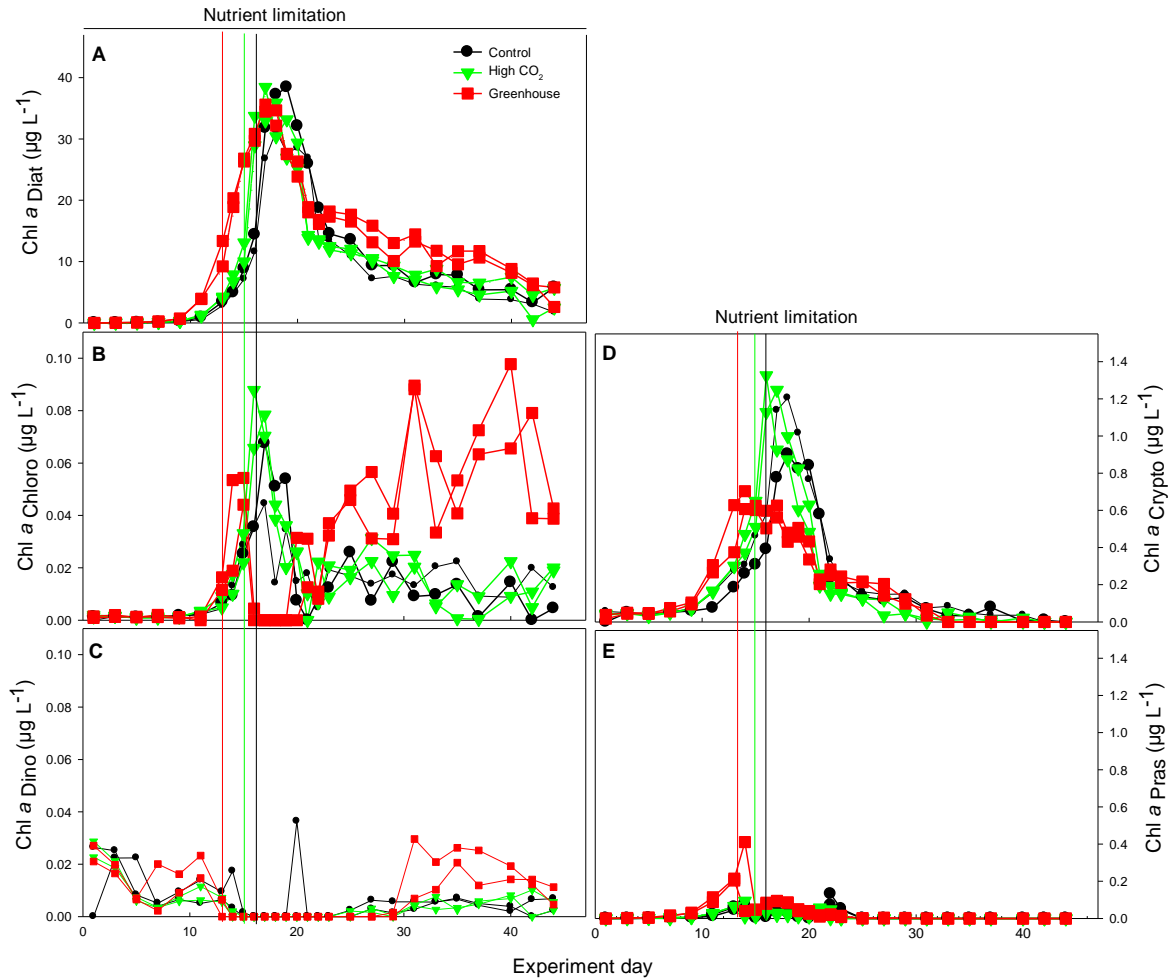


Figure 7. Chlorophyll *a* equivalent concentrations of: A) Diatoms, B) Chlorophytes, C) Dinophytes, D) Cryptophytes and E) Prasinophytes analyzed by CHEMTAX. Vertical lines indicate time of nitrate depletion; red line corresponds to Greenhouse treatment, green line to High CO_2 and black to Control treatment.

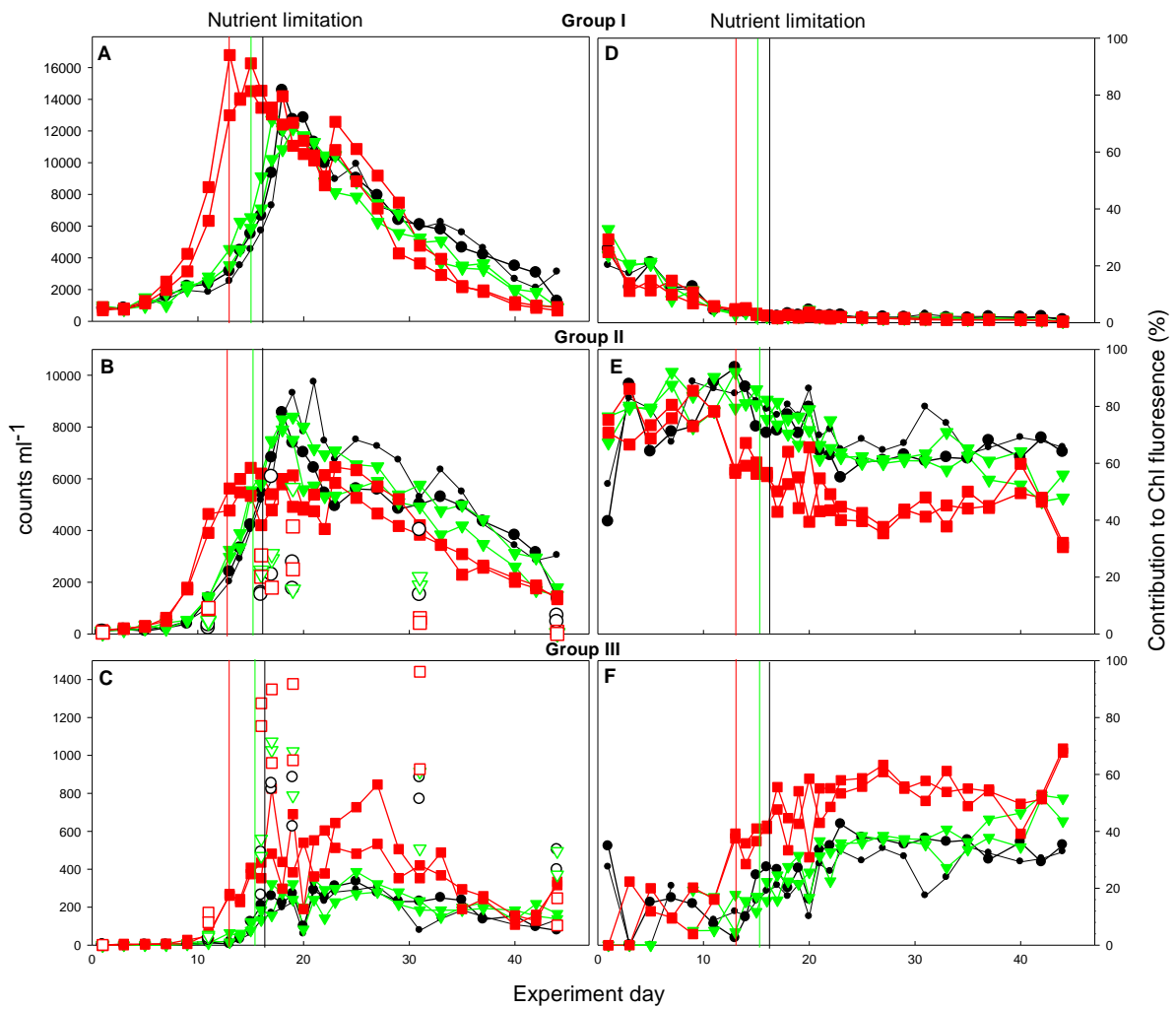


Figure 8. Cell counts according to group sizes (left panel) and percent contribution to total Chlorophyll fluorescence (right panel). Filled symbols are based on flow cytometry and empty symbols in B and C represent groups from microscopic counts grouped into relevant size categories. Color coding according to Figure 1. Vertical lines indicate time of nitrate depletion; red line corresponds to Greenhouse treatment, green line to High CO_2 and black to Control treatment.

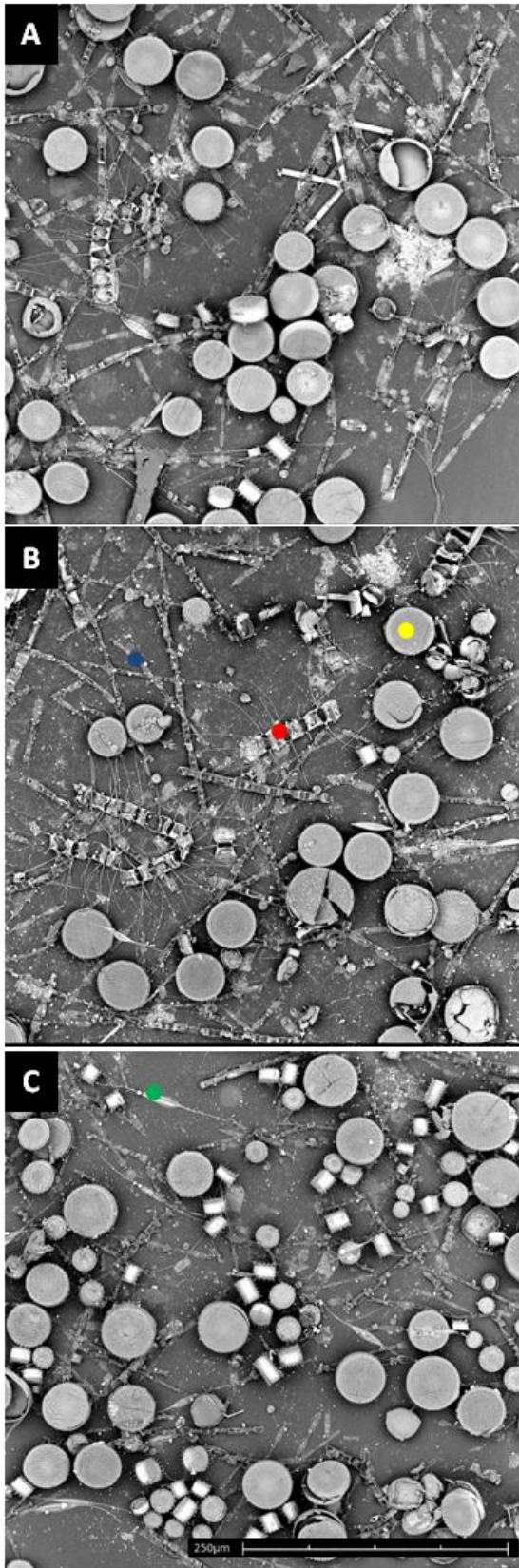
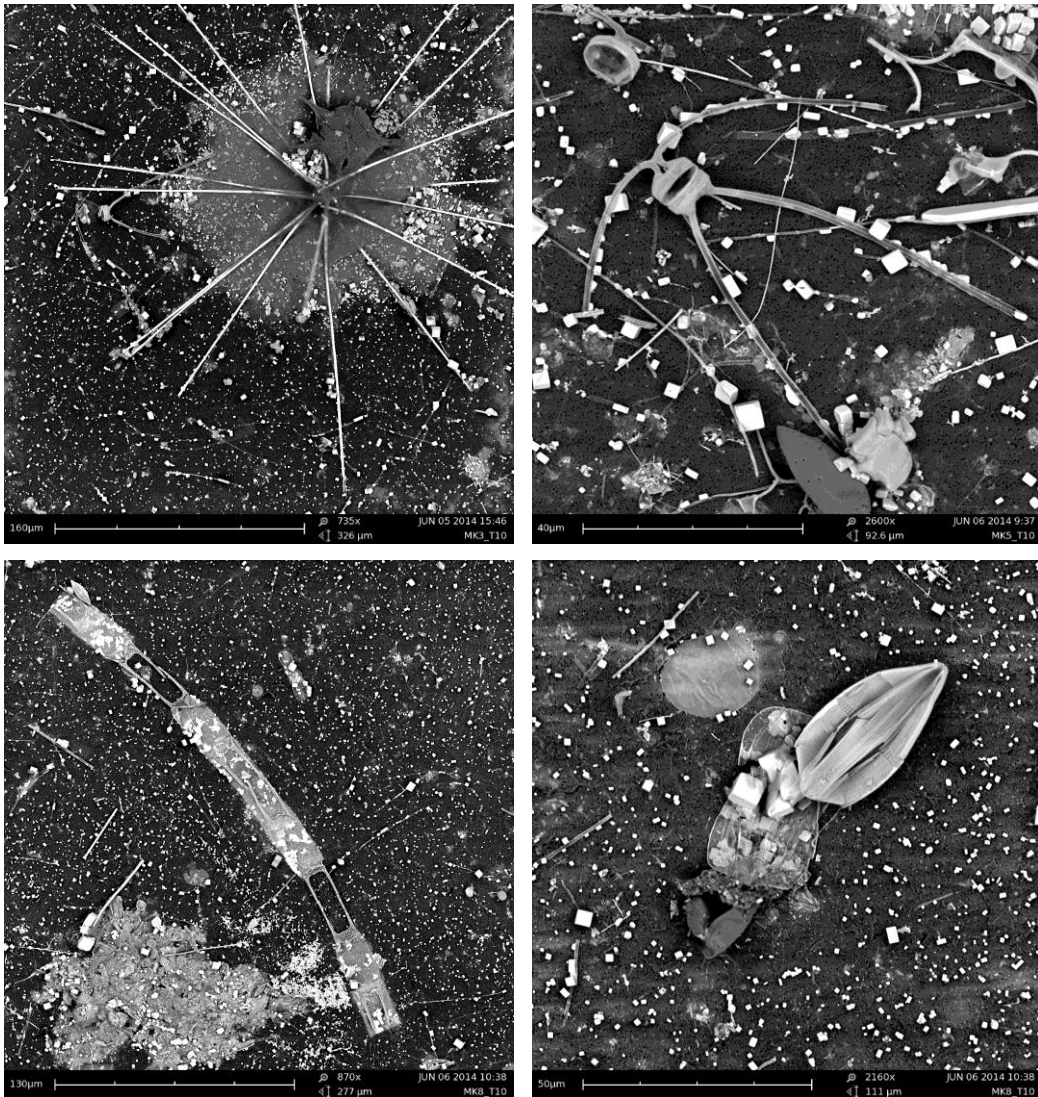


Figure 9. Representative scanning electron microscopy pictures of species composition on day 19 of the experiment under A) Control, B) High CO₂ and C) Greenhouse conditions. Yellow dot: *Thalassiosira* sp, red dot: 'large' *Chaetoceros* sp, green dot: *Nitzschia* sp and blue dot: *S. costatum*.

Chapter III



Scanning electron microscope pictures of different plankton species during a summer bloom in the Mediterranean Sea

Nor does abundance necessarily relate to importance. Carbon is only the fifteenth most common element, accounting for a very modest 0.048 per cent of Earth's crust, but we would be lost without it. What sets the carbon atom apart is that it is shamelessly promiscuous. It is the party animal of the atomic world, latching on to many other atoms (including itself) and holding tight, forming molecular conga lines of hearty robustness – the very tick of nature necessarily to build proteins and DNA.

Bill Bryson

Particulate and dissolved organic matter dynamics during a nutrient- induced phytoplankton bloom under ocean acidification and warming scenarios

Scarlett Sett¹, Souad Annane², Gustavo Ferreyra², Francesca Vidussi³, Bezhad Mostajir³, Carolina Cantoni⁴, Anna Luchetta⁴ and Ulf Riebesell¹

¹ GEOMAR Helmholtz Centre for Ocean Research Kiel, Düsternbrooker Weg 20, 24105 Kiel, Germany

² Institut des Sciences de la Mer (ISMER), Université du Québec à Rimouski (UQAR), Rimouski, Québec G5L 3A1, Canada

³ Ecosystemes Lagunaires UMR 5119 CNRS-Université Montpellier 2- IRD-IFREMER, Station Méditerranéenne de l'environnement Littoral, Sete, France

⁴ CNR- National Research Council of Italy, ISMAR – Marine Sciences Institute in Trieste, Viale Romolo Gessi 2, 34123 Trieste, Italy

Abstract

Mesocosm experiments were conducted in the Mediterranean Sea (South of France) to investigate the individual and combined effects of ocean acidification and warming on the build-up and decline of particulate and dissolved organic matter (POM and DOM, respectively) during a nutrient-induced phytoplankton bloom. Four treatments were set up in triplicates under the following conditions: (1) Control - **C** (*in situ* temperature and $p\text{CO}_2$), (2) Acidified - **A** (*in situ* temperature, initially +400 $\mu\text{atm } p\text{CO}_2$ above control), (3) Warming - **T** (+3°C above control, *in situ* $p\text{CO}_2$) and (4) Combined acidified and warming - **TA** (+3°C and initially +400 $\mu\text{atm } p\text{CO}_2$ above control). Once target temperature and $p\text{CO}_2$ levels were established, nutrients were added to induce phytoplankton growth. Changes in POM and DOM were monitored during 12 days. After addition of inorganic nutrients, POM increased to maximum concentrations. POM build-up was enhanced in the acidified treatments (A and TA) while lowest POM build-up was observed in the warmed treatment (T). DOC concentrations were slightly higher in the acidified treatments (A and TA) while DON and DOP remained relatively stable for the duration of the experiment. Transparent exopolymer particle concentration, TEP, increased after nutrient additions and was three fold higher in the acidified treatment compared to the control. Elemental stoichiometry of POM was carbon-enriched and remained higher than Redfield proportions in all treatments.

Chapter III

Introduction

Increasing anthropogenic CO₂ in the atmosphere is leading to changes in the climate system at an unprecedented pace while affecting all natural systems on Earth (Parmesan & Yohe, 2003). While the effects of climate change have been partially mitigated by the ocean's capability to absorb and sequester CO₂ and heat (Sabine *et al.*, 2004; Levitus *et al.*, 2012) there have been serious consequences for the ocean's chemical and physical properties. Increasing CO₂ concentrations in the atmosphere have exacerbated the natural "greenhouse effect" on Earth and increased global average temperatures. An increase of 2.5-5.1°C in the Mediterranean regions is projected by the end of the century, depending on emission scenario by the IPCC 2014 (Field *et al.*, 2014). Additionally, increasing atmospheric CO₂ has also modified the carbonate chemistry speciation of seawater towards an increase in bicarbonate ions [HCO₃²⁻] and dissolved CO₂ and a decrease in carbonate ions [CO₃²⁻] and pH in a process known as ocean acidification, OA (Wolf-Gladrow *et al.*, 1999; Caldeira & Wickett, 2003). With the continuous utilization of fossil fuels pH is projected to decrease by ~0.4 units towards the end of this century (Orr *et al.*, 2005). These changes in the ocean's chemical and physical properties will potentially modify marine biogeochemical cycling (Riebesell & Tortell, 2011; Rees, 2012) but the challenge remains on to what extent and in which directions (i.e. positive or negative feedbacks) the marine environment will respond.

Up to date, the individual effect of temperature and CO₂ on natural phytoplankton communities has been extensively studied through mesocosm experiments. Independently, both factors have been reported to modify primary production, PP (Hein & Sand-Jensen, 1997; Schippers *et al.*, 2004; Tortell *et al.*, 2008; Egge *et al.*, 2009; Lewandowska *et al.*, 2012; Engel *et al.*, 2013) species community composition (Tortell *et al.*, 2002, 2008; Hare *et al.*, 2007; Feng *et al.*, 2009; Lewandowska & Sommer, 2010; Brussaard *et al.*, 2013) and biomass buildup (Keller *et al.*, 1999; Isla *et al.*, 2008; O'Connor *et al.*, 2009; Lassen *et al.*, 2010; Taucher *et al.*, 2012; Wohlers-Zöllner *et al.*, 2012; Biermann *et al.*, 2014). Warming is expected to enhance heterotrophic over autotrophic processes therefore modifying energy transfer across the food web and redistributing carbon flow into the dissolved rather than the particulate pool (Wohlers *et al.*, 2009). Furthermore, changes in community composition are of particulate importance because primary and secondary production are recognized as key components of carbon fluxes modifying food web structure and ecosystem productivity (Legendre & Rivkin, 2002).

Our experiments were conducted in the Thau lagoon (France). This region in the Mediterranean Sea is of particular interest due to their economically productive shellfish farming (Gangnery *et al.*, 2003). If the transfer of energy from primary producers to higher trophic levels in these ecosystems would be disrupted, it would lead to serious socio-economical implications. Therefore, a factorial mesocosm experiment was carried out with warming, OA and a combination of

Chapter III

both to investigate if these environmental drivers would modify phytoplankton biomass buildup (POM) and dissolved organic matter (DOM) dynamics during a nutrient-induced summer bloom. The corresponding increases in temperature and CO₂ were according to projections by the IPCC 2014 for the end of this century.

Materials and Methods

Experimental set-up

A mesocosm experiment was carried out between the 30th of May and 11th of June 2012 at the MEDIMEER facilities (Mediterranean Platform for Marine Ecosystem Experimental Research) in the South of France at the shore of the coastal Thau Lagoon in Sete (43°24'49"N, 3°41'19"E). Twelve mesocosm bags (3 m long and 1.2 m wide, made of vinylacetate mixed-polyethylene) were fixed to individual floating structures anchored to a platform. Mesocosms were submerged 2 m and covered by a transparent dome to prevent contamination and water exchange in case of rain or high wave activity. Additionally, a transparent floating lid (same material as mesocosm bags) was placed on the water surface to minimize gas exchange with the atmosphere. Mesocosm bags were filled simultaneously from screened (1000 mm) subsurface lagoon water up to a volume of ~2300 l. Each mesocosm was equipped with a pump which ensured homogenization of the water column (see Nougier *et al.*, 2007 for details). Four treatments were set-up in triplicates: Control – “C” (*in situ* pCO₂ and temperature), Acidified – “A” (*in situ* temperature and initially +400 µatm pCO₂ above *in situ*), Temperature – “T” (*in situ* pCO₂ and +3°C above *in situ*) and Acidified + Temperature – “TA” (+400 µatm pCO₂ and +3°C above *in situ*). Increased pCO₂ and temperature levels were chosen according to projections by the IPCC 2014.

Temperature, pCO₂ and nutrient manipulation

Temperature and CO₂ manipulations were performed over a period of several days. Water temperature in treatments T and TA was increased by using a submersible heating element (12 kW, Galvatec) suspended at mid depth of the mesocosm bag (Nougier *et al.*, 2007). Temperature was increased in a 2-day stepwise manner (i.e. 1.5°C d⁻¹) to a final temperature difference of +3°C above the Control treatment. Temperature was monitored every 30 seconds by sensors (Campbell scientific 107) positioned at three different depths in the bag and maintained at +3°C above the control with daily fluctuations using a Campbell scientific data logger (CR23X).

For the CO₂ manipulation, filtered seawater from the lagoon was aerated with pure CO₂ (99.9995%) for at least 4 hrs prior to the manipulation. The addition of CO₂-enriched water was to increase dissolved inorganic carbon (DIC) in treatments A and TA while leaving total alkalinity (A_T) relatively constant, mimicking what happens in the ocean (Schulz *et al.*, 2009). Target CO₂

Chapter III

concentrations were +400 $\mu\text{atm } p\text{CO}_2$ above the control, which represent levels projected by end of this century. The CO_2 manipulation was performed over a 3-day stepwise manner (T_1 - T_3). Additionally, in order to minimize gas exchange with the atmosphere we placed transparent floating lids on the water surface of the mesocosms. The lids remained in place throughout the experiment and were only lifted once a day during sampling.

The addition of dissolved inorganic nutrients on T_5 was meant to initiate the phytoplankton bloom. Nutrients were added according to Redfield proportions: 4 $\mu\text{M NaNO}_3$, 0.25 $\mu\text{M KHPO}_4$, 4 $\mu\text{M Na}_2\text{O}_3\text{Si} \cdot 5 \text{H}_2\text{O}$.

General sampling

Sampling was carried out daily starting at 8:30 a.m. and lasted approximately 2 hrs. Water samples were taken at mid-depth by two methods: 1) with a hand-operated water sampler (5 L Niskin bottle, daily cleaned and rinsed with acid) and 2) with a hand-operated pump into 20 L polycarbonate canisters (daily cleaned and rinsed with acid). Water samples from the Niskin bottle were taken for dissolved organic carbon, nitrogen and phosphorous (i.e. DOC, DON and DOP, respectively) as well as carbonate chemistry parameters (i.e. DIC, A_T and pH) and carefully transferred to their specific containers with Teflon tubing. Water samples for biogeochemical and biological variables were taken from the 20 L canisters. Canisters were gently mixed before sub-sampling to ensure homogenous water samples.

Biological and chemical analysis

Samples for A_T and pH were taken directly from the Niskin bottle into the respective Nalgene bottle or glass cuvette (i.e. A_T and pH, respectively) and measured immediately. A_T samples were poisoned with HgCl_2 and measured 24 hrs later. Samples were measured with an automatic potentiometric titrator Metrohm 685 according to Hernandez-Ayon *et al.*, 1999. Samples for determination of pH (total scale, pH_{total}) were measured using a double-wavelength spectrophotometric procedure with a dye indicator according to Clayton & Byrne, 1993. Measurements for A_T and pH were calibrated against certified reference material batch 117 (CRM, Dickson, 2010). Unfortunately, a large portion of the DIC samples (>40%) was lost during transport and thus the concentrations were calculated from measured A_T and pH_{total} , temperature, salinity and nutrients (i.e. phosphate and silicate). Constants from Mehrbach *et al.* 1973 refitted by Dickson and Millero 1987 for K_1 and K_2 and Dickson for KHSO_4 were used to calculate carbonate chemistry parameters with the program CO2SYS (Lewis & Wallace, 1998).

Samples for dissolved inorganic nutrients nitrate (NO_3^-), nitrite (NO_2^-), and phosphate (PO_4^{3-}) were filtered through GF/F and analyzed on a segmented flow autoanalyzer (SEAL QuAAtro)

Chapter III

according to Hansen & Koroleff, 1999. Samples for dissolved silicate were filtered through cellulose acetate filters and measured according to Hansen & Koroleff, 1999.

Samples for Chl *a* were filtered (200 mbar) onto GF/F filters and immediately frozen at -80°C until analysis. Extraction of Chl *a* was with 95% methanol and analyzed via HPLC (High Pressure Liquid Chromatography) according to Zapata *et al.*, 2000. The HPLC was calibrated using commercial standards (DHI and Sigma).

Particulate and dissolved organic matter

Samples for particulate organic carbon and nitrogen (POC and PON, respectively) and particulate organic phosphorous (POP) were filtered (200 mbar) onto pre-combusted GF/F (450°C for 5 hrs) and stored at -20°C. Prior to analysis, filters for POC/PON were placed in a desiccator above fuming acid (37% HCl) for 2 hours to remove all inorganic carbon and subsequently dried overnight at 60 °C. POC/PON samples were measured simultaneously with a EuroVector elemental analyzer according to Sharp, 1974. POP samples were oxidized to orthophosphate with Oxysolv (MERCK) and measured according to Hansen & Koroleff, 1999. Biogenic silicate (BSi) samples were filtered (200 mbar) onto cellulose acetate filters and stored at -20°C. BSi samples were measured spectrophotometrically according to Hansen & Koroleff, 1999.

Samples for dissolved organic carbon, nitrogen and phosphorus (DOC, DON and DOP, respectively) were filtered through pre-combusted GF/F (450°C for 5 hrs) with a STEPDOS pump (continuous flow of 100 mL min⁻¹) into 20 mL glass vials (i.e. DOC) and 100 mL nalgene bottles (i.e. DON/DOP) and immediately frozen. DOC samples were analyzed according to Wurl & Min Sin, 2009 using a HTCO method (high-temperature catalytic oxidation) on a Shimadzu TOC-V. A calibration against deep-sea reference material was performed to test for accuracy of the method. DON/DOP samples were oxidized with Oxisolv (MERCK) into dissolved N and P and measured in a two-channel autoanalyzer (SEAL QuAArto) according to Hansen & Koroleff, 1999. DON and DOP concentrations were obtained by subtracting DIN and DIP concentrations, respectively.

Calculation of maximum biomass buildup and losses

Maximum build-up of POM was calculated by subtracting the initial stock after nutrient addition (concentrations on T5, \pm standard deviation of triplicates) from each experimental day. In most cases, maximum POM concentrations was two days after nutrient depletion and to account for variability the average of the two highest consecutive days was taken as maximum buildup. Losses of POM were calculated by subtracting final concentrations (T12) from initial stock after nutrient addition (concentration on T5, \pm standard deviation of triplicates).

Chapter III

Results and Discussion

This mesocosm study investigated the effects OA (A treatment), warming (T treatment) and combined OA and warming (TA treatment) conditions on the POM and DOM dynamics during a nutrient-induced phytoplankton bloom in the Mediterranean Sea. However, the initial low nutrient concentrations and high Chl *a* and POM concentrations could have indicated that the plankton community was in a post bloom phase when water for the experiments was collected. During the first phase of the experiment (days 1 to 5) decreasing concentrations of Chl *a* and BSi were observed in all treatments and indicated decreasing autotrophic biomass, whereas POC, PON and POP only show slight fluctuations (Figure 3, 4D-F, 5B).

Initial experimental conditions

Temperature and $p\text{CO}_2$ manipulations were performed in a step-wise manner to prevent initial shocks to the community by drastically changing environmental conditions (Figure 1).

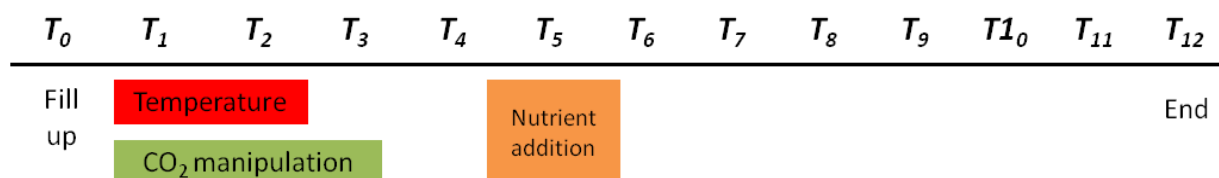


Figure 1. Timeline of experimental manipulations. Starting from filling (T_0) to CO₂ manipulation over a 3-day stepwise manner (T_1 - T_3), temperature manipulation over 2 days (T_1 - T_2) and nutrient manipulation on day 5 once CO₂ and temperature target levels were established (T_5).

Temperature at the beginning of the experiment (T_1) was on average 22.1 ± 0.03 °C. Target temperatures in the warmed treatments (i.e. T and TA) of + 3°C above *in situ* conditions were established on T_3 . Temperatures in the C and A treatment were 23.1 ± 0.03 °C and 25.6 ± 0.6 °C in the T and TA treatments on T_3 (Figure 2B). Temperature was monitored with sensors every 30 sec and natural fluctuations in the C and A treatments were followed in the warmed mesocosms (T and TA) while keeping the ~3°C difference. Temperature decreased during the experiment from their respective target values on T_3 to final values on T_{12} of 20.4 ± 0.03 °C in the C and A treatments and 23.5 ± 0.08 °C in the T and TA treatments (Figure 2B).

$p\text{CO}_2$ was increased in the acidified treatments (A + TA) by additions of enriched CO₂ water over a period of 3 days from initial values of 471 ± 14 on T_1 to target levels of 874 ± 42 μatm $p\text{CO}_2$ on T_4 (Figure 2A). A difference of ~400 μatm above the C treatment was established in the A and TA treatments. Once target levels were established, $p\text{CO}_2$ decreased faster in the acidified treatments (A and TA) up to T_8 when values stabilized. A slight increase was observed in all treatments on day T_{10} followed by a decrease at the end of the experiment on T_{12} . Levels remained slightly higher in the

Chapter III

acidified treatments (A and TA) at the end of the experiment on T12 compared to the C and T treatments.

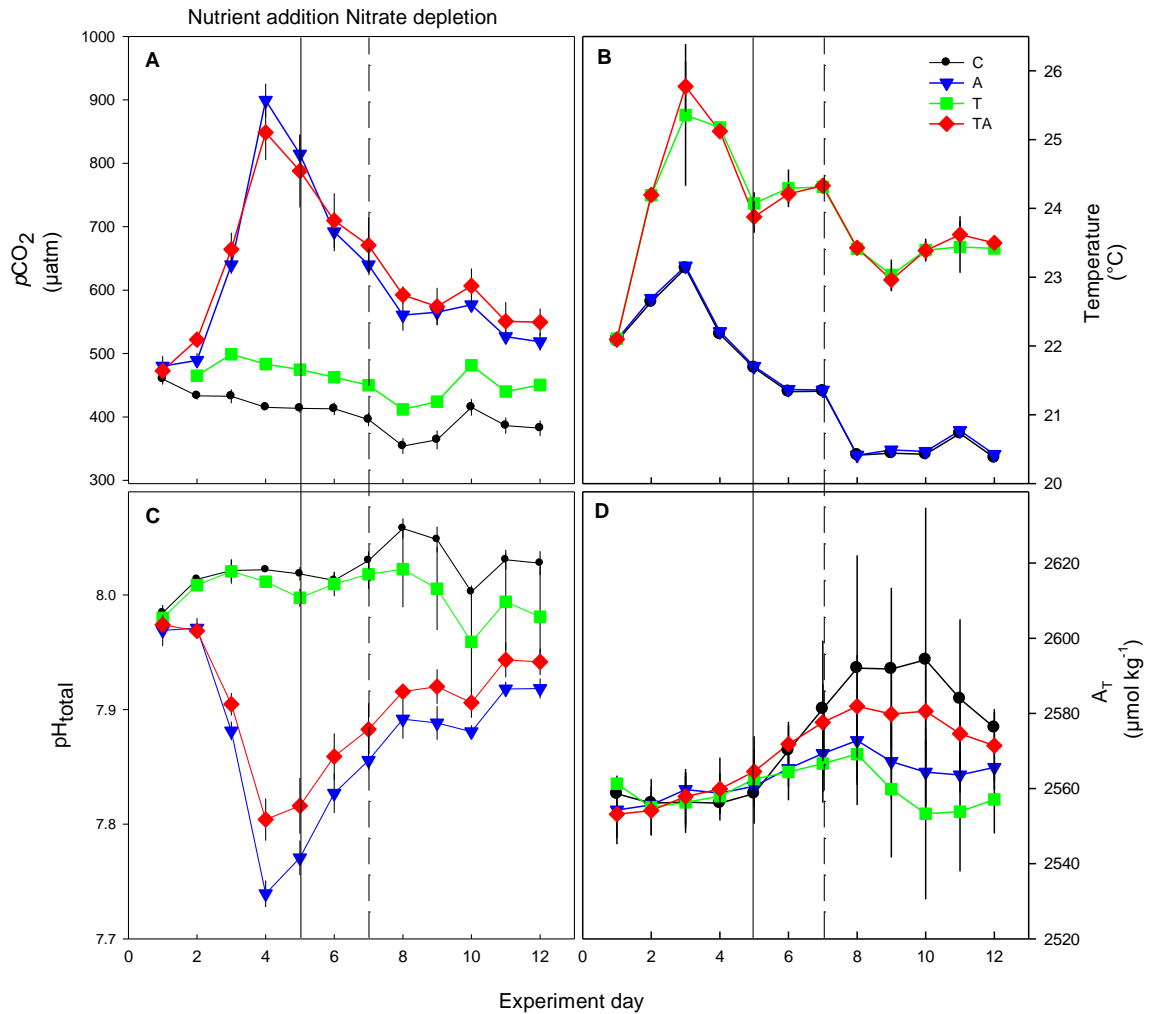


Figure 2. Carbonate chemistry and temperature during the experiment. A) partial pressure of CO_2 ($p\text{CO}_2$), B) temperature ($^\circ\text{C}$), C) pH (total scale) and D) total alkalinity – A_T . Solid vertical line indicates nutrient addition and dashed line indicates nitrate depletion.

Concomitant to the increase in $p\text{CO}_2$ in the acidified treatments (A and TA), pH was decreased from an initial average of 7.971 ± 0.01 to 7.739 ± 0.01 in the A and 7.804 ± 0.02 in the TA treatment (Figure 2C). Thereafter, pH values in the A and TA treatments increased rapidly until the end of the experiment. pH in the C and T treatments slightly increased at the beginning of the experiment by ~ 0.05 units and then remained stable up to T8 where highest values were observed followed by a decrease. Final pH in the C and T treatments was close to initial values while those in the A and TA treatments were ~ 0.1 units lower than initial values. Initial A_T was $\sim 2555.9 \pm 5.74 \mu\text{mol kg}^{-1}$ and slightly increased during the experiment (Figure 2D). Highest A_T was observed between T8-T10 in the C treatment with $2592.1 \pm 30 \mu\text{mol kg}^{-1}$, $2581.9 \pm 14 \mu\text{mol kg}^{-1}$ in the TA, $2572.88 \pm 12 \mu\text{mol kg}^{-1}$

Chapter III

kg⁻¹ in the A and 2569.1±14 μmol kg⁻¹ in the T treatment. Thereafter A_T decreased on all mesocosms to initial concentrations.

Uptake of inorganic nutrients and bloom development

Once the temperature and pCO₂ treatments were established the addition of inorganic nutrients was performed on T5 (Figure 1). Inorganic nutrients were added according to Redfield proportions to final concentrations of 4 μmol L⁻¹ NO₃⁻, 0.25 μmol L⁻¹ PO₄⁻³ and 4 μmol L⁻¹ Si(OH)₂ and simulated a natural up-welling event of after a storm or due to river discharge in this region. The addition of nutrients was performed on the evening of T5 and therefore, nutrient concentrations on T6 show that NO₃ was ~1.98 ± 0.3 μmol L⁻¹ which would indicate that half of the addition on day T5 (~4 μmol L⁻¹ NO₃) was taken up overnight, the same applies to PO₄.

Following the addition of nutrients on T5, a phytoplankton bloom developed in all mesocosms and was characterized by increasing Chl *a* and a rapid drawdown of inorganic nutrients (Figure 3 and 4A-C). NO₃ was the only nutrient to go under limitation 3 days after the addition and then slightly increased and remained at low levels (Figure 4A). PO₄ remained at low but detectable concentrations and Si remained high after addition on T5 (data still under validation, Figure 4B-C).

Chl *a* decreased during the first 5 days of the experiment when treatment conditions were being established (i.e. temperature and pCO₂) but rapidly increased after nutrient addition on T5 (Figure 3). On average Chl *a* increased from 1.35 ± 0.3 μg Chl *a* L⁻¹ on T5 to maximum concentrations of 3.1 ± 0.3 μg Chl *a* L⁻¹ in the Control, 4.0 ± 0.3 μg Chl *a* L⁻¹ in the A, 3.7 ± 0.1 μg Chl *a* L⁻¹ in the T and 4.5 ± 0.2 μg Chl *a* L⁻¹ in the TA treatment on T7. Although initial Chl *a* concentrations were similar between the treatment, Chl *a* in the control always showed the lowest values compared to the other treatments (Figure 3). No acceleration in the timing of peak Chl *a* due to warming was observed during our experiments and peak concentrations were highest in the TA treatment. Maximum Chl *a* concentrations matched to the peaks in marker specific pigments of diatoms, dinoflagellates and prymnesiophytes (Figure 3, 4).

Community composition derived from HPLC pigment analysis

The initial phytoplankton community was very similar between the different treatments and was composed of diatoms (60%), dinoflagellates (15%), prymnesiophytes (10%), green algae (10%), cryptophytes (8%) and cyanobacteria (2%)(Figure 4). Two days after the addition of inorganic nutrients peaks in pigment markers were observed in all treatments (Figure 4). Initially, diatoms followed the same temporal development pattern as Chl *a*, decreasing in the first part of the experiment (i.e. T1-T5) and after nutrient addition increasing to maximum concentrations on T7 (Figure 4A). A second diatom peak was observed in the warmed treatments (T and TA) on T9, however this was only

Chapter III

observed in the T treatment in total Chl *a* (Figure 3 and 4A). Contribution from diatoms during maximum Chl *a* was ~50% with lowest values observed in the Control treatment. Dinoflagellates remained stable during the first part of the experiment (i.e. T1-T6) and increased after the addition of nutrients to peak concentrations on T8 (Figure 4B). Dinoflagellates showed highest contribution to total Chl *a* in the TA treatment. Prymnesiophytes were the only group which showed an increase during the first part of the experiment (i.e. T1-T6) with slightly higher values in the TA treatment (Figure 4C). After nutrient addition prymnesiophytes increased again to maximum concentrations but their contribution to total Chl *a* during peak concentrations was ~20% and thereafter decreased until the end of the experiment. Green algae contributed ~5-8% to total Chl *a* during peak concentrations but increased towards the end of the experiment (Figure 4D). Contribution from cryptophytes and cyanobacteria during peak Chl *a* was ~2-4% (combined) and remained at about those levels throughout the experiments.

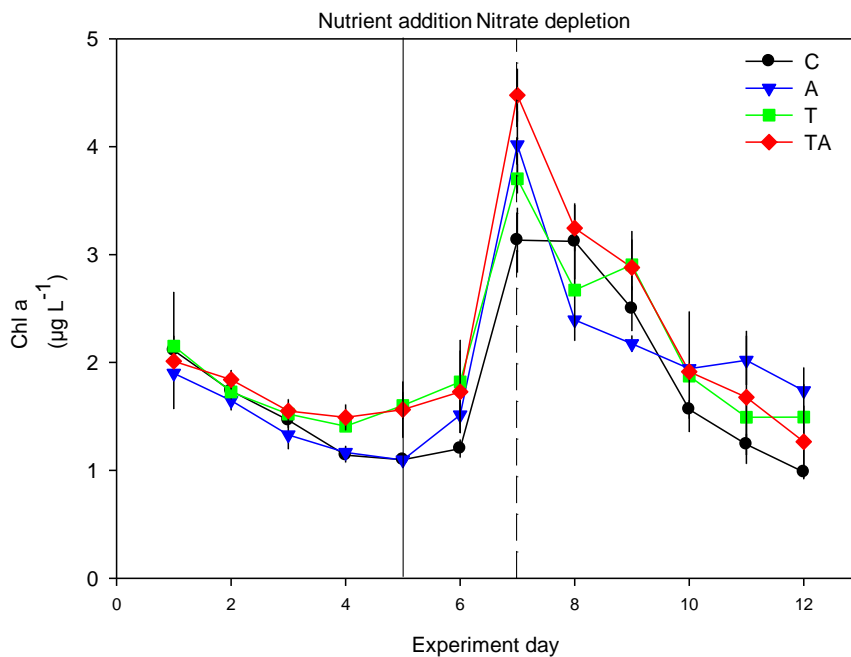


Figure 3. Development of Chlorophyll *a* during the experiment. Solid vertical line indicates nutrient addition and dashed line indicates nitrate depletion.

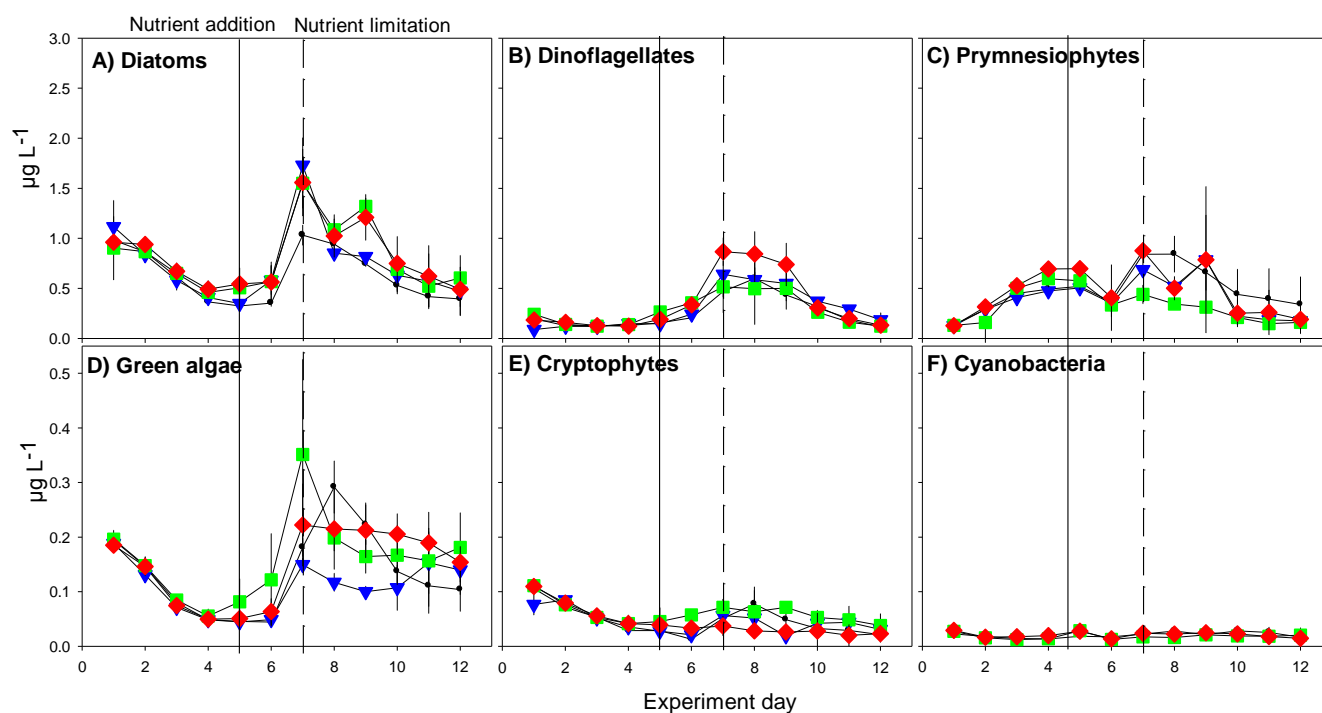


Figure 4. Temporal development of Chl *a* equivalent concentrations of A) diatoms, B) dinoflagellates, C) prymnesiophytes and D) green algae, E) cryptophytes and F) cyanobacteria. Color coding according to Figure 1. Note different scales on top and bottom figures.

Temporal development of particulate and dissolved organic matter

The temporal development of particulate organic matter (POM) followed as expected when nutrients become available for growth. Maximum buildup of particulate organic carbon (POC), particulate organic nitrogen (PON), particulate organic phosphorus (POP) and biogenic silica (BSi) was observed 2-3 days after nutrient addition (Figure 5D-F, 6B). While the uptake of inorganic nutrients was similar between the treatments differences in the incorporation into their respective particulate organic pools were observed (Figure 5). PON increased on average from $5.7 \pm 0.6 \mu\text{mol N L}^{-1}$ (T1) to maximum concentrations of $8.2 \pm 0.9 \mu\text{mol N L}^{-1}$ in the C, $9.0 \pm 0.5 \mu\text{mol N L}^{-1}$ in the A, $8.1 \pm 0.9 \mu\text{mol N L}^{-1}$ in the T and $8.9 \pm 0.6 \mu\text{mol N L}^{-1}$ in the TA treatment on T7. Highest PON concentrations were observed in the acidified treatments (i.e. A and TA treatments, Figure 5D). POP increased on average from $0.34 \pm 0.03 \mu\text{mol P L}^{-1}$ to maximum concentrations of 0.41 ± 0.03 in the C, $0.45 \pm 0.01 \mu\text{mol P L}^{-1}$ in the A, $0.38 \pm 0.04 \mu\text{mol P L}^{-1}$ in the T and $0.42 \pm 0.003 \mu\text{mol P L}^{-1}$ in the TA treatment on T6-T7 (Figure 5E). Highest POP concentrations were observed in the A treatment. BSi decreased from T1 to T5 and increased after nutrient addition (Figure 5F). BSi reached maximum concentrations on T9 of $3.5 \pm 0.3 \mu\text{mol L}^{-1}$ in the C, $5.5 \pm 0.1 \mu\text{mol L}^{-1}$ in the A, $4.2 \pm 0.9 \mu\text{mol L}^{-1}$ in the T and $3.7 \pm 0.6 \mu\text{mol L}^{-1}$ in the TA treatment.

Chapter III

POC initially increased from 51.3 ± 4 to $65.3 \pm 6 \mu\text{mol C L}^{-1}$ on the first two days of the experiment and then decreased. While little change was observed in POC in the C treatment ($58.7 \pm 4.7 \mu\text{mol C L}^{-1}$) POC in the other treatments increased to maximum concentrations of $73.1 \pm 7.5 \mu\text{mol C L}^{-1}$ in the A, $56.5 \pm 3.3 \mu\text{mol C L}^{-1}$ in the T and $71.0 \pm 1.3 \mu\text{mol C L}^{-1}$ in the TA treatment. Highest POC build-up was observed in the acidified treatments, A and TA (Figure 6B). TEP concentrations at the beginning of the experiment was $43.5 \pm 4.02 \mu\text{mol C L}^{-1}$ in all treatments and remained relatively stable up to nutrient addition on T5 (Figure 6D). After nutrient addition, TEP increased in all treatments but most pronouncedly in the A treatment (Figure 6D). Peak TEP concentrations in the C were $79.8 \pm 18 \mu\text{mol C L}^{-1}$, $136.8 \pm 26 \mu\text{mol C L}^{-1}$ in the A, $76.7 \pm 4.17 \mu\text{mol C L}^{-1}$ in the T and $79.6 \pm 6.8 \mu\text{mol C L}^{-1}$ in the TA treatment. Lowest TEP concentrations were observed in the warmed treatment (i.e. T treatment) throughout the experimental period while the control (C) and the combined treatment (TA) remained similar to one another for the duration of the experiment.

Treatment	POC _{max} ($\mu\text{mol L}^{-1}$)	PON _{max} ($\mu\text{mol L}^{-1}$)	POP _{max} ($\mu\text{mol L}^{-1}$)	BSi _{max} ($\mu\text{mol L}^{-1}$)
C	58.7 ± 4.7	8.2 ± 0.9	0.41 ± 0.03	3.5 ± 0.3
A	73.1 ± 7.5	9.0 ± 0.5	0.45 ± 0.01	5.5 ± 0.1
T	56.5 ± 3.3	8.1 ± 0.9	0.38 ± 0.04	4.2 ± 0.9
TA	71.0 ± 1.3	8.9 ± 0.6	0.42 ± 0.003	3.7 ± 0.6
	POC _{loss} ($\mu\text{mol L}^{-1}$)	PON _{loss} ($\mu\text{mol L}^{-1}$)	POP _{loss} ($\mu\text{mol L}^{-1}$)	BSi _{loss} ($\mu\text{mol L}^{-1}$)
C	18.03 ± 4.5	1.4 ± 0.3	0.2 ± 0.04	2.1 ± 0.3
A	14.3 ± 3.7	0.21 ± 0.4	0.02 ± 0.005	1.1 ± 1.7
T	36.4 ± 7.4	3.9 ± 0.4	0.12 ± 0.1	1.2 ± 0.1
TA	26.1 ± 7.5	1.9 ± 0.3	0.09 ± 0.004	2.6 ± 0.3

Table 1. Maximum build-up and losses of POC, PON, POP and BSi (\pm standard deviation between replicates).

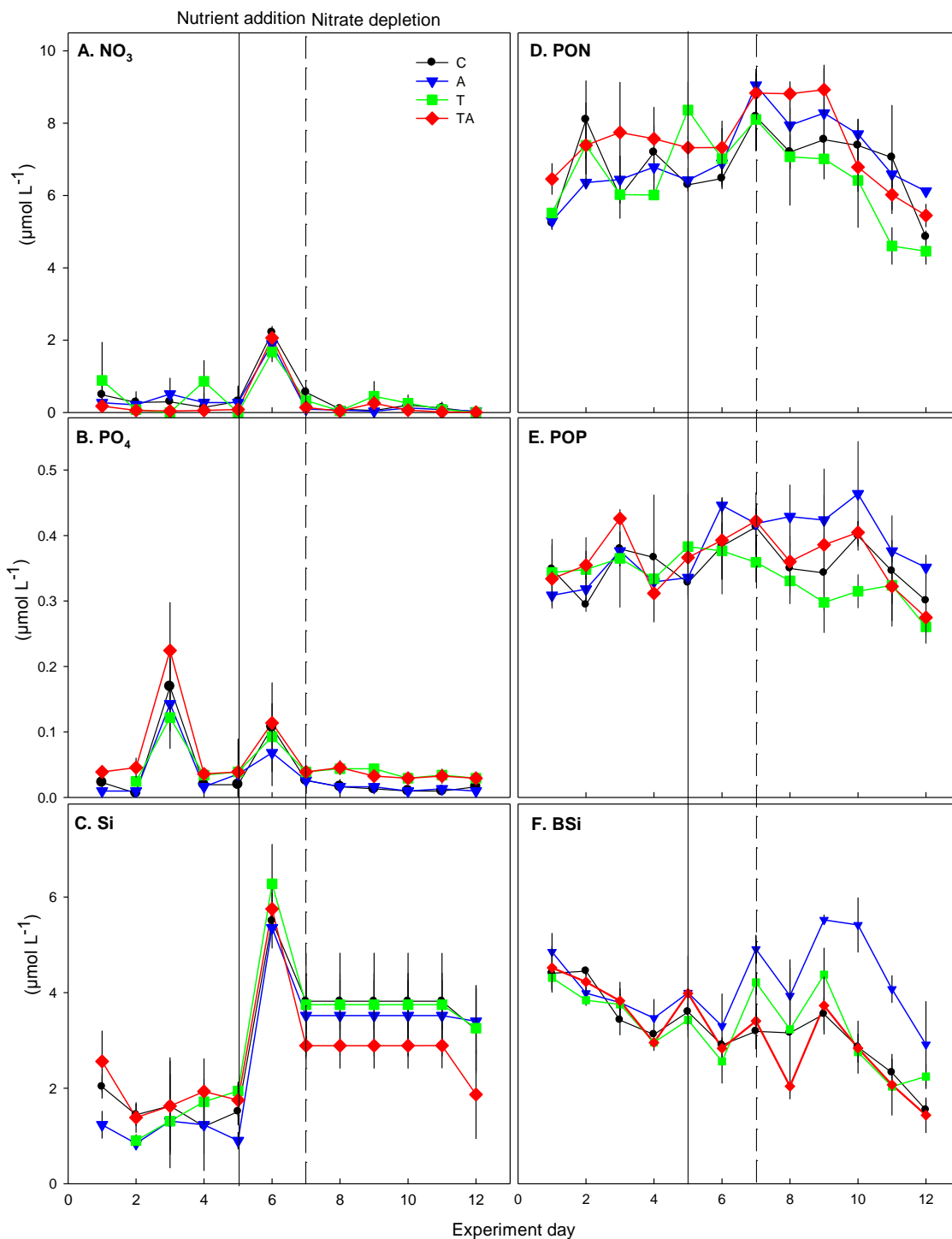


Figure 5. Temporal dynamics of inorganic nutrients A) nitrate, B) phosphate, C) silicate (non validated data) and D) particulate organic nitrogen, E) particulate organic phosphorous and F) biogenic silicate. Solid vertical line indicates nutrient addition and dashed line indicates nitrate depletion.

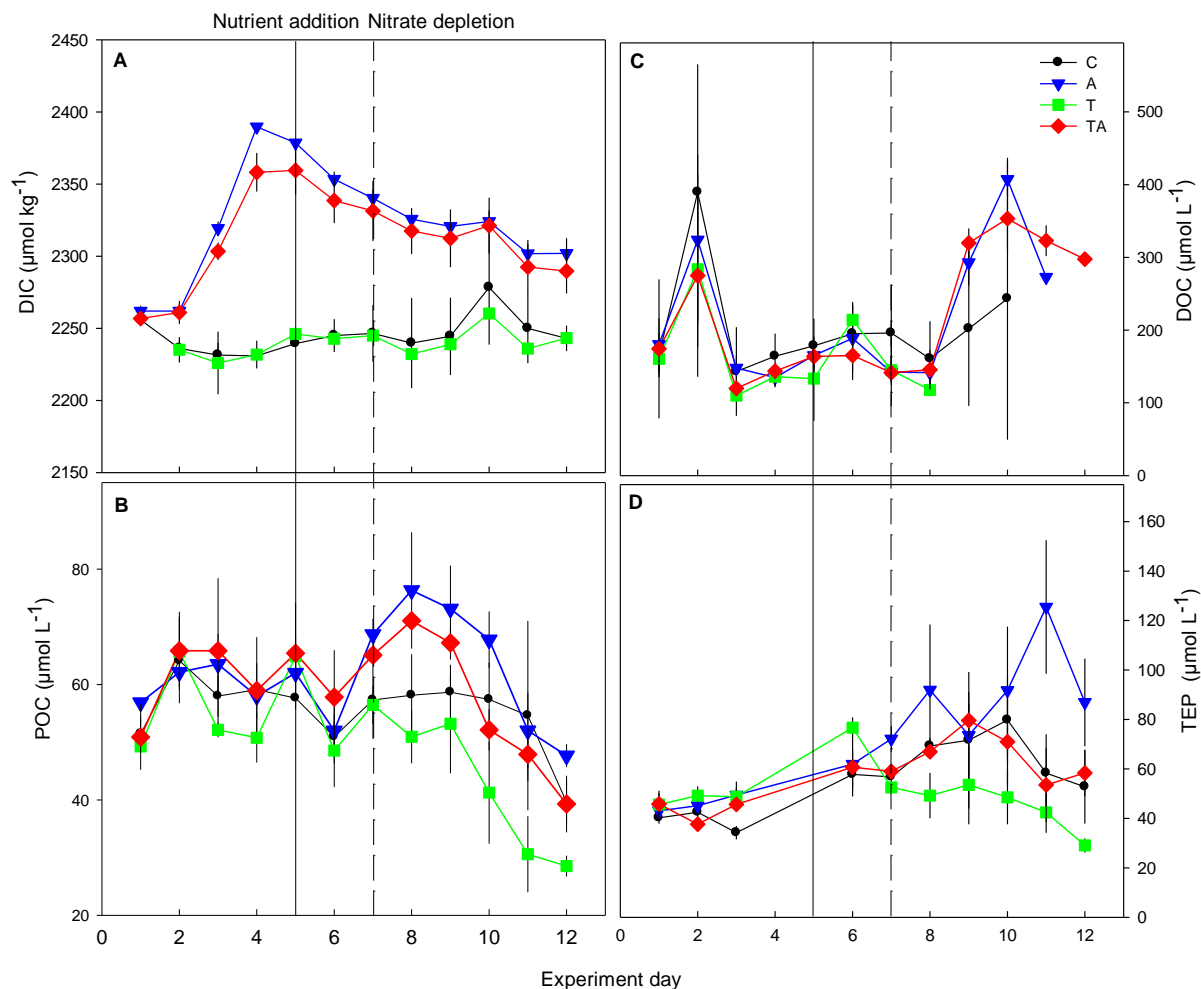


Figure 6. Carbon dynamics during the experiment. A) Dissolved inorganic carbon, B) particulate organic carbon, C) dissolved organic carbon and D) transparent exopolymer particles. Solid vertical line indicates nutrient addition and dashed line indicates nitrate depletion.

Warming decreased maximum POM build-up in our experiments similarly to what was reported in the literature with natural communities (Vidussi *et al.*, 2011; Wohlers-Zöllner *et al.*, 2012). The decreased biomass accumulation under warmed conditions that Vidussi *et al.* reported was in response to enhanced grazing activity of consumers over producers and therefore producer biomass being top down controlled. While Wohlers *et al.* suggested that during their experiments it was rather a temperature-driven shift in the balance between heterotrophic and autotrophic processes which lead to decreased biomass buildup and favored accumulation of DOM. Highest losses of POM were observed in the warmed treatment (T) (Table 1).

Interestingly, was the enhanced biomass build-up of POM under the combined warming and acidification conditions (Figure 5D-G, Figure 6B) potentially suggesting that the negative effects of increased temperature could have been partially compensated at higher CO_2 (both A and TA treatments). The A treatment showed the highest values for maximum biomass build-up in all POM

Chapter III

parameters and would suggest a positive response of plankton biomass to CO₂ enrichment in our experiments.

Enhanced TEP production was observed under acidified conditions (A treatment, Figure 6D). Formation and accumulation of TEP was calculated to account for ~10-35% of POC after nutrient depletion during mesocosm experiments with natural phytoplankton communities exposed to CO₂ enrichment (Engel *et al.*, 2004, 2014) as well as warming (Piontek *et al.*, 2009; Wohlers-Zöllner *et al.*, 2012). Lowest TEP concentrations were observed in the warming treatment and highest in the acidified. TEP concentrations on the combined TA treatment behaved similarly to the Control throughout the experimental period (Figure 6D). Our results would suggest that the individual rather than the combined effects of OA and warming affected TEP production.

DOC concentrations almost double from T1 to T2 in all treatments and then decreased to $132.01 \pm 33 \mu\text{mol L}^{-1}$ on T3 (Figure 6C). After nutrient addition DOC slightly increased in the T treatment and remained stable in the C, A and TA treatments. Thereafter, highest DOC concentrations were observed in the A and TA treatments on T10 (Figure 6C). Unfortunately, DOC samples after T8 for the T treatment were lost during transport. Accumulation of DOC was observed in both acidified treatments, A and TA after nutrient limitation (Figure 6C). Increasing DOC concentrations after a phytoplankton bloom have been commonly observed during mesocosm experiments investigating the effects of CO₂ enrichment in natural phytoplankton communities (Engel *et al.*, 2005, 2014) as well as warming (Wohlers *et al.*, 2009; Taucher *et al.*, 2012). Production and accumulation of DOC is associated with extracellular release of phytoplankton photosynthetic products, sloppy eating by grazers or cell lysis by viruses (Carlson, 2002). Most likely in our experiments, and commonly during exponential growth phase in bloom events, DOC originates from the extracellular release of photosynthetic products (Biddanda & Benner, 1997) and/or channelled from carbon overconsumption (Kähler & Koeve, 2001). Furthermore, nutrient limiting conditions are also known to favor the accumulation of DOC after the bloom peak (Zweifel *et al.*, 1993; Thingstad *et al.*, 1997) and indeed, concentrations started to increase once nitrate depletion started on T8 of the experiment. DON and DOP concentrations slightly increased after nutrient limitation and highest concentrations were attained ~2-3 days earlier in the T treatment compared to the rest (Figure 7). Maximum DON concentrations (after nutrient limitation) were on average $\sim 9.8 \pm 0.07 \mu\text{mol L}^{-1}$. DOP increased to maximum concentrations of $0.37 \pm 0.7 \mu\text{mol L}^{-1}$ between T8-T10 in all treatments. Besides the earlier timing of maximum DON and DOP concentrations in the warmed treatment (T), no trends were observed.

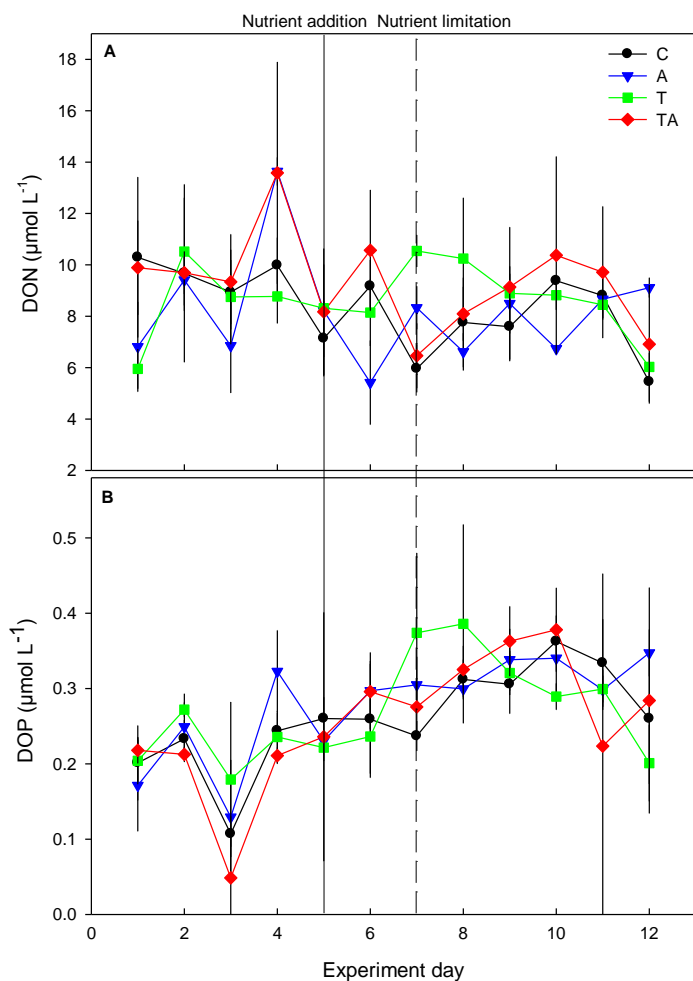


Figure 7. Development of A) dissolved organic nitrogen and B) dissolved organic phosphorus during the experiment. Solid vertical line indicates nutrient addition and dashed line indicates nitrate limitation.

Elemental stoichiometry

POM showed slightly higher assimilation of carbon over nitrogen and phosphorus in relation to Redfield proportions during the experiment in all treatments (Figure 8A-C). POC:PON at the beginning of the experiment was slightly higher in the C and A treatment with ~ 10 mol:mol and ~ 8 mol:mol in the T and TA treatments. POC:PON decreased over time and reached lowest values of ~ 7.5 on T7 of the experiment, two days after nutrient addition. Thereafter, POC:PON slightly increased and the A treatment showed the highest POC:PON values (~ 9) compared to the other treatments which remained relatively stable at $\sim 7.5-8$ (Figure 8A). POC:POP at the beginning of the experiment was higher in the A treatment with ~ 170 while the C, T and TA treatments started at $\sim 135-145$ (Figure 8B). After the addition of nutrients on T5, POC:POP decreased and another peak was observed when nitrate was depleted coinciding with the POC peak on T8. The fluctuation of PON:POP remained similar during the experiment with no trends between the treatments.

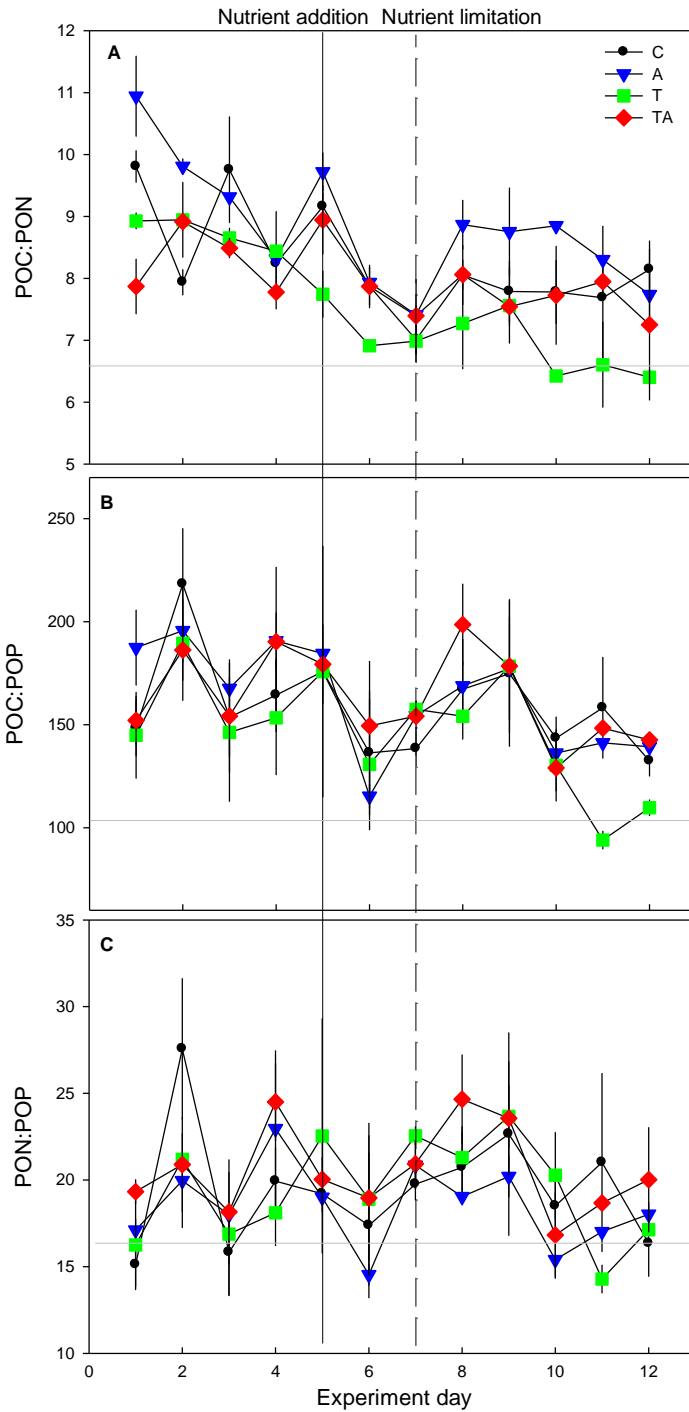


Figure 8. Elemental stoichiometry of POM. A) POC:PON, B) POC:POP and C) PON:POP. Vertical solid line represent day of nutrient addition and dashed line represents day of nitrate depletion. Grey horizontal lines represent expected Redfield proportions of A) 6:1, B) 106:1 and C) 16:1. Color coding according to Figure 1.

The response of marine phytoplankton to expected changes in environmental factors as a consequence of climate change will determine the functioning of marine ecosystems in the upcoming decades. While the majority of experiments studying the effects of climate change in plankton communities have focused on the individual effects of environmental stressors, it was recently suggested that the interactive effects (rather than the sum of the individual) could provide more realistic responses (Christensen *et al.*, 2006). The results from our experiments suggested that when both stressors changed simultaneously (i.e. temperature and CO₂) an increase in phytoplankton

Chapter III

biomass buildup could potentially translate into higher energy potentially transferable to higher trophic levels thus increasing productivity of the system (in terms of shellfish farming) since there seems to be a positive correlation between phytoplankton biomass and successful growth of oysters (Brown & Hartwick, 1988).

References

- Biddanda B, Benner R (1997) Carbon, nitrogen, and carbohydrate fluxes during the production of particulate and dissolved organic matter by marine phytoplankton. *Limnology and Oceanography*, **42**, 506–518.
- Biermann A, Engel A, Riebesell U (2014) Changes in organic matter cycling in a plankton community exposed to warming under different light intensities. *Journal of Plankton Research*, **36**, 658–671.
- Brown J, Hartwick E (1988) Influences of temperature, salinity and available food upon suspended culture of the Pacific oyster, *Cassostrea gigas*: I Absolute and allometric growth. *Aquaculture*, **70**, 231–251.
- Brussaard CPD, Noordeloos a. a. M, Witte H, Collenteur MCJ, Schulz K, Ludwig a., Riebesell U (2013) Arctic microbial community dynamics influenced by elevated CO₂ levels. *Biogeosciences*, **10**, 719–731.
- Caldeira K, Wickett M (2003) Anthropogenic carbon and ocean pH. *Nature*, **425**, 2003.
- Carlson C (2002) Production and removal processes. In: *Biogeochemistry of Marine Dissolved Organic Matter* (eds Hansell D, Carlson C), pp. 91–189. Elsevier Science.
- Christensen MR, Graham MD, Vinebrooke RD et al. (2006) Multiple anthropogenic stressors cause ecological surprises in boreal lakes. *Global Change Biology*, **12**, 2316–2322.
- Clayton T, Byrne R (1993) Spectrophotometric seawater pH measurements: total hydrogen ion concentration scale concentration scale calibration of m-cresol purple and at-sea results. *Deep Sea Research Part I*, **40**, 2115–2129.
- Dickson A (2010) Standards for Ocean Measurements. *Oceanography*, **23**, 34–47.
- Egge JK, Thingstad TF, Larsen A et al. (2009) Primary production during nutrient-induced blooms at elevated CO₂ concentrations. *Biogeosciences*, **6**, 877–885.
- Engel A, Delille B, Jacquet S et al. (2004) Transparent exopolymer particles and dissolved organic carbon production by *Emiliana huxleyi* exposed to different CO₂ concentrations : a mesocosm experiment C : N C : P. *Aquatic Microbial Ecology*, **34**, 93–104.
- Engel A, Zondervan I, Beaufort L et al. (2005) Testing the direct effect of CO₂ concentration on a bloom of the coccolithophorid *Emiliana huxleyi* in mesocosm experiments Marie-Dominique Pizay. *Limnology and Oceanography*, **50**, 493–507.

Chapter III

- Engel A, Borchard C, Piontek J et al. (2013) CO₂ increases ¹⁴C primary production in an Arctic plankton community. *Biogeosciences*, **10**, 1291–1308.
- Engel A, Piontek J, Grossart H-P et al. (2014) Impact of CO₂ enrichment on organic matter dynamics during nutrient induced coastal phytoplankton blooms. *Journal of Plankton Research*, **0**, 1–17.
- Feng Y, Hare C, Leblanc K et al. (2009) Effects of increased pCO₂ and temperature on the North Atlantic spring bloom. I. The phytoplankton community and biogeochemical response. *Marine Ecology Progress Series*, **388**, 13–25.
- Field C, Barros V, Dokken D et al. (2014) IPCC, 2014: Summary for Policymakers. In: *Climate Change 2014: Impacts, Adaptation and Vulnerability. Contribution of Working Group II to the Fifth Assessment Report of the Intergovernmental Panel on Climate Change*, pp. 1–32. Cambridge University Press, United Kingdom and New York.
- Gangnery A, Chabirand J, Lagarde F et al. (2003) Growth model of the Pacific oyster, *Crassostrea gigas*, cultured in Thau Lagoon (Mediterranee, France). *Aquaculture*, **215**, 267–290.
- Hansen H, Koroleff F (1999) Determination of nutrients. In: *Methods of seawater analysis*, 3rd edn (eds Grasshoff K, Kremling K, Ehrhardt M), pp. 159–228. Wiley VCH, Weinheim.
- Hare C, Leblanc K, DiTullio G et al. (2007) Consequences of increased temperature and CO₂ for phytoplankton community structure in the Bering Sea. *Marine Ecology Progress Series*, **352**, 9–16.
- Hein M, Sand-Jensen K (1997) CO₂ increases oceanic primary production. *Nature*, **384**, 526–527.
- Hernandez-Ayon J, Belli S, Zirino A (1999) pH, alkalinity and total CO₂ in coastal seawater by potentiometric titration with a difference derivative readout. *Analytica Chimica Acta*, **394**, 101–108.
- Isla JA, Lengfellner K, Sommer U (2008) Physiological response of the copepod *Pseudocalanus* sp. in the Baltic Sea at different thermal scenarios. *Global Change Biology*, **14**, 895–906.
- Kähler P, Koeve W (2001) Marine dissolved organic matter: can its C : N ratio explain carbon overconsumption? *Deep Sea Research Part I*, **48**, 49–62.
- Keller A, Oviatt CA., Walker H et al. (1999) Predicted impacts of elevated temperature on the magnitude of the winter-spring phytoplankton bloom in temperate coastal waters: A mesocosm study. *Limnology and Oceanography*, **44**, 344–356.
- Lassen MK, Nielsen KD, Richardson K et al. (2010) The effects of temperature increases on a temperate phytoplankton community — A mesocosm climate change scenario. *Journal of Experimental Marine Biology and Ecology*, **383**, 79–88.
- Legendre L, Rivkin R (2002) Fluxes of carbon in the upper ocean: regulation by food-web control nodes. *Marine Ecology Progress Series*, **242**, 95–109.
- Levitus S, Antonov J, Boyer T et al. (2012) World ocean heat content and thermosteric sea level change (0-2000 m) 1955-2010. *Geophysical Research Letters*, **39**.

Chapter III

- Lewandowska A, Sommer U (2010) Climate change and the spring bloom: a mesocosm study on the influence of light and temperature on phytoplankton and mesozooplankton. *Marine Ecology Progress Series*, **405**, 101–111.
- Lewandowska AM, Breithaupt P, Hillebrand H et al. (2012) Responses of primary productivity to increased temperature and phytoplankton diversity. *Journal of Sea Research*, **72**, 87–93.
- Lewis E, Wallace D (1998) Program developed for CO₂ system calculations [Internet] ORNL/CDIAC-105. OakRidge (Tennessee): Carbon Dioxide Information Analysis Center.
- Nouguier J, Mostajir B, LeFloch E et al. (2007) An automatically operated system for simulating global change temperature and ultraviolet B radiation increases: application to the study of aquatic ecosystem responses in mesocosm experiments. *Limnology and Oceanography: Methods*, **5**, 269–279.
- O'Connor MI, Piehler MF, Leech DM et al. (2009) Warming and resource availability shift food web structure and metabolism. *PLoS biology*, **7**, e1000178.
- Orr JC, Fabry VJ, Aumont O et al. (2005) Anthropogenic ocean acidification over the twenty-first century and its impact on calcifying organisms. *Nature*, **437**, 681–6.
- Parmesan C, Yohe G (2003) A globally coherent fingerprint of climate change impacts across natural systems. *Nature*, **421**, 37–42.
- Piontek J, Händel N, Langer G et al. (2009) Effects of rising temperature on the formation and microbial degradation of marine diatom aggregates. *Aquatic Microbial Ecology*, **54**, 305–318.
- Rees AP (2012) Pressures on the marine environment and the changing climate of ocean biogeochemistry. *Philosophical transactions. Series A, Mathematical, physical, and engineering sciences*, **370**, 5613–35.
- Riebesell U, Tortell P (2011) Effects of ocean acidification on pelagic organisms and ecosystems. In: *Ocean Acidification*, pp. 99–116. Oxford University Press.
- Sabine CL, Feely R, Gruber N et al. (2004) The oceanic sink for anthropogenic CO₂. *Science*, **305**, 367–371.
- Schippers P, Lurling M, Scheffer M (2004) Increase of atmospheric CO₂ promotes phytoplankton productivity. *Ecology Letters*, **7**, 446–451.
- Schulz KG, Ramos JB, Zeebe RE et al. (2009) CO₂ perturbation experiments: similarities and differences between dissolved inorganic carbon and total alkalinity manipulations. *Biogeosciences*, **6**, 2145–2153.
- Sharp JH (1974) Improved analysis for particulate organic carbon and nitrogen from seawater. *Limnology and Oceanography*, **19**, 984–989.
- Taucher J, Schulz KG, Dittmar T et al. (2012) Enhanced carbon overconsumption in response to increasing temperatures during a mesocosm experiment. *Biogeosciences*, **9**, 3531–3545.

Chapter III

- Thingstad T, Hagstrom A, Rassoulzadegan F (1997) Accumulation of degradable DOC in surface waters : Is it caused by a malfunctioning microbial loop ? *Limnology and Oceanography*, **42**, 398–404.
- Tortell P, DiTullio G, Sigman D et al. (2002) CO₂ effects on taxonomic composition and nutrient utilization in an Equatorial Pacific phytoplankton assemblage. *Marine Ecology Progress Series*, **236**, 37–43.
- Tortell PD, Payne CD, Li Y et al. (2008) CO₂ sensitivity of Southern Ocean phytoplankton. *Geophysical Research Letters*, **35**, L04605.
- Vidussi F, Mostajir B, Fouilland E et al. (2011) Effects of experimental warming and increased ultraviolet B radiation on the Mediterranean plankton food web. *Limnology and Oceanography*, **56**, 206–218.
- Wohlers J, Engel A, Zöllner E et al. (2009) Changes in biogenic carbon flow in response to sea surface warming. *Proceedings of the National Academy of Sciences of the United States of America*, **106**, 7067–72.
- Wohlers-Zöllner J, Biermann A, Engel A et al. (2012) Effects of rising temperature on pelagic biogeochemistry in mesocosm systems: a comparative analysis of the AQUASHIFT Kiel experiments. *Marine Biology*, **159**, 2503–2518.
- Wolf-Gladrow D, Riebesell U, Burkhardt S (1999) Direct effects of CO₂ concentration on growth and isotopic composition of marine plankton. 461–476.
- Wurl O, Min Sin T (2009) Analysis of Dissolved and Particulate Organic Carbon with the HTCO Technique. In: *Practical guidelines for the analysis of seawater* (ed Wurl O), pp. 33–48. CRC Press Taylor and Francis group.
- Zapata M, Rodrigues F, Garrido J (2000) Separation of chlorophylls and carotenoids from marine phytoplankton: A new HPLC method using a reversed phase C-8 column and pyridine-containing mobile phases. *Marine Ecology Progress Series*, **195**, 29–45.
- Zweifel U, Norrman B, Hagstrom A (1993) Consumption of dissolved organic carbon by marine bacteria and demand for inorganic nutrients. *Marine Ecology Progress Series*, **101**, 23–32.

Chapter III

Synthesis and future perspectives

Synthesis

The results compiled in this doctoral thesis from experimental work show the importance of investigating the interactive rather than the individual effects of environmental stressors to develop a better understanding of the response of marine ecosystems in a future ocean (Hoffman *et al.*, 2003; Christensen *et al.*, 2006; Gruber, 2011). The work in this thesis focused on the response of key phytoplankton species to changes in CO₂ and temperature expected by the end of this century and potential consequences for marine biogeochemical cycling. Two phytoplankton functional groups were studied in this thesis: coccolithophores (**Chapter I**) and diatoms (**Chapter II and III**). Both groups are key players in the marine carbon cycle (Sarhou *et al.*, 2005; Boyd *et al.*, 2010) and thus could influence the ocean's capability to take up excess CO₂ from the atmosphere via photosynthesis (De La Rocha & Passow, 2007; Passow & Carlson, 2012). The successful growth of phytoplankton in the ocean is determined by the right combination of environmental conditions of which light, nutrients and temperature play key roles and all three are expected to change in the context of climate change (Beardall & Stojkovic, 2006; Gruber, 2011). Although the exact magnitude in which they are expected to change is only a prediction, they are expected to modulate primary productivity in the ocean with considerable consequences for biogeochemical cycling and export potential (Gruber, 2011; Passow & Carlson, 2012). However, looking at all these parameters simultaneously is beyond the scope of this doctoral thesis and from this point forward I will only focus on ocean acidification (OA) and warming.

Effects of climate change on phytoplankton physiology

Culture experiments have been used in biology as key tools to understand phytoplankton physiology under controlled laboratory conditions (Lakeman *et al.*, 2009). However, the results from these types of experiments would not necessarily portray their response in nature where competition for resources, competition with other species or a combination of different environmental stressors might play a stronger role. Nevertheless, they do provide rather valuable information on the *physiological capabilities* of an organism and their metabolic thresholds, which would otherwise be difficult to investigate in the field. Results from experiments in **Chapter I** provide valuable information on the sensitivity of key metabolic processes to OA and how warming modulates this sensitivity. Our results showed that two important bloom forming coccolithophore species shifted their optimum CO₂ concentrations for metabolic processes towards higher concentrations at elevated temperatures. This has significant implications when assessing the success of coccolithophores in the future ocean. Over the past decades, coccolithophores gained considerable attention from scientists all over the world because OA considerably decreased calcification rates and increased coccolith malformation (Riebesell *et al.*, 2000; Ridgwell *et al.*, 2009; Hoppe *et al.*, 2011). The majority of results suggested that at a 'lower pH' future ocean scenario, this

Synthesis and future perspectives

key phytoplankton group would be facing serious problems to produce their CaCO₃ shells. Moreover, since CO₂ is released in the process of calcification a decrease in phytoplankton calcification rates would most likely translate into a potential negative feedback to atmospheric CO₂ and increase CO₂ storage capacity in the ocean (Riebesell *et al.*, 2000). While OA is a non-debatable and ongoing process that will affect marine ecosystems in the future (Riebesell & Tortell, 2011), it is not expected to occur in isolation but rather simultaneously with other environmental stressors (Gruber, 2011). The results from our culture experiments looking at both drivers showed the importance of temperature in not only enhancing growth and production rates (i.e. calcification and photosynthesis) but also in modulating the sensitivity of these processes to OA. The shift in CO₂ optima suggested that the negative effects of OA were partially compensated at higher temperatures where higher metabolic rates (and inorganic carbon demand) benefited more from substrate availability than were negatively affected by low pH.

Furthermore, our results also showed that both species had highest growth and production rates at temperatures ~10°C higher to those experienced at their isolation sites suggesting a potential physiological flexibility which would allow them to exploit climatic anomalies. Indeed, the latitudinal expansion of coccolithophore blooms in relation to warming has been reported in the Bering and North Sea and Southern Ocean (Merico *et al.*, 2004; Cubillos *et al.*, 2007; Beaugrand *et al.*, 2013).

Lastly, the results from our physiological experiments enabled us to propose a conceptual model which would help explain much of the discrepancies found in coccolithophore literature (Ridgwell *et al.*, 2009; Hoppe *et al.*, 2011). We proposed that the response of a coccolithophore strain to OA can be neutral, positive or negative depending on the temperature at which it was cultured and the strain specific temperature optima (Figure 1). This highlights that the physiological response of coccolithophores (and any organism for that matter) can only be judged accurately when interpreted in the proper eco-physiological context of a given species or strain. If a sound understanding of the importance and influence of experimental conditions on the organisms' response is missing, the interpretation of results can be misleading because all responses can be attained if cultured at specific conditions.

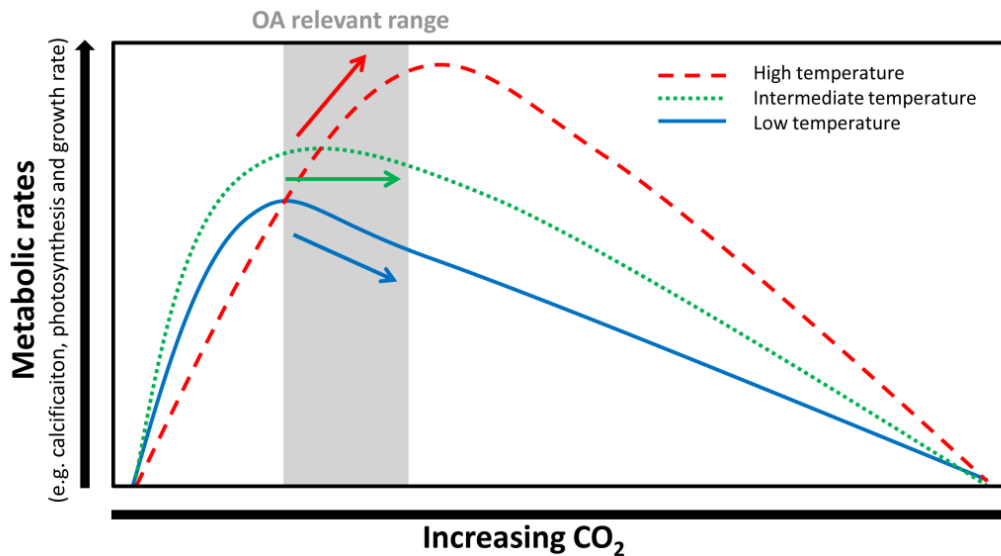


Figure 1. Conceptual graph depicting the modulating effect of temperature on the OA sensitivity of key metabolic processes in coccolithophores. The arrows emphasize the trends of key metabolic processes (i.e. growth, photosynthesis and calcification) vs. CO₂ concentration, grey area represents the relevant range for future OA, ~280-1000 $\mu\text{atm } p\text{CO}_2$. Source: Sett *et al.*, 2014.

While physiological studies give us information on physiological capabilities of an organism, what will ultimately determine the success of aquatic ecosystems will come from a more complex web of trophic interactions. Therefore it is crucial to investigate and try to understand responses at a community level (e.g. including more than one species and when possible more than one trophic level) and what it would mean for the future functioning of marine ecosystems.

The use of mesocosms to study whole community responses

Recently, mesocosms (i.e. experimental enclosures) have become a very useful tool to investigate the effects of environmental stressors from a whole community approach which includes more than one trophic level (Berg *et al.*, 2009). It is a compromise between the highly controlled conditions of laboratory experiments and the more realistic *in situ* manipulations (which can be much more difficult to conduct). The advantages of having a high degree of realism at the cost of replication seem like a fair tradeoff when whole community responses are of interest (Berg *et al.*, 2009). Investigating ecosystem community responses under the combined effect of environmental stressors, although more complex, could provide more realistic results than when stressors are investigated separately (Hoffman *et al.*, 2003; Christensen *et al.*, 2006). Indeed, Christensen *et al.* demonstrated that, during experiments in boreal lakes, the interaction of three environmental stressors (i.e. drought, OA and warming) better explained the response of producers and consumers biomass over a 20 year period as compared to when the stressors were investigated individually. In their experiments, the synergistic positive effects of the three stressors on consumer biomass came

Synthesis and future perspectives

as an unexpected surprise since previous experiments showed negative effects of the same stressors when investigated individually (Christensen *et al.*, 2006 and references therein). In fact, the results from our experiments in **Chapter II** and **Chapter III** investigating the combined effect of OA and warming showed responses which could have not been inferred from individual stressor experiments.

Experiments investigating the effects of global warming on the spring bloom plankton succession in the Kiel Bight were performed yearly from 2005-2012 with indoor mesocosms (Sommer *et al.*, 2012). Most likely, the lack of experiments with OA in these types of mesocosms (indoor) came from limitations on appropriate methods for CO₂ manipulation. The use of enriched CO₂ air by bubbling the experimental water proved to be an ineffective method since the permanent flow of air bubbles produced a layer of foam on the water surface and disturbed the delicate phytoplankton. On the other hand, if the method of enriched CO₂ water were to be used, the gas exchange fluxes would be extremely fast due to the large surface to volume ratio (indoor mesocosms are ~1.5 m in diameter and ~1 m in depth). Furthermore, another important factor for gas exchange would be the continuous mixing with the propellers which gently mixed the water column. Thus the enriched CO₂ water additions would be lost within hours and no proper CO₂ manipulation would be achieved. Therefore we developed transparent floating lids to minimize gas exchange (Figure 2). This meant only one, initial CO₂ enrichment event at the beginning of the experiment was necessary and thereafter for the plankton community to proceed with the natural alterations to the seawater carbonate chemistry. Tests to verify that the lids would serve the function of minimizing gas exchange were performed prior to the experiments in **Chapter II**. CO₂ enrichment additions were performed in two mesocosms, one with a lid and one without. In the mesocosm without the lid, the addition of CO₂ enriched water was lost within 48 hrs while the mesocosm with the lid minimized the gas exchange processes (Czerny *et al.*, 2013). During the experiments described in **Chapter II**, the floating lids remained on top of the water column throughout the duration of the experiment. The use of N₂O as a gas tracer allowed for calculation of gas exchange rates according to the specific temperature and CO₂ levels in the different treatments. Similar lids were also used during experiments described in **Chapter III**, unfortunately however, no samples for N₂O were taken during the latter experiments. Whereas the lids proved to be effective in minimizing gas exchange, caution needs to be taken when using them. The presence of a floating lid also provides an additional surface for biofilm formation and eventually an area of organic matter accumulation when experiments last longer than 6-8 weeks. Furthermore, when phytoplankton are buoyant (e.g. cyanobacterial mats), this set-up would not work properly because they would attach directly to the bottom of the lid and no representative sampling of a homogenous water mass would be possible.

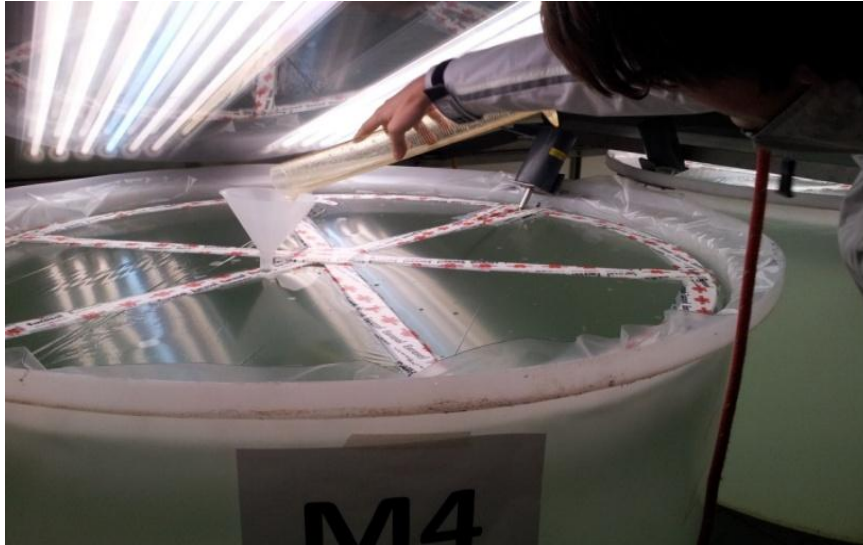


Figure 2. Indoor mesocosm with transparent floating lid. Addition of enriched CO₂ water and daily sampling was performed without lifting the lids throughout the experiment.

Effects of climate change on natural phytoplankton communities

While the effects of ocean acidification (Delille *et al.*, 2005; Kim *et al.*, 2006; Riebesell *et al.*, 2007; Tortell *et al.*, 2008; Schulz *et al.*, 2013; Engel *et al.*, 2014) and warming (Keller *et al.*, 1999; O'Connor *et al.*, 2009; Lassen *et al.*, 2010; Taucher *et al.*, 2012; Wohlers-Zöllner *et al.*, 2012; Biermann *et al.*, 2014) on natural phytoplankton communities have been extensively studied independently, there seems to be limited data on the combined effects (Hare *et al.*, 2007; Feng *et al.*, 2009; Kim *et al.*, 2011). However, ocean acidification and warming are two processes expected to occur simultaneously in the future (Gruber, 2011) and while the results from multi-stressor experiments are much more complicated to interpret they also could provide more realistic results on potential responses of the marine environment. Most importantly, any modifications at the phytoplankton community composition level of an ecosystem (regardless of which direction it occurs) are crucial to understand because primary and secondary production are recognized as key components of carbon fluxes modifying food web structure and ecosystem productivity (Legendre & Rivkin, 2002).

Results from the mesocosm experiments in **Chapter II** revealed that under combined OA and warming conditions (i.e. 'Greenhouse' treatment) there was a shift in the phytoplankton community composition towards larger diatom species. Although the shift towards larger diatoms was not observed in the "High CO₂" treatment and a temperature effect cannot be ruled out completely, we found some evidence suggesting that the shift was most likely due to the combination of both parameters. Similar experiments exclusively studying warming in the Kiel Bight spring plankton community reported that one of the recurrent (and strong) trends in community composition was the negative correlation of large diatom biomass with warming (Sommer & Lengfellner, 2008; Lewandowska & Sommer, 2010). This result is rather strong considering that some of the

Synthesis and future perspectives

experiments were in different years with most likely different community compositions, and with other stressors simultaneously tested such as light (Sommer & Lengfellner, 2008; Lewandowska & Sommer, 2010). Moreover, incubation experiments with the North Atlantic spring bloom showed that while diatoms were favored at high CO₂ conditions only in the combined treatment (“Greenhouse”) was the shift to larger diatom species detected. Likewise during CO₂ enrichment experiments with natural diatom communities, larger diatoms proliferated over smaller species (Tortell *et al.*, 2008; Feng *et al.*, 2010). These results are not surprising since diatoms, in general, are known to operate effective CO₂ concentrating mechanisms and to benefit from high CO₂ substrate availability (Yoshimura *et al.*, 2013). Nevertheless, small picoeukaryotes have also been reported to benefit during CO₂ enrichments experiments over other phytoplankton groups (Brussaard *et al.*, 2013; Schulz *et al.*, 2013; Yoshimura *et al.*, 2013). Moreover, the shift in size could have implications for the sinking of particulate organic matter. In fact, the loss of organic matter at the end of the experiments was significantly higher in the Greenhouse treatment suggesting that the shift in size towards larger diatoms did play a role in determining loss processes at the end of the bloom.

Results from experiments in **Chapter III** showed that high CO₂, individually and in combination with warming, enhanced biomass build-up during a nutrient-induced summer bloom. Since most of the literature with natural phytoplankton communities have reported a negative effect of enhanced temperature on biomass build-up (Keller *et al.*, 1999; Sommer & Lengfellner, 2008; O’Connor *et al.*, 2009; Lassen *et al.*, 2010; Vidussi *et al.*, 2011; Wohlers-Zöllner *et al.*, 2012; Biermann *et al.*, 2014) we suggest that this response was most likely compensated by increasing CO₂ availability. It would be interesting to verify whether the combination of these two stressors inhibited/decreased growth and grazing activities of consumers (consumer data under evaluation) and whether top down control was diminished, as opposed to when warming was investigated alone (Vidussi *et al.*, 2011). The experiments in **Chapter III** were conducted in a region of the Mediterranean Sea (Thau lagoon) of particular interest due to their economically productive shellfish farming (Gangnery *et al.*, 2003) and thus it was crucial to understand how the effects of climate change (in our case OA and warming) would affect productivity in this ecosystem. If the transfer of energy in these ecosystems would be disrupted as a response to changing environmental conditions, it could lead to serious socio-economical implications. Brown & Hartwick showed that high phytoplankton biomass (represented by Chl *a*) correlated positively with successful oyster growth (i.e. increased weight and shell height) in British Columbia (Brown & Hartwick, 1988). Therefore, if the results from our experiments in **Chapter III** could serve as a representative response of this ecosystem to climate change, we could infer that enhanced phytoplankton biomass (under combined OA and warming) could potentially translate into less C recycled in the microbial loop and more transfer to higher trophic levels thereby enhancing productivity in this region.

Synthesis and future perspectives

Implications for coastal ecosystems

In general, natural variability in coastal ecosystems usually surpasses values expected by the end of the century in terms of pH and $p\text{CO}_2$ levels (Hofmann *et al.*, 2011; Melzner *et al.*, 2012) and thus makes these areas an interesting ecosystem to examine under the effects of rising CO_2 and temperature expected in the upcoming decades. This natural variability in seawater carbonate chemistry (i.e. pH, $p\text{CO}_2$, CO_2) is dominated by physical, biological processes or a combination of both depending on the season. Variability due to physical processes are mostly dominant in winter and early spring when storms mix the water column and provide nutrients to the upper ocean, as well as rich CO_2 waters upwelled from deeper depths and usually when biological activity is low because of low light availability. In spring and summer however, biological processes dominate because environmental conditions (e.g. availability of light and nutrients) induce fast growth of phytoplankton and zooplankton which in turn drive variability of the system. From a physiological point of view, this natural variability could provide the organisms at these sites with some sort of resilience to changing environmental conditions. However, this would not be the case if they are already at the extremes of their physiological capabilities (Hofmann *et al.*, 2011). For example, there is strong evidence supporting that marine phytoplankton from areas with large annual temperature fluctuations have broader thermal tolerance curves than those in stable environments (i.e. temperate coastal versus tropical phytoplankton, Thomas *et al.*, 2012; Boyd *et al.*, 2013). This has also been the case for marine invertebrates (i.e. barnacles) from highly fluctuating CO_2 environments showing more tolerance to increasing CO_2 compared to those from stable CO_2 habitats (Pansch *et al.*, 2014). Huertas *et al.*, 2011 suggested that the biogeographical origin of an organism could help determine their success in a changing environment allowing those from highly dynamic ecosystems to acclimate better. If this would be the case, then it could be an additional explanation, besides the physiological response, as to why the changes in phytoplankton community composition we observed in the 'Greenhouse' treatment did not occur in the OA treatment of experiments in **Chapter II**. The community could have already experienced those levels ($\sim 900 \mu\text{atm } p\text{CO}_2$) in the earlier months and those levels were not a stress factor during our experiments.

Future perspectives

Given that at this point in time there is quite a large amount of experimental data (from laboratory, mesocosm and field experiments) it would be interesting to begin correlating experimental data with biological and chemical data from field observation platforms. For example, field observations over the past 50 years in the northeast Atlantic and North Sea showed an increase in the ratio of diatoms to dinoflagellates which positively correlated with warming and windy conditions (Hinder *et al.*, 2012). To follow up on the results from experiments in **Chapter II** it would

Synthesis and future perspectives

be interesting to investigate whether these results were driven by diatoms of a specific species or size. For example, Wasmund *et al.*, 2008 reported that during spring blooms in the Kiel Fjord there was a natural transition from 'larger' diatoms (such as *Chaetoceros* sp and *Thalassiosira* sp) during the first phase to smaller ones (such as *Skeletonema*) when the water column stabilized. However, an earlier stabilization of the water column in a particular year (e.g. 2003) prevented larger species start with the spring bloom and instead *Skeletonema* dominated the phytoplankton bloom. Furthermore, they reported that early spring blooms (i.e. starting in February-March) were more intense and the diatom contribution to total phytoplankton biomass was higher than when they occur later (i.e. starting in March-April). It would be interesting to look more closely at the correlations between phytoplankton community composition and biological and chemical parameters to verify which parameters are of key importance when driving the shifts and/or biogeographical expansion of species.

To follow up on the results from experiments in **Chapter II**, physiology experiments similar to the ones performed in **Chapter I** with coccolithophores could be carried out with diatoms of different sizes and species. These types of experiments could increase our understanding of the physiological responses of different sized diatoms to the individual and synergistic effects of OA and warming and elucidate some potential reasons why the groups responded the way they did in our experiments: Was the observed shift to larger species in the 'Greenhouse' treatment in our experiments a physiological response (i.e. larger species would benefit over smaller ones given specific environmental conditions) or was it merely due to larger species dominating the initial community composition and therefore already having an advantage over smaller ones?

Additionally, during our experiments, the combination of different methods to analyze experimental data also proved to be crucial. For example, during the analysis of phytoplankton community composition, if both the data from the HPLC and flow cytometry would not have been used in combination we would have probably missed the shift in size towards large diatoms or which was the group which contributed mostly to total Chl *a*. If only the flow cytometry data would have been used, we would have detected the shift in size but we would not have been able to determine which phytoplankton group was driving this shift. If only the HPLC data would have been used, we would have determined that diatoms were the dominating phytoplankton group contributing to total Chl *a* but we would have missed the very important piece of information on the shift in size.

Furthermore, prior to conducting experiments with natural communities I would suggest to monitor the environment were experiments would be performed in order to create experimental setups which would be relevant for that specific community. For example, for the mesocosm experiments described in **Chapter II**, the levels for the OA treatment should have been much higher than ~900 μatm $p\text{CO}_2$ since the community in November/December already experienced levels of

Synthesis and future perspectives

~700 μatm $p\text{CO}_2$. This could be another possible explanation as to why there was minimal response in the OA treatment where levels were only ~400 μatm $p\text{CO}_2$ higher than the control.

References

- Beardall J, Stojkovic S (2006) Microalgae under Global Environmental Change : Implications for Growth and Productivity , Populations and Trophic Flow. *ScienceAsia*, **1**, 1–10.
- Beaugrand G, McQuatters-Gollop A, Edwards M et al. (2013) Long-term response of North Atlantic calcifying plankton to climate change. *Nature Climate Change*, **3**.
- Berg G, Brooks M, Chen C et al. (2009) *Enclosed experimental ecosystems and scale: tools for understanding and managing coastal ecosystems* (eds Petersen J, Kennedy V, Dennison W, Kemp W). Springer.
- Biermann A, Engel A, Riebesell U (2014) Changes in organic matter cycling in a plankton community exposed to warming under different light intensities. *Journal of Plankton Research*, **36**, 658–671.
- Boyd PW, Strzepek R, Fu F et al. (2010) Environmental control of open-ocean phytoplankton groups: Now and in the future. *Limnology and Oceanography*, **55**, 1353–1376.
- Boyd PW, Rynearson TA, Armstrong E a et al. (2013) Marine phytoplankton temperature versus growth responses from polar to tropical waters--outcome of a scientific community-wide study. *PLoS one*, **8**, e63091.
- Brown J, Hartwick E (1988) Influences of temperature, salinity and available food upon suspended culture of the Pacific oyster, *Cassostrea gigas*: I Absolute and allometric growth. *Aquaculture*, **70**, 231–251.
- Brussaard CPD, Noordeloos AAM, Witte H et al. (2013) Arctic microbial community dynamics influenced by elevated CO_2 levels. *Biogeosciences*, **10**, 719–731.
- Christensen MR, Graham MD, Vinebrooke RD et al. (2006) Multiple anthropogenic stressors cause ecological surprises in boreal lakes. *Global Change Biology*, **12**, 2316–2322.
- Cubillos J, Wright S, Nash G et al. (2007) Calcification morphotypes of the coccolithophorid *Emiliana huxleyi* in the Southern Ocean: changes in 2001 to 2006 compared to historical data. *Marine Ecology Progress Series*, **348**, 47–54.
- Czerny J, Schulz KG, Ludwig A et al. (2013) Technical Note: A simple method for air–sea gas exchange measurements in mesocosms and its application in carbon budgeting. *Biogeosciences*, **10**, 1379–1390.
- Delille B, Harlay J, Zondervan I et al. (2005) Response of primary production and calcification to changes of $p\text{CO}_2$ during experimental blooms of the coccolithophorid *Emiliana huxleyi*. *Global Biogeochemical Cycles*, **19**.
- Engel A, Piontek J, Grossart H-P et al. (2014) Impact of CO_2 enrichment on organic matter dynamics during nutrient induced coastal phytoplankton blooms. *Journal of Plankton Research*, **0**, 1–17.

Synthesis and future perspectives

- Feng Y, Hare C, Leblanc K et al. (2009) Effects of increased pCO₂ and temperature on the North Atlantic spring bloom. I. The phytoplankton community and biogeochemical response. *Marine Ecology Progress Series*, **388**, 13–25.
- Feng Y, Hare CE, Rose JM et al. (2010) Interactive effects of iron, irradiance and CO₂ on Ross Sea phytoplankton. *Deep Sea Research Part I: Oceanographic Research Papers*, **57**, 368–383.
- Gangnery A, Chabirand J, Lagarde F et al. (2003) Growth model of the Pacific oyster, *Crassostrea gigas*, cultured in Thau Lagoon (Mediterranee, France). *Aquaculture*, **215**, 267–290.
- Gruber N (2011) Warming up, turning sour, losing breath: ocean biogeochemistry under global change. *Philosophical Transactions of the Royal Society A*, **369**, 1980–96.
- Hare C, Leblanc K, DiTullio G et al. (2007) Consequences of increased temperature and CO₂ for phytoplankton community structure in the Bering Sea. *Marine Ecology Progress Series*, **352**, 9–16.
- Hinder SL, Hays GC, Edwards M et al. (2012) Changes in marine dinoflagellate and diatom abundance under climate change. *Nature Climate Change*, **2**, 271–275.
- Hoffman JR, Hansen LJ, Klinger T (2003) Interactions between UV radiation and temperature limit inferences from single-factor experiments. *Journal of Phycology*, **39**, 268–272.
- Hofmann GE, Smith JE, Johnson KS et al. (2011) High-frequency dynamics of ocean pH: a multi-ecosystem comparison. *PLoS one*, **6**, e28983.
- Hoppe CJM, Langer G, Rost B (2011) *Emiliana huxleyi* shows identical responses to elevated pCO₂ in TA and DIC manipulations. *Journal of Experimental Marine Biology and Ecology*, **406**, 54–62.
- Huertas IE, Rouco M, López-Rodas V et al. (2011) Warming will affect phytoplankton differently: evidence through a mechanistic approach. *Proceedings. Biological sciences / The Royal Society*, **278**, 3534–43.
- Keller A, Oviatt CA, Walker HA et al. (1999) Predicted impacts of elevated temperature on the magnitude of the winter-spring phytoplankton bloom in temperate coastal waters: A mesocosm study. *Limnology and Oceanography*, **44**, 344–356.
- Kim J-M, Lee K, Shin K et al. (2006) The effect of seawater CO₂ concentration on growth of a natural phytoplankton assemblage in a controlled mesocosm experiment. *Limnology and Oceanography*, **51**, 1629–1636.
- Kim J-M, Lee K, Shin K et al. (2011) Shifts in biogenic carbon flow from particulate to dissolved forms under high carbon dioxide and warm ocean conditions. *Geophysical Research Letters*, **38**.
- De La Rocha CL, Passow U (2007) Factors influencing the sinking of POC and the efficiency of the biological carbon pump. *Deep Sea Research Part II: Topical Studies in Oceanography*, **54**, 639–658.
- Lakeman MB, von Dassow P, Cattolico RA (2009) The strain concept in phytoplankton ecology. *Harmful Algae*, **8**, 746–758.

Synthesis and future perspectives

- Lassen MK, Nielsen KD, Richardson K et al. (2010) The effects of temperature increases on a temperate phytoplankton community — A mesocosm climate change scenario. *Journal of Experimental Marine Biology and Ecology*, **383**, 79–88.
- Legendre L, Rivkin R (2002) Fluxes of carbon in the upper ocean: regulation by food-web control nodes. *Marine Ecology Progress Series*, **242**, 95–109.
- Lewandowska A, Sommer U (2010) Climate change and the spring bloom: a mesocosm study on the influence of light and temperature on phytoplankton and mesozooplankton. *Marine Ecology Progress Series*, **405**, 101–111.
- Melzner F, Thomsen J, Koeve W et al. (2012) Future ocean acidification will be amplified by hypoxia in coastal habitats. *Marine Biology*, **160**, 1875–1888.
- Merico A, Tyrrell T, Lessard EJ et al. (2004) Modelling phytoplankton succession on the Bering Sea shelf: role of climate influences and trophic interactions in generating *Emiliana huxleyi* blooms 1997–2000. *Deep Sea Research Part I: Oceanographic Research Papers*, **51**, 1803–1826.
- O'Connor MI, Piehler MF, Leech DM et al. (2009) Warming and resource availability shift food web structure and metabolism. *PLoS biology*, **7**, e1000178.
- Pansch C, Schaub I, Havenhand J et al. (2014) Habitat traits and food availability determine the response of marine invertebrates to ocean acidification. *Global Change Biology*, **20**, 765–777.
- Passow U, Carlson C (2012) The biological pump in a high CO₂ world. *Marine Ecology Progress Series*, **470**, 249–271.
- Ridgwell A, Schmidt DN, Turley C et al. (2009) From laboratory manipulations to Earth system models: scaling calcification impacts of ocean acidification. *Biogeosciences*, **6**, 2611–2623.
- Riebesell U, Tortell P (2011) Effects of ocean acidification on pelagic organisms and ecosystems. In: *Ocean Acidification*, pp. 99–116. Oxford University Press.
- Riebesell U, Zondervan I, Rost B et al. (2000) Reduced calcification of marine plankton in response to increased atmospheric CO₂. *Nature*, **407**, 2–5.
- Riebesell U, Schulz KG, Bellerby RGJ et al. (2007) Enhanced biological carbon consumption in a high CO₂ ocean. *Nature*, **450**, 545–8.
- Sarthou G, Timmermans KR, Blain S et al. (2005) Growth physiology and fate of diatoms in the ocean: a review. *Journal of Sea Research*, **53**, 25–42.
- Schulz KG, Bellerby RGJ, Brussaard CPD et al. (2013) Temporal biomass dynamics of an Arctic plankton bloom in response to increasing levels of atmospheric carbon dioxide. *Biogeosciences*, **10**, 161–180.
- Sett S, Bach LT, Schulz KG et al. (2014) Temperature Modulates Coccolithophorid Sensitivity of Growth, Photosynthesis and Calcification to Increasing Seawater pCO₂. *PloS one*, **9**, e88308.
- Sommer U, Lengfellner K (2008) Climate change and the timing, magnitude, and composition of the phytoplankton spring bloom. *Global Change Biology*, **14**, 1199–1208.

Synthesis and future perspectives

- Sommer U, Adrian R, Bauer B et al. (2012) The response of temperate aquatic ecosystems to global warming: novel insights from a multidisciplinary project. *Marine Biology*, **159**, 2367–2377.
- Taucher J, Schulz KG, Dittmar T et al. (2012) Enhanced carbon overconsumption in response to increasing temperatures during a mesocosm experiment. *Biogeosciences*, **9**, 3531–3545.
- Thomas MK, Kremer CT, Klausmeier C et al. (2012) A global pattern of thermal adaptation in marine phytoplankton. *Science (New York, N.Y.)*, **338**, 1085–8.
- Tortell PD, Payne CD, Li Y et al. (2008) CO₂ sensitivity of Southern Ocean phytoplankton. *Geophysical Research Letters*, **35**, L04605.
- Vidussi F, Mostajir B, Fouilland E et al. (2011) Effects of experimental warming and increased ultraviolet B radiation on the Mediterranean plankton food web. *Limnology and Oceanography*, **56**, 206–218.
- Wasmund N, Göbel J, Bodungen B V. (2008) 100-years-changes in the phytoplankton community of Kiel Bight (Baltic Sea). *Journal of Marine Systems*, **73**, 300–322.
- Wohlers-Zöllner J, Biermann A, Engel A et al. (2012) Effects of rising temperature on pelagic biogeochemistry in mesocosm systems: a comparative analysis of the AQUASHIFT Kiel experiments. *Marine Biology*, **159**, 2503–2518.
- Yoshimura T, Suzuki K, Kiyosawa H et al. (2013) Impacts of elevated CO₂ on particulate and dissolved organic matter production: microcosm experiments using iron-deficient plankton communities in open subarctic waters. *Journal of Oceanography*, **69**, 601–618.

Acknowledgments

First and foremost, I would like to thank my supervisor Ulf Riebesell for letting me be part of this wonderful research group. Having the opportunity to work with one of the best in the field was a very rewarding experience. Thanks also to my second supervisor Andreas Oschlies for always having an open door and being so supportive and encouraging.

During these past 5 years not only did I grow professionally but I was also fortunate enough to have met some of the most amazing characters and build relationships which will last me a lifetime. I will never forget the past years in Kiel as part of this working group and my mini German family.

While the *'thank you list'* could go on for pages, I would like to take some time to specially thank two people in particular: Kai and Lenni. Without your kind supervision and all the time you invested in explaining things to me (mathematically and what not) I owe you the world. You both trusted in me and a big part of finishing this thing was thanks to your words of encouragement and always telling me I could do it. For this and for everything you guys did for me...I will be forever in debt. You are the big brothers I always wanted and I love you both very much.

A special thanks to my thesis editors Allanah and Ivonne, for taking the time to look over grammatical mistakes that I could no longer see...I will try to repay it in the future to both of you 😊 You went above and beyond friendship duties and I really do appreciate it.

To my office mates Janina and Jan B for always being so supportive and having fun topics to discuss when working was not an option ;) you guys are next...you can do it!

To my friends who were always encouraging (the scientists and the non scientists) for not only making my stay in Germany unforgettable but for filling my life with so much joy 😊 here goes the list in alphabetical order not to offend anyone (cause I love everyone): Alessio, Bei, Chris S, Jassi, Jan C, Jon, Judith, Karina, Kerstin, Lionel, Linn, Luisa, Magda, Manu, Micha, Tim, Renata, Silke, Yury.....and so on.

Last but not least.

A mis papas y mi hermana, porque sin ellos nada fuera posible, por siempre apoyarme en todas las decisiones que tome y siempre tener palabras alentadoras para seguir creciendo profesional y emocionalmente. Estas metas alcanzadas son mas lindas porque las puedo compartir con ustedes (a pesar de la distancia). Y lo mejor siempre queda de ultimo, al amor de mi vida, por siempre apoyarme en todas mis decisiones y ser paciente los ultimos meses (o siempre?) y por creer en mi (aunque no sepa derivar). Te amo y soy muy afortunada al haberte encontrado y llevar una vida tan maravillosa a tu lado.

Acknowledgments

Curriculum Vitae

Scarlett Sett, M.Sc.

■ Personal Information

Nationality: Guatemalan
Place of birth: Guatemala City, Guatemala
Date of birth: 02.05.1984

■ Education

Jan. 2011 – Sept 2014 Biological Oceanography
PhD student Biological Oceanography / Marine Biogeochemistry
GEOMAR Helmholtz Centre for Ocean Research Kiel, Germany

Oct. 2007 – Nov. 2010 Biological Oceanography
Master of Science (M.Sc.)
GEOMAR Helmholtz Centre for Ocean Research Kiel, Germany

Aug. 2003 – Aug. 2007 Marine Biology
Bachelor of Science (B.Sc.)
University of West Florida, Pensacola, Fl. USA

■ Courses

July 2012 *Darwin Summer School on Biogeosciences*
Darwin Center for Biogeosciences
Utrecht, Holland

August 2009 *Summer School on The Coastal Zone and its Management*
Sino-German Initiative
Qingdao, China

June 2008 *Summer School on Conservation Biology*
International Graduate School of Conservation Biology
Rovinj, Croatia

■ Honors and Awards

- Stipendium Teaching Assistant
Christian-Albrechts-Universität
Winter 2010, Spring 2011
- Latin American and Caribbean Scholarship
University of West Florida
Fall 2003 – Fall 2007
- President's Honor List
University of West Florida
Summer 2005, 2006
Fall 2006
- Dean's Honor List
University of West Florida
Fall 2004

■ Publication list

Barcelos e Ramos J, Schulz KG, Brownlee C, **Sett S**, Azevedo EB (2014) Effects of increasing seawater carbon dioxide concentrations on chain formation of the diatom *Asterionellopsis glacialis*. PLoS ONE 9(3): e90749. doi:10.1371/journal.pone.0090749

Sett, S., Bach, L.T., Schulz, K.G., Koch-Klavsen, S., Lebrato, M., and Riebesell, U. *Temperature modulates coccolithophorid sensitivity of growth, photosynthesis and calcification to increasing seawater pCO₂*. (2014) PLoS ONE 9(2): e88308. doi:10.1371/journal.pone.0088308

Müller, M. N., Lebrato, M., Riebesell, U., Barcelos e Ramos, J., Schulz, K. G., Blanco-Ameijeiras, S., **Sett, S.**, Eisenhauer, A., and Stoll, H. M. (2014) *Influence of temperature and CO₂ on the strontium and magnesium composition of coccolithophore calcite*. Biogeosciences 11, 1065-1075. doi:10.5194/bg-11-1065-2014, 2014.

Bach, L., Riebesell, U., **Sett, S.**, Febiri, S., Rzepka, P. and Schulz, K. G. (2012) *An approach for particle sinking velocity measurements in the 3–400 µm size range and considerations on the effect of temperature on sinking rates*. Marine Biology, 159 (8). pp. 1853-1864. DOI 10.1007/s00227-012-1945-2.

Blanco-Ameijeiras, S., Lebrato, M., Stoll, H. M., Iglesias-Rodriguez, M. D., Mendez-Vicente, A., **Sett, S.**, Müller, M. N., Oschlies, A. and Schulz, K. (2012) *Removal of organic magnesium in coccolithophore carbonates*. Geochimica et Cosmochimica Acta, 89 . pp. 226-239. DOI 10.1016/j.gca.2012.04.043.

Eidesstattliche Erklärung

Hiermit bestätige ich, dass die vorliegende Arbeit mit dem Titel:

Interactive effects of ocean acidification and warming on marine phytoplankton –from physiology to biogeochemical cycling

von mir selbstständig verfasst worden ist und keine weiteren Quellen und Hilfsmittel als die angegebenen verwendet wurden. Die vorliegende Arbeit ist unter Einhaltung der Regeln guter wissenschaftlicher Praxis der Deutschen Forschungsgemeinschaft entstanden und wurde weder im Rahmen eines Prüfungsverfahrens an anderer Stelle vorgelegt noch veröffentlicht. Ich erkläre mich einverstanden, dass diese Arbeit an die Bibliothek des GEOMAR und die Universitätsbibliothek der CAU weitergeleitet wird.

Kiel, den 17.Sept 2014

Scarlett Sett